Dissertation ETH No. 19908

Stochastic Model Predictive Control for Energy Efficient Building Climate Control

A dissertation submitted to
ETH Zurich

for the degree of
Doctor of Sciences

presented by

Frauke Oldewurtel

Dipl.-Wirtsch.-Ing., TU Braunschweig
Master of Science, Georgia Institute of Technology
born 09.11.1980
citizen of Germany

accepted on the recommendation of

Prof. Dr. Manfred Morari, examiner
Dr. Jürg Tödtli, co-examiner

2011

Stochastic Model Predictive Control for Energy Efficient Building Climate Control

Frauke Oldewurtel

Dissertation ETH Zürich No. 19908

To my parents

Contents

Abstract xi

Zusammenfassung xiii

Acknowledgments xvii

Notation xix

List of Acronyms xxi

List of Figures xxiii

List of Tables xxiv

1 Introduction 1
- 1.1 Outline and Contribution . . . 3
- 1.2 Publications . . . 6

I Background 9

2 Building Climate Control 11
- 2.1 Introduction . . . 11
- 2.2 Literature Survey . . . 12
- 2.3 Positioning of the Work . . . 13

3 Model Predictive Control for Building Climate Control 17
- 3.1 Mathematical Preliminaries . . . 17
  - 3.1.1 Set Theory . . . 17
  - 3.1.2 System and Control Theory . . . 18
- 3.2 Receding Horizon Control . . . 20
  - 3.2.1 MPC for Building Climate Control . . . 22
  - 3.2.2 Nominal MPC . . . 26

3.2.3 Deterministic MPC/ Certainty Equivalence MPC 27
3.2.4 Robust MPC 28
3.2.5 Chance Constrained Stochastic MPC 31

II Computationally Efficient MPC under Uncertainty 33

4 Tractable Approximations of Chance Constrained Stochastic MPC 35
4.1 Introduction 35
4.1.1 Main Idea and Outline 35
4.1.2 Dealing with Uncertainty 36
4.1.3 Definition of Constraints 37
4.2 Problem Setting 38
4.3 Affine Disturbance Feedback for Stochastic MPC 40
4.4 Chance Constraint Reformulations 43
4.4.1 Quantile Function 43
4.4.2 Bounds on the Disturbance Set 44
4.4.3 Fixed Feedback 46
4.5 Numerical Example 47
4.6 Conclusions 51

5 Blocking Parameterization of Affine Disturbance Feedback MPC 53
5.1 Introduction 53
5.1.1 Blocking for Reducing Computational Complexity 53
5.1.2 Main Idea and Outline 54
5.2 Problem Setting 54
5.2.1 Affine Disturbance Feedback Input Parameterization 54
5.2.2 Expectation Based Disturbance Feedback MPC Problem 56
5.3 Complexity Reduction via Blocking 57
5.3.1 Blocking Parameterization 57
5.3.2 Prediction Constraint Relaxation 57
5.3.3 Reduction of Computational Complexity 61
5.4 Numerical Example 62
5.5 Conclusions 65

III Investigations in Building Climate Control 67

6 Simulation Environment 69
6.1 Introduction 69

6.2 Building Types 72
6.3 HVAC Systems 72
6.4 Control Settings 76
6.5 Disturbances 78
6.5.1 Weather 79
6.5.2 Internal Gains 79
6.6 Simulation Software 80
6.7 Control Strategies and Benchmarks for Building Climate Control 81
6.7.1 Classification of Control Problem 81
6.7.2 Rule Based Control 81
6.7.3 Deterministic MPC 82
6.7.4 Chance Constrained Stochastic MPC 82
6.7.5 Performance Bound 83
6.8 Implementation of MPC for Building Climate Control 84
6.8.1 Step 1: Weather Prediction at Building Site 84
6.8.2 Step 2: Modeling 87
6.8.3 Step 3: Formulate Optimization Problem 91
6.8.4 Step 4: Solve Optimization Problem 94
6.8.5 Step 5: Apply Control Action 94
6.9 Overview of Simulation Settings 94

7 Use of Weather Predictions and MPC 97
7.1 Introduction 97
7.1.1 Main Idea and Ouline 97
7.2 Building Simulation Framework 98
7.3 Controller Assessment Concept 98
7.4 Investigations 99
7.4.1 Theoretical Energy Savings Potential 100
7.4.2 Practical Energy Savings Potential 100
7.5 Results 102
7.5.1 Theoretical Energy Savings Potential 102
7.5.2 Practical Energy Savings Potential 104
7.6 Conclusions 108

8 Use of Occupancy Predictions and MPC 109
8.1 Introduction 109
8.1.1 Use of Occupancy Information for Building Automation 109
8.1.2 Use of Occupancy Models in for Building Automation 110
8.1.3 Main Idea and Outline 110

8.2 Building Simulation Framework . . . 111
8.2.1 Building and HVAC Model . . . 111
8.2.2 Building Cases and HVAC Systems . . . 112
8.2.3 Control settings . . . 112
8.2.4 Disturbances . . . 113
8.2.5 Control formulation . . . 115
8.3 Occupancy Model . . . 116
8.4 Investigations . . . 118
8.5 Results . . . 122
8.5.1 Homogeneous occupancy . . . 122
8.5.2 Alternating occupancy . . . 122
8.6 Discussion . . . 125
8.6.1 Choice of Investigation Setup . . . 125
8.6.2 Simulation Results . . . 126
8.7 Conclusions . . . 127

9 Use of Dynamic Electricity Prices and MPC 129
9.1 Introduction . . . 129
9.2 Building Simulation Framework . . . 130
9.2.1 Building and HVAC Model . . . 130
9.2.2 Building Cases and HVAC Systems . . . 131
9.2.3 Control Settings . . . 131
9.2.4 Disturbances . . . 131
9.2.5 Control Formulation . . . 132
9.2.6 Electricity Tariffs . . . 132
9.3 Dynamic Electricity Tariff . . . 133
9.3.1 Basic Construction . . . 133
9.3.2 Support Vector Regression . . . 136
9.3.3 Construction of Price Vector for MPC Controller . . . 138
9.4 Investigations . . . 138
9.5 Results . . . 139
9.5.1 Qualitative Differences . . . 139
9.5.2 Quantitative Differences . . . 139
9.6 Conclusions . . . 142

Appendix 143
A Expression of Matrices in Augmented Model . . . 143
B Proof of Theorem 4.16 . . . 143
C Computation of Problem 4.18 . . . 144

D Monotonicity of NRPE Use Depending on $(\beta_{\text{vac}}, \beta_{\text{occ}})$ 145
E Homogeneous Occupancy, Absolute Savings 147

Bibliography **148**

Abstract

This thesis is concerned with the development of Model Predictive Control (MPC) strategies for energy efficient building climate control. Because a large fraction of the world's energy is consumed in buildings and refurbishments are expensive, there is a strong motivation for a more energy efficient control. The aim is to use the inherent thermal storage capacity of the building to optimize Heating, Ventilation, and Air Conditioning (HVAC) by using MPC with weather and occupancy predictions. MPC is a control technique which is characterized by its ability to handle constrained control problems using a model for predicting the future behavior of a system and using optimization routines to determine the control input. The thesis starts with a background on building climate control and MPC, in the second part two theoretical developments are presented, and the last part describes three investigations in the field of building climate control.

Two important features in building climate control give rise to a stochastic MPC formulation. First, the uncertainty in the weather predictions is of major importance and second, motivated by definitions in building standards, comfort constraints do not have to be fulfilled at all times, but can be expressed as chance constraints. A stochastic MPC formulation is developed that is tractable for large-scale systems such as buildings. An uncertain linear system with polytopic constraints on the input and chance constraints on the state that is subject to additive Gaussian disturbances is considered. The proposed formulation combines the use of Affine Disturbance Feedback, a formulation successfully applied in robust control, with a tractable deterministic reformulation of the chance constraints.

The aforementioned Affine Disturbance Feedback suffers from a high computational complexity due to a significant increase in decision variables. This problem is addressed for a linear system subject to additive, bounded disturbances and polytopic constraints on input and state. So-called move-blocking is an effective method of reducing the computational complexity of MPC problems. Unfortunately, move-blocking precludes the use of terminal constraints as a means of enforcing strong feasibility. A method for enforcing strong feasibility of nominal move-blocking MPC problems that was recently developed is generalized here and employed for the purpose of enforcing strong feasibility of blocking Affine Disturbance Feedback MPC problems.

The last part of the thesis presents three investigations in the field of building climate control.

The first investigation is concerned with the proposed stochastic MPC formulation and the use of weather predictions. As a first step the potential of MPC for building climate control is assessed by means of a large-scale factorial simulation study considering different types of buildings and HVAC systems at four representative European sites. Then for selected representative cases the control performance of the proposed stochastic MPC is investigated as well as the impact of the accuracy of weather predictions on the control performance and the tunability of stochastic MPC. The findings suggest that stochastic MPC outperforms current control practice in terms of both, energy efficiency and occupant comfort.

Second, an investigation of the importance of occupancy predictions in building climate control is presented. An MPC controller which controls the building with a fixed occupancy schedule is used as a benchmark. The energy use of this benchmark is compared with those of three other control strategies: first, the same MPC controller that uses the same schedule for control as the benchmark, but adjusts lighting in case of (instantaneous measurement of) vacancy; second, the same MPC controller that uses the same schedule for control as the benchmark, but adjusts lighting and ventilation in case of (instantaneous measurement of) vacancy; and third, the same MPC controller as the benchmark, but using a perfect prediction of the future occupancy. The results show that taking into account occupancy information in building climate control has a significant energy savings potential. For some cases, however, a large part of this potential can already be captured by taking into account instantaneous occupancy measurements.

The third investigation is concerned with the reduction of peak electricity demand by adopting a dynamic electricity tariff and MPC in building climate control. The use of a dynamic electricity tariff based on the spot market price and current grid load level is proposed. This tariff can be directly incorporated in the MPC problem and serve as an incentive for the building controller to act in a grid-friendly manner. Since the tariff is only available for a limited time window into the future, least-squares support vector machines for electricity price forecasting are used to provide the MPC controller with the necessary estimated dynamic electricity prices for the whole prediction horizon. It is shown that the peak electricity demand of buildings can be significantly reduced, making this study an example for a successful implementation of Demand Response in building climate control.

Zusammenfassung

Diese Arbeit beschäftigt sich mit der Entwicklung von modellprädiktiven Regelungsstrategien (MPC) für eine energieeffiziente Gebäudeklimaregelung. Die Tatsache, dass ein grosser Teil des weltweiten Energiekonsums auf Gebäude entfällt und dass Renovierungen teuer sind, ist eine starke Motivation für eine energieeffizientere Regelung. Das Ziel ist, die inherente thermische Speicherfähigkeit des Gebäudes zu nutzen, um Heizen, Ventilation und Kühlung (HVAC) durch Verwendung von MPC mit Wetter- und Belegungsprognosen zu optimieren. MPC ist eine Regelungsmethode, die sich durch ihre Fähigkeit zur Behandlung von beschränkten Regelungsproblemen auszeichnet und ein Model zur Vorhersage des zukünftigen Verhaltens des Systems verwendet sowie Optimierungsroutinen, um die Stellgrössen zu bestimmen. Die Arbeit beginnt mit dem Hintergrund zu Gebäudeklimaregelung und MPC, im zweiten Teil werden zwei theoretische Entwicklungen präsentiert und im letzten Teil werden drei Untersuchungen im Feld der Gebäudeklimaregelung beschrieben.

Zwei wichtige Merkmale in der Gebäudeklimaregelung führen zur Betrachtung einer stochastischen MPC Formulierung. Erstens ist die Unsicherheit in den Wetterprognosen von grosser Wichtigkeit und zweitens müssen, motiviert durch die Gebäudestandards, Komfortbeschränkungen nicht zu allen Zeiten eingehalten werden, sondern können als Chance-Beschränkungen aufgefasst werden. Eine stochastische MPC Formulierung wird entwickelt, die für grosse Systeme wie Gebäude geeignet ist. Ein unsicheres lineares System mit polytopischen Beschränkungen auf dem Eingang und Chance-Beschränkungen auf dem Zustand, das additiven Störungen unterworfen ist, wird betrachtet. Die vorgeschlagene Formulierung verbindet die Verwendung von Affine Disturbance Feedback, einer Formulierung, die erfolgreich in der robusten Regelung verwendet wird, mit einer deterministischen Reformulierung der Chance-Beschränkungen.

Das bereits erwähnte Affine Disturbance Feedback leidet an einer hohen Rechenkomplexität durch eine signifikante Erhöhung der Entscheidungsvariablen. Dieses Problem wird für ein lineares System mit additiven beschränkten Störungen und polytopischen Beschränkungen auf Eingang und Zustand betrachtet. So genanntes Move-Blocking ist eine effektive Methode zur Reduktion der Rechenkomplexität von MPC Problemen. Leider schliesst Move-Blocking die Verwendung von Terminal Constraints zur Garantie von Strong Feasibility aus. Eine Methode, um Strong Feasibility für nominale

Move-Blocking MPC Probleme zu garantieren wurde kürzlich entwickelt und wird hier generalisiert und angewendet, um Strong Feasibility für Blocking Affine Disturbance Feedback MPC Probleme zu garantieren.

Der letzte Teil der Arbeit präsentiert drei Untersuchungen für den Bereich Gebäudeklimaregelung.

Die erste Untersuchung beschäftigt sich mit der vorgeschlagenen stochastischen MPC Formulierung und der Verwendung von Wetterprognosen. Als erster Schritt wird das Potential von MPC für die Gebäudeklimaregelung durch eine grosse faktorielle Simulationsstudie mit unterschiedlichen Typen von Gebäuden und HVAC Systemen an vier repräsentativen europäischen Standorten bestimmt. Dann wird für eine Auswahl von repräsentativen Fällen das Regelverhalten des vorgeschlagenen stochastischen MPC Reglers untersucht, sowie der Einfluss der Qualität der Wetterprognosen auf das Regelverhalten und die Möglichkeit des Tunings von stochastischem MPC. Die Resultate deuten darauf hin, dass stochastisches MPC die momentane Regelpraxis verbessert und zwar sowohl im Hinblick auf Energieeffizienz als auch auf Komfort.

Zweitens wird eine Untersuchung über die Bedeutung von Belegungsprognosen in der Gebäudeklimaregelung präsentiert. Ein MPC Regler, der das Gebäude mithilfe eines fixierten Standardbelegungsplans regelt, wird als Benchmark verwendet. Der Energieverbrauch dieses Benchmarks wird mit drei anderen Regelstrategien verglichen: erstens, dem gleichen MPC Regler, der den gleichen Belegungsplan zur Regelung verwendet wie der Benchmark, aber das Licht im Falle von (instantan gemessener) Abwesenheit ausschaltet; zweitens, der gleiche MPC Regler, der den gleichen Belegungsplan zur Regelung verwendet wie der Benchmark, aber das Licht und die Lüftung im Falle von (instantan gemessener) Abwesenheit ausschaltet; und drittens, der gleiche MPC Regler wie der Benchmark, der aber eine perfekte Vorhersage über die zukünftige Belegung verwendet. Die Resultate zeigen, dass die Verwendung von Information über die Belegung in der Gebäudeklimaregelung ein signifikantes Energiesparpotential besitzt. Allerdings kann ein grosser Teil dieses Potentials bereits durch die Verwendung von instantanen Belegungsmessungen abgeschöpft werden.

Die dritte Untersuchung beschäftigt sich mit der Reduktion der Spitzen im Elektrizitätsbedarf durch die Verwendung von dynamischen Elektrizitätstarifen und MPC in der Gebäudeklimaregelung. Die Verwendung eines dynamischen Elektrizitätstarifs, der auf dem Spotmarktpreis und der momentanen Netzlast basiert, wird vorgeschlagen. Dieser Preis kann direkt im MPC Problem berücksichtigt werden und als Anreiz für den Gebäuderegler für ein netzfreundliches Verhalten dienen. Da der Tarif nur für ein begrenztes Zeitfenster in die Zukunft verfügbar ist, werden Least-Squares Support Vector Machines zur Elektrizitätspreisvorhersage verwendet, um für den MPC Regler die notwendigen geschätzen dynamischen Elektrizitätspreise für den gesamten Vorher-

sagehorizont zur Verfügung zu stellen. Es wird gezeigt, dass die Spitzen im Elektrizitätsbedarf von Gebäuden signifikant reduziert werden können. Daher ist diese Studie ein Beispiel für die erfolgreiche Implementierung von Demand Response in der Gebäudeklimaregelung.

Acknowledgments

First of all I would like to thank Professor Manfred Morari for being my supervisor. Professor Morari provided me with guidance and support throughout the years, but also with freedom to discover which directions I would like to emphasize during my PhD. I would also like to thank him for providing an excellent working environment and for bringing so many interesting and diverse people together. I am very grateful for having been part of such an inspiring and motivating environment as the Automatic Control Laboratory at ETH Zurich.

I would like to thank Colin N. Jones for supervising me on a weekly basis. I am deeply indebted for his constant support, for the detailed technical discussions, and for his advice.

I am very grateful to Jürg Tödtli for kindly agreeing to be in my examination committee. More importantly, he is the reason that I started working on the OptiControl project and that I did my PhD at ETH, since it is due to an incidental meeting of Jürg Tödtli and myself during my diploma studies that I got to know about this project.

My thanks go to all project members of the OptiControl project, who shared with me their expertise on meteorology, building physics, and building control, amongst them D. Gyalistras (project leader); M. Gwerder, C. Gähler, B. Illi, D. Habermacher (Siemens Building Technologies); T. Frank, V. Dorer, B. Lehmann, K. Wirth (EMPA); V. Stauch, P. Steiner, and F. Schubiger (MeteoSwiss). I am grateful for the privilege of having experienced the work on an industry project and meeting people, who showed me a different perspective on many questions.

It was nice to see the 'building group' grow while being at IfA; by PhD students, but also by visitors. I very much enjoyed working with Philipp Rostalski, David Sturzenegger, Roy Smith, Alessandra Parisio, Clara Verhelst, Jan Sirkoy, Sam Privara, Jiri Cigler, and Boris Vega Lara. I have learned a lot from them!

It was a pleasure to work with Ravi Gondhalekar, who taught me a lot about the usefulness of invariant sets. His humorous comments in write-ups are unrivaled.

I also enjoyed very much working with Andreas Ulbig and Professor Göran Andersson, who enabled me to extend my work to the area of electricity grids. This also motivated me to continue my work in this direction.

My thanks go to 'my' master students, Fabian Ullmann, Tobias Baltensperger, Thomas Burtscher, and Milan Korda for their excellent work.

I also would like to thank Georg Schildbach, David Sturzenegger, Jan Siroky, Milan Korda, Ravi Gondhalekar, Alessandra Parisio, Sam Privara, and Jiri Cigler for proofreading this thesis.

What made my PhD really enjoyable was the amazing group of inspiring people at IfA. They are not only inspiring in a scientific sense, but simply great people. I remember many wonderful moments and I consider these experiences invaluable and unforgettable.

In addition to the people mentioned above I would like to thank the following people. Let me start with Urban Mäder and Kristian Nolde, who were my officemates in ETL K22.3 for the first half of my PhD. We had very interesting discussions on one of Zurich's prime balconies. Thanks for the wonderful time! My thanks go to Melanie Zeilinger, who started at the same time as me and was always there; in particular, we shared many hotel rooms on many conferences (unforgettable is our trip to the great wall!), my 'brothers' Yannis Lymperopoulos and Akin Sahin (thanks for your protection and insights about life!), our Mexican Cristian Grossmann, Antonello Caruso (the Italian teacher), Helfried Peyrl, Miroslav Baric, Ioannis Fotiou, Andreas Kuhn, Giorgos Chaloulos, Andreas Milias, Kostas Koutroumpas, Kostas Margellos, Alexander Fuchs, Joe Warrington, Claudia Fischer, John Lygeros, Aldo Zgraggen, Stefan Richter, Manfred Quack, Peyman Mohajerin (watch your grammar!), Andreas Hempel, Stephan Huck (how did you get this motorcycle in my office?!?), Robert Nguyen, Khoa Nguyen, Debasish Chatterjee, Peter Hokayem, Maryam Kamgarpour (gole sorch), Robin Vujanic, Christian Conte (tablesoccer expert), Paul Goulart, Sébastien Mariéthoz, Stefan Almér, Davide Raimondo, Frank Christophersen, Federico Ramponi, Riccardo Porreca, Jack DiGiovanni, Tyler Summers, Sean Summers, Alexander Domahidi, Nikolaos Kariotoglou, Jakob Ruess, Bratislav Svetozarevic, Marko Tanaskovic, Bart van Parys, Thomas Besselmann, and Daniel Axehill (order intended to be non-existing).

I am eternally grateful to my family and friends. In particular, I would like to thank my parents that always gave me faith, love, and strength. Without their support, I would not be here. Last, but foremost, I would like to thank Georg for his constant love and support.

Zurich, August 2011 *Frauke Oldewurtel*

Notation

Throughout the thesis, scalars and vectors are denoted with lower cases letters ($a, b, ...,$ $\alpha, \beta, ...$), matrices are denoted with upper case letters ($A, B, ..., \mathbf{A}, \mathbf{B}$), and sets are denoted with upper case blackboard bold letters ($\mathbb{X}, \mathbb{U}, ..., \mathbb{N}, \mathbb{R}$) for constraint sets and number sets and with upper case calligraphic letters ($\mathcal{A}, \mathcal{B}, ...$) for general sets.

General Operators and Relations

$\cdot$	general placeholder
...	and so forth
$:=$	left-hand side is defined by the right-hand side
$\vert$	such that
$\in$	is element of (belongs to)
$\forall$	for all
$\exists$	there exists
$\notin$, $\nexists$	/ denotes negation
$\wedge$	and
$\Rightarrow$	implies

Sets, Spaces, and Set Operators

$\{\cdot, ...\}$	set or sequence
$\emptyset$	empty set
$\mathbb{R}$	real numbers
$\mathbb{R}_{+0}$	set of non-negative real numbers
$\mathbb{R}^n$	space of n-dimensional (column) vectors with real entries
$\mathbb{R}^{n\times m}$	space of n by m matrices with real entries
$\mathbb{N}$	natural numbers (non-negative integers), $\mathbb{N}_+ := \mathbb{N}\backslash\{0\}$
$\mathbb{N}_j^k$	set of consecutive non-negative integers $\{j, \ldots, k\}$
$(\subset)$ $\subseteq$	(strict) subset
$(\supset)$ $\supseteq$	(strict) superset
$\backslash$	set difference
$\times$	Cartesian product, $\mathbb{X} \times \mathbb{Y} = \{(x, y) \vert x \in \mathbb{X}, y \in \mathbb{Y}\}$
$\mathbb{S}^N$	Cartesian product of $\mathbb{S}$, $\mathbb{S} \times \ldots \times \mathbb{S}$, N times with itself

Operators on Vectors and Matrices

$[\cdot, \cdot, ...]$	a matrix (or a vector)
$<, \leq, =, >, \geq$	element-wise comparison of vectors
v^T	row vector, transpose of a vector
$\|v\|$	(any) vector norm
$\|v\|_1$	l_1-norm or vector 1-norm (sum of absolute values)
$\|v\|_2$	l_2-norm or vector 2-norm (Euclidian norm)
$\|v\|_\infty$	l_∞-norm or vector ∞-norm (largest absolute element)
$\mathbf{I}$	identity matrix (of appropriate dimension)
$\mathbf{I}_{\{n\}}$	identity matrix of dimension $n \times n$
$\mathbf{0}$	zero matrix (of appropriate dimension)
$\mathbf{0}_{\{n,m\}}$	zero matrix of dimension $n \times m$
M^T	transpose of a matrix
M^{-1}	inverse of the square matrix
$M \succ (\succeq)\ 0$	matrix M is positive (semi)definite
$\|M\|$	(any) matrix norm
$\|M\|_1$	induced matrix 1-norm
$\|M\|_2$	induced matrix 2-norm
$\|M\|_\infty$	induced matrix ∞-norm
$A \otimes B$	Kronecker product of matrices $A \in \mathbb{R}^{n \times m}$ and $B \in \mathbb{R}^{p \times q}$, $A \otimes B := \begin{bmatrix} a_{11}B & \dots & a_{1m}B \\ \vdots & \ddots & \vdots \\ a_{n1}B & \dots & a_{nm}B \end{bmatrix}$

Systems and Control Theory

n_x	number of states, $n_x \in \mathbb{N}_+$
n_u	number of inputs, $n_u \in \mathbb{N}_+$
n_w	number of disturbances, $n_w \in \mathbb{N}_+$
x	state, $x \in \mathbb{R}^{n_x}$
u	control input, $u \in \mathbb{R}^{n_u}$
w	disturbance, $w \in \mathbb{R}^{n_w}$
$\mathbb{X}$	set of state vectors, $\mathbb{X} \subseteq \mathbb{R}^{n_x}$
$\mathbb{U}$	set of control inputs, $\mathbb{U} \subseteq \mathbb{R}^{n_u}$
$\mathbb{W}$	set of disturbances, $\mathbb{W} \subseteq \mathbb{R}^{n_w}$

Probability Theory

$\Pr[\cdot]$	probability measure
$\mathrm{E}[\cdot]$	expectation with respect to probability measure Pr
$\mathcal{N}(\bar{w}, \Sigma)$	multivariate normal (Gaussian) distribution with mean $\bar{w}$ and covariance Σ

List of Acronyms

ADF	Affine Disturbance Feedback
ANN	Artificial Neural Network
ARIMA	Autoregressive Integrated Moving Average
BDS	Bounds on Disturbance Set
CE	Certainty Equivalence
CI	Controlled invariant
CLP	Closed loop prediction
DR	Demand Response
FF	Fixed Feedback
HVAC	Heating, Ventilation, Air Conditioning
IAQ	Indoor air quality
LP	Linear program
LS	Least Squares
LTI	Linear time invariant
LQR	Linear quadratic regulator
LQG	Linear quadratic Gaussian
LUG	Lugano
MCI	Maximum controlled invariant
MPC	Model Predictive Control
MRCI	Maximum robust controlled invariant
MSM	Marseille Marignane
NRPE	Non-renewable primary energy
OLP	Open loop prediction
QCQP	Quadratically constrained quadratic program
QF	Quantile Function
QP	Quadratic program
RBC	Rule-Based Control
RC	Resistance-capacitance
RCI	Robust controlled invariant
SFHOCP	Stochastic finite horizon optimal control problem
SMA	Zurich

SMPC	Stochastic Model Predictive Control
SOC	Second order cone
SVM	Support Vector Machines
TABS	Thermally Activated Building System
WHW	Wien Hohe Warte

List of Figures

3.1 MPC scheme for building climate control 22

4.1 Outside temperature, solar radiation, and internal heat gains 48
4.2 Energy use versus $\alpha_{\mathbf{x},j}$ 50
4.3 Room temperature profile 50
4.4 Heating input 50
4.5 Relation of energy use and probability of violations 51

5.1 Dog walking schematic 63
5.2 Nominal trajectories with proposed controllers 65
5.3 Disturbed trajectories with proposed controllers 66

6.1 Thermal RC network model 71
6.2 Schematic representation of two building zones 72
6.3 Room temperature set points for heating and cooling 76
6.4 Example of diurnal occupancy profiles for weekdays 80
6.5 Decision flow of the MPC strategy for building control 85
6.6 Simple example model for constructing the differential equation 87

7.1 Controller assessment concept 98
7.2 Joint cumulative distribution function 103
7.3 Average prediction horizon length 104
7.4 Comparison of PB, DMPC, RBC, and SMPC 105
7.5 Comparison of SMPC and RBC for Cases 1, 2, 3, 7, 17, and 18 105
7.6 Room temperature profile of Case 3 in Table 7.1 using RBC 106
7.7 Room temperature profile of Case 3 in Table 7.1 using SMPC 106
7.8 Comparison of SMPC with different weather predictions 107
7.9 Tuning of SMPC 107

8.1 Two-zone model 111
8.2 Standard weekly occupancy profile 115
8.3 Vacancy and occupancy histograms 117
8.4 Random occupancy time series 118

8.5 Homogeneous occupancy, relative savings 123
8.6 Alternating occupancy, relative savings 124

9.1 Evolution of spot prices, grid load, and dynamic tariff 135
9.2 Hourly electricity tariff forecasts for Zurich, 1-22 July 2007 137
9.3 Reducing peak electricity demand by shifting radiator usage 140
9.4 Relative peak demand reduction for different room setups 141

D.1 Relative energy savings versus different values of $(\beta_{\text{vac}}, \beta_{\text{occ}})$ 146
E.2 Homogenous occupancy, absolute savings 147

List of Tables

3.1 Common types of cost functions 24
3.2 Common types of constraints 25

5.1 Comparison of blocking schemes 66

6.1 Building types differ in terms of four parameters 73
6.2 Five HVAC systems and their automated subsystems 75
6.3 Control settings 77
6.4 Sites for the weather measurements 78
6.5 Values for internal gains levels 79
6.6 Disturbance parameters 80
6.7 Overview of simulation settings 95

7.1 Investigated cases for practical savings potential 101

8.1 Building types for investigation of occupancy information 112
8.2 Variants of occupancy handling in controller 120
8.3 Occupancy patterns 120
8.4 Parameters for investigation of occupancy information 121

9.1 Building types for investigation of dynamic electricity prices 131
9.2 Overview of electricity tariffs 132
9.3 Correlation of variable tariffs with spot price and grid load time-series . 136
9.4 Parameters for investigation of electricity prices 138

1 Introduction

The increased interest in building climate control both in academia as well as from industry and policy makers is due to several developments. On the one hand the world is facing a drastic need to reduce its energy consumption while a large part of today's energy in industrialized countries is consumed in buildings. Since in industrialized countries the main building stock is already in place and refurbishments are very expensive, new building designs can only help to a certain extent and energy efficient control of the existing buildings becomes important. On the other hand modern technologies (e.g., increase in computational power, availability of low-cost sensors, high-quality weather predictions, and advanced control techniques) enable new possibilities for an energy efficient building climate control or for looking at buildings as entities in a smart grid, whose thermal storage capacity can be used to shift electricity demands.

The current control practice in building control is *Rule Based Control* (RBC). These controllers consist of rules of the form "if *condition*, then *action*" and involve a large number of threshold values and parameters that need to be determined. The control performance critically depends on the tuning of these parameters. But with the rising complexity of *Heating, Ventilation, and Air Conditioning* (HVAC) systems a good tuning of RBC controllers becomes more and more difficult.

Model Predictive Control (MPC) is a modern control technique that has been successfully applied in many areas due to its ability to handle constrained control problems. At each sampling time, the optimal control action is obtained by solving a constrained finite horizon optimal control problem for the current state of the plant. When applied in building climate control, this means that at the current point in time a plan for heating, cooling, and ventilation is formulated for the next several hours to days, based on predictions of the upcoming weather conditions. Predictions of any other disturbances (e.g., occupancy), time-dependencies of the control costs (e.g., dynamic electricity prices), or of the constraints (e.g., thermal comfort range) can be readily included in the optimization.

Besides its ability to handle constrained control problems, one reason frequently given why MPC can lead to energy savings in building climate control is the aforementioned ability to easily incorporate weather forecasts and make use of the building as a thermal storage, the underlying assumption being that with knowledge of the future weather,

the low energy cost actuators (e.g., blinds, cooling tower) can be used to prepare the building for the future weather conditions and the high energy cost actuators (e.g., radiators, chillers) can be avoided as much as possible. The use of weather forecasts in building climate control is, however, not straightforward, since the weather forecasts are subject to errors, which introduces uncertainty to the resulting control problem. In order to achieve a good control performance, it is crucial to properly account for these uncertainties in the controller. A second reason why MPC is well suited for building climate control is the fact that building standards require the room temperature to be satisfied not at all times, but allow for violations during a predefined (small) fraction of the year, which can be included in the MPC problem with the formulation of so-called chance constraints, i.e. constraints that have to be fulfilled with a given probability. This gives rise to a stochastic MPC formulation for building climate control, which is developed and investigated in this thesis.

Besides the weather, a second important influence on buildings originates from the buildings' occupants, both in terms of the heat gains that are introduced to the building and in terms of the constraints due to the need of meeting the occupants' comfort. Today, occupancy information is used only in form of *schedules* in building climate control, often in addition with instantaneous adjustments of lighting, sometimes in addition with instantaneous adjustment of both lighting and ventilation based on occupancy sensor measurements. It appears, however, desirable to take into account information about long-term vacancies (business trips, holidays, illnesses) in order to achieve an energy efficient building climate control, whereas the benefit of this information can be expected to depend on the considered building and HVAC system. In this work the potential benefit of long-term vacancy information is investigated and an advanced control strategy using occupancy predictions is compared with simple control strategies that are based on current measurements.

A third area, in which the application of MPC in building climate control can be beneficial is in the area of electricity grids and dynamic electricity tariffs. From an electricity network perspective, it is important to reduce the peak electricity demands, since the peaks determine the necessary capacity of the network. Price signals can be used as an economic incentive for consumers to shift their electricity demand in time according to the price signal and hence behave in a grid-friendly manner. When using MPC, this price signal can be directly incorporated in the formulation of the optimization problem. So far, many authors have considered the consequences from a grid perspective under the assumption that the consumers would react in a predefined way. In this work the problem is considered from the end-consumer perspective and the reaction to dynamic electricity prices assuming a perfect building response is investigated.

This PhD was carried out in the framework of the OptiControl project, involving the project partners Siemens Building Technologies, EMPA, MeteoSwiss, and Gruner AG and was sponsored by Swisselectric Research, CCEM-CH, and Siemens Building Technologies (www.opticontrol.ethz.ch).

1.1 Outline and Contribution

Part I

Part I introduces some background material that is relevant for the developments in this thesis and it positions the thesis in the research area it deals with.

Chapter 2

Chapter 2 gives some background on current control practice in building climate control and provides a brief literature survey as well as a positioning of the work.

Chapter 3

Chapter 3 starts with giving some mathematical preliminaries that are needed in this thesis and then discusses different formulations of MPC in view of applying them to building climate control. In particular, it provides an overview of the different types of MPC formulation that are dealt with in this thesis and introduces the terminology.

Part II

Part II is concerned with computationally efficient MPC under uncertainty. Different formulations involving Affine Disturbance Feedback, a parametrization of the control inputs, are developed and two different cases are investigated: in the first one, dealt with in Chapter 4, a chance-constrained problem with a stochastic disturbance having unbounded support is considered, whereas in the second one, treated in Chapter 5, hard constraints and a bounded disturbance are dealt with.

Chapter 4

The developments in Chapter 4 are motivated by the application of building climate control. We consider an uncertain linear system with polytopic constraints on the

inputs and chance constraints on the states that is subject to additive Gaussian disturbances. The proposed formulation combines the use of Affine Disturbance Feedback, a formulation successfully applied in robust control, with a tractable deterministic reformulation of the chance constraints. Different chance constraint reformulations are compared and analyzed on a small-scale example and a formulation which is tractable for large-scale systems, such as buildings, is developed. This method is investigated for application in building climate control in Chapter 7 of Part III.

Chapter 5

The use of Affine Disturbance Feedback goes along with an increase in decision variables. Chapter 5 deals with the problem of the high computational complexity of Affine Disturbance Feedback MPC problems for uncertain systems with hard constraints and bounded disturbances. So-called move-blocking is an effective method of reducing the computational complexity of MPC problems. Unfortunately, move-blocking precludes the use of terminal constraints as a means of enforcing strong feasibility of MPC problems. Hence, move-blocking MPC has traditionally been employed without rigorous guarantees of constraint satisfaction. An existing method for enforcing strong feasibility of nominal move-blocking MPC problems is generalized and employed for the purpose of enforcing strong feasibility of blocking Affine Disturbance Feedback robust MPC problems. Furthermore, the effectiveness of different Affine Disturbance Feedback blocking strategies is investigated by means of a numerical example.

Part III

Part III is concerned with investigations in building climate control. First, an overview of the OptiControl project and the definition of the simulation environment is given. Then, three topics are investigated in detail: use of weather predictions, use of occupancy information, and use of a dynamic electricity tariff.

Chapter 6

Chapter 6 explains the choices of the investigated building and HVAC systems and introduces the simulation environment. Within the framework of the OptiControl project, the project partners developed a Matlab-based simulation software for simulating different building types and HVAC-systems with different controllers and under different weather conditions. This software was used for obtaining the simulation results described in this thesis. In the first part of this chapter, the underlying assumptions, the

modeling approach, and the available simulation setups are introduced. In the second part of this chapter all control strategies and benchmarks are explained in detail and the implementation of MPC for building climate control is described.

Chapter 7

Chapter 7 deals with applying the developed methods introduced in Chapter 4 to building climate control and assessing their performance. First, alternative investigated control strategies and benchmarks are introduced and discussed, and the implementation of weather forecasts and MPC is explained in detail. Then the assessment procedure for the control strategies as well as the different investigations are introduced and finally, the results of the investigations are presented and discussed.

Chapter 8

In Chapter 8 the influence of occupancy information on building climate control is assessed. A model for generating occupancy and vacancy patterns is developed and evaluated with empirical data. The influence of occupancy information depending on different building types and occupancy patterns is then investigated by applying MPC and occupancy predictions. The results are compared to simple control strategies that account for occupancy based on instantaneous measurements. Different occupancy layouts are considered reflecting the heat transfer between building zones if these are not homogeneously occupied.

Chapter 9

Chapter 9 deals with the reduction of peak electricity demand in building climate control by adopting a dynamic electricity tariff and MPC. The use of a recently developed time-varying, hourly-based electricity tariff for end-consumers is proposed, that has been designed to truly reflect marginal costs of electricity provision, based on spot market prices as well as on electricity grid load levels. The electricity tariff can be readily included into the MPC cost function, however, since this electricity tariff is only available for a limited time window into the future, least-squares support vector machines for electricity tariff price forecasting are used to provide the MPC controller with the necessary estimated time-varying costs for the whole prediction horizon. In the given context, the dynamic tariff provides an economic incentive for the building controller to adjust control actions in case of high spot market electricity prices and high grid load levels, respectively. It can be shown that peak electricity demand

of buildings can be significantly reduced, which makes this study an example for the successful implementation of Demand Response in the field of building climate control.

1.2 Publications

The work presented in this thesis was done in close collaboration with various colleagues and is largely based on previous publications which are listed in the following.

Part II

Chapter 4 is based on the following publications:

F. Oldewurtel, C.N. Jones, A. Parisio, M. Morari
Stochastic Model Predictive Control for Energy Efficient Building Climate Control
Submitted to IEEE Transactions on Control Systems Technology.

A first part of the work was presented in the conference paper:

F. Oldewurtel, C.N. Jones, M. Morari
A tractable Approximation of Chance Constrained Stochastic MPC based on Affine Disturbance Feedback
IEEE Conference on Decision and Control, Cancun, Mexico, 2008, [OJM08].

Chapter 5 is based on the following publication:

F. Oldewurtel, R. Gondhalekar, C.N. Jones, M. Morari
Blocking Parameterizations for Improving the Computational Tractability of Affine Disturbance Feedback MPC Problems
IEEE Conference on Decision and Control, Shanghai, China, 2009, [OGJM09].

Part III

Chapter 7 is based on the following publications:

F. Oldewurtel, A. Parisio, C.N. Jones, D. Gyalistras, M. Gwerder, V. Stauch, B. Lehmann, M. Morari
Use of Model Predictive Control and Weather Predictions for Energy Efficient Building Climate Control
Energy Buildings, 45:15-27, February 2012, [OPJ+12].

The basic ideas and main results were presented in the following conference papers:

F. Oldewurtel, A. Parisio, C.N. Jones, M. Morari, D. Gyalistras, M. Gwerder, V. Stauch, B. Lehmann, K. Wirth
Energy Efficient Building Climate Control using Stochastic Model Predictive Control and Weather Predictions
American Control Conference, Baltimore, USA, 2010, [OPJ+10].

F. Oldewurtel, D. Gyalistras, M. Gwerder, C.N. Jones, A. Parisio, V. Stauch, B. Lehmann, M. Morari
Increasing Energy Efficiency in Building Climate Control using Weather Forecasts and Model Predictive Control
Clima - RHEVA World Congress, Antalya, Turkey, 2010, [OGG+10].

D. Gyalistras, M. Gwerder, F. Oldewurtel, C.N. Jones, M. Morari, B. Lehmann, K. Wirth, V. Stauch
Analysis of Energy Savings Potentials for Integrated Room Automation
Clima - RHEVA World Congress, Antalya, Turkey, 2010, [GGO+10].

Chapter 8 is based on the following publication:

F. Oldewurtel, D. Sturzenegger, M. Morari
Importance of Occupancy Information for Building Climate Control
Submitted to Applied Energy.

Chapter 9 is based on the following publication:

F. Oldewurtel, A. Ulbig, A. Parisio, G. Andersson, M. Morari
Reducing Peak Electricity Demand in Building Climate Control using Real-Time Pricing and Model Predictive Control
IEEE Conference on Decision and Control, Atlanta, USA, 2010, [OUP+10].

Part I

Background

2 Building Climate Control

This chapter gives a brief introduction to building climate control, a literature survey, and it summarizes the positioning of this work.

2.1 Introduction

Energy efficient management of building systems plays a major role in minimizing overall energy consumption and costs since, worldwide, the residential and commercial sectors use 2589 Mtoe (mega tonnes of oil equivalent) of energy, which accounts for almost 40% of final energy use in the world; and in European countries, 76% of this energy goes towards comfort control in buildings - *Heating, Ventilation, and Air Conditioning* (HVAC) [Lau08]. Because of the long lifespan of buildings and high cost of refurbishments, it is urgent to increase the energy efficiency of the existing HVAC systems, i.e. to reduce the energy use and utility costs while guaranteeing comfort for the buildings' occupants. A natural idea to reduce energy consumption is to further exploit low energy cost actuators and to make use of the thermal storage capacity of the building. For doing so, a plan of the upcoming boundary conditions for the building, in particular the weather, needs to be made.

Current control solutions for building climate control are based on so-called *Rule Based Controllers* (RBC). They provide control solutions by applying rules of the form "if *condition*, then *action*" and depend on a large number of threshold values and parameters that need to be defined in order to describe the conditions and actions. The performance of these controllers critically depends on the quality of the chosen parameters, whereas a good choice becomes more and more difficult in view of the growing complexity of HVAC systems and the desire to additionally integrate more information, e.g., weather forecasts.

Hence, there are two main drivers for looking into new control solutions for building climate control (in the following referred to as building control): first, the ability to use weather predictions in order to reduce the energy consumption of buildings and second, the ability to efficiently handle the increasingly complex HVAC systems and comfort requirements.

The reasons for *Model Predictive Control* (MPC) in buildings being rarely used until now are primarily the difficulties/costs of obtaining a model of an (individual) building that can be used in the MPC controller and the fact that energy costs played a minor role in the past compared to today. Using the energy savings potential of buildings by applying MPC has however become more realistic recently due to several developments: There is a drastic increase in computational power as well as the possibility to shift computations to external servers/clouds. The use of simulation tools in building planning is becoming standard and can help to obtain models for the MPC controller. The quality of weather predictions is increasing and hence their usefulness for building control. Energy costs are rising and finally, there is a desire to handle time-varying electricity prices, which MPC does in a straightforward manner.

2.2 Literature Survey

The use of disturbance predictions, in particular weather predictions, for building control has been investigated in several works [AOT07, BRM06, CZU03, GT85, GT05, HKLF05]. A link to the cited papers and a more extensive bibliography can be found on the OptiControl website [Opt11]. In these studies the predictive strategies are shown to be more efficient when compared to conventional, non-predictive strategies for thermal control of buildings. In [GT85] the authors compared different predictive controllers taking into account weather predictions with a non-predictive strategy for a solar domestic hot water system. The simulation results showed that in particular for a small storage tank, the predictive control strategies achieved a lower energy cost compared to the non-predictive strategy. In [HFK04a, HFK04b, HKLF05] the use of a short-term weather predictor based on observed weather data for the control of active and passive building thermal storage was explored. The predicted variables included ambient air temperature, relative humidity, and solar radiation. In [MBH$^+$09] the implementation of MPC for a chilled water plant was investigated. A predictive control strategy using a forecasting model of outdoor air temperature was investigated in [CZU03] for intermittently heated radiant floor heating systems. The experimental results showed that the predictive control strategy saved between 10% and 12% energy during the cold winter months compared to the existing conventional control strategy. In [SOCP11] the authors described the testing of MPC for a heating system on a real building in Prague. Energy savings in a predictive Integrated Room Automation (IRA) were investigated in [GT05]. The proposed model predictive strategy manipulated the passive thermal storage of the building based on predicted future disturbances while respecting comfort bounds for the room temperature. The predictive control outperformed the non-predictive control, because the room temperature could be kept within its comfort

bounds with minimum energy, i.e. low energy cost actuators were exploited as much as possible. The effect of automated blinds and lighting control on heating and cooling requirements were studied in [BRM06]; the authors investigated the reduction of the annual primary energy usage in building control for the case of Rome. In the study of [AOT07], the influence of occupant behavior on energy consumption was investigated in a single room occupied by one person. The simulated occupant could manipulate six controls, such as turning on or off the heat and adjusting clothing. The simulation results showed that occupant behavior significantly affects the energy consumption in the room.

In conclusion, from the literature it can be learned that predictive control strategies as well as including automated blinds and lighting in the control action provide potential benefits for energy efficient building control.

2.3 Positioning of the Work

The goal is to investigate how energy consumption in building control can be minimized while respecting comfort constraints. This section outlines the aspects of building control that this thesis focuses on.

The *comfort requirements* in a building address various aspects, the most important being room temperature, illuminance, and indoor air quality (IAQ); the latter usually referring to the CO_2-level. In order to achieve a comfortable room climate also other aspects play an important role, like humidity, air movement/velocity, or air stratification; and the requirements and perception of comfort vary clearly in between different persons. A comprehensive study on comfort is given in [Fan70]. In this thesis the consideration of comfort constraints is limited to temperature, illuminance, and CO_2. The definition of these comfort constraints is based on the building standard EN 15251 [EN 07].

The focus of this work is on office buildings, since they typically involve energy intensive HVAC systems and account for a large fraction of the energy consumption, which has been steadily increasing in the last years [LPL08]. Furthermore, offices have very distinct usage profiles. Comfort requirements apply when offices are occupied, i.e. during working days and during daytime, but on weekends and during the nights setbacks can be applied, i.e. the comfort constraints are relaxed. With conventional control strategies, the handling of these setbacks is quite difficult, whereas in MPC the time-varying constraints can be easily incorporated. Also, offices are usually equipped with more advanced *Building Management Systems* (BMS). A BMS is a computer-based control system installed in buildings, that controls and monitors the building's

HVAC, lighting, blind positioning, as well as fire and security systems. This can be favorable for using MPC, because more sensor data is available and/or there is more possibilities of actuation.

A BMS consists of both software and hardware and has, as defined according to the standard EN ISO 16484 [EN 04], a hierarchical topology consisting of three layers: the *management level*, the *automation level*, and the *field level*. The control is usually split from a functional point of view into two layers: high-level control and low-level control. The high-level controller determines setpoints and modes whereas the low-level controller simply tracks the set-points given by the corresponding high-level controller. In this thesis new control strategies for high-level control are investigated. This is because the task of high-level control is very complex giving room for improvement for advanced strategies that properly take into account the different sources of information, in particular predictions about weather and occupancy.

Fire and security have traditionally been treated separately from the control of HVAC, although their integration might be beneficial in future implementations in terms of taking into account the information about occupancy available from the security system in the control of the HVAC system. In this work, the primary interest is in the energy savings potential and ability to reduce peak electricity demands, therefore, the focus is set on HVAC, lighting, and blind positioning.

The considered application is *Integrated Room Automation* (IRA). IRA deals with the automated control of heating, ventilation, air-conditioning, blind positioning, and electric lighting of a room or building zone [BK04]. It is mainly used in office buildings and its advantages are twofold. It provides high comfort since the comfort requirements are addressed room-wise. And it is generally considered to be energy efficient since it automatically adapts the energy input to the individual room requirements and can therefore prevent unnecessary energy input in case of vacancies. IRA is hence seen as the most promising automation setup for energy efficient building control and high user comfort [BK04].

Building dynamics are slow and the building is subject to intermittent disturbances, i.e. the weather as well as the building's appliances and occupants, who generate heat, CO_2, and set demands for temperature, illuminance, and air quality. This gives rise to a constrained control problem (because of the occupants' comfort requirements as well as the limited capacity of the actuators) and the aim is to use weather predictions in order to efficiently use the thermal storage capacity of the building. MPC is an ideal framework to tackle this problem and is investigated for the use in building control in this thesis.

To summarize the positioning of this work in building control, the control of office buildings is considered; the considered comfort constraints are on temperature, illu-

minance, and CO_2; the high-level control is addressed; and the IRA application is considered. The goal is to investigate the energy savings potential of applying MPC together with weather and occupancy predictions in building control as well as to investigate the potential to reduce the peak electricity demands when applying MPC with a dynamic electricity tariff.

3 Model Predictive Control for Building Climate Control

This chapter consists of two parts, the first part deals with some mathematical preliminaries and the second part discusses MPC, in particular in view of applying it to building climate control.

The mathematical definitions given in this thesis are all standard and can be found for example in [Bla99, Ker00, Roc70]. More information on MPC can be found in [RM09, Mac02, ML99, GPM89] and the references therein.

3.1 Mathematical Preliminaries

3.1.1 Set Theory

Definition 3.1 (Convex set). A set $\mathcal{S} \subseteq \mathbb{R}^{n_s}$ is *convex* if the line segment connecting any pair of points of $\mathcal{S}$ lies entirely in $\mathcal{S}$, i.e.

$$s_1, s_2 \in \mathcal{S}, \quad 0 \leq \kappa \leq 1 \quad \Rightarrow \quad \kappa s_1 + (1-\kappa) s_2 \in \mathcal{S} \ . \tag{3.1}$$

Definition 3.2 (Affine set). A set $\mathcal{S} \subseteq \mathbb{R}^{n_s}$ is *affine* if

$$\alpha s_1 + (1-\alpha) s_2 \in \mathcal{S} \text{ for any } s_1, s_2 \in \mathcal{S} \text{ and } \alpha \in \mathbb{R} \ . \tag{3.2}$$

Definition 3.3 (ϵ-ball). The open n_x-dimensional ϵ-ball in $\mathbb{R}^{n_x}$ around a given (center) point $x_c \in \mathbb{R}^{n_x}$ is the set

$$\mathcal{B}_\epsilon(x_c) := \{x \in \mathbb{R}^{n_x} |\ \|x - x_c\| < \epsilon\} \ , \tag{3.3}$$

where the radius $\epsilon > 0$ and $\|\cdot\|$ denotes any vector norm (most commonly the Euclidean vector norm $\|\cdot\|_2$).

Definition 3.4 (Closed set). A set $\mathcal{S} \subseteq \mathbb{R}^{n_s}$ is *closed* if every point not in $\mathcal{S}$ has a neighborhood disjoint from $\mathcal{S}$, i.e.

$$\forall x \notin \mathcal{S}, \ \exists\ \epsilon > 0 \ \text{ such that } \ \mathcal{B}_\epsilon(x) \cap \mathcal{S} = \emptyset \ . \tag{3.4}$$

Definition 3.5 (Bounded set). A set $\mathcal{S} \subseteq \mathbb{R}^{n_s}$ is *bounded* if it is contained inside some ball $\mathcal{B}_r(\cdot)$ of finite radius r, i.e.

$$\exists\, r < \infty,\ s \in \mathbb{R}^{n_s} \ \text{ such that } \ \mathcal{S} \subseteq \mathcal{B}_r(s)\ . \tag{3.5}$$

Definition 3.6 (Compact set). A set $\mathcal{S} \subseteq \mathbb{R}^{n_s}$ is *compact* if it is closed and bounded.

3.1.2 System and Control Theory

Definition 3.7 (Discrete-time system).

$$x_{t+1} = Ax_t + Bu_t + Ew_t \qquad \text{Linear time invariant (LTI)} \tag{3.6}$$

$$x_{t+1} = Ax_t + Bu_t + Vv_t + Ew_t \qquad \text{LTI with external input} \tag{3.7}$$

with time step $t \in \mathbb{N}$, system state $x_t \in \mathbb{R}^{n_x}$, control input $u_t \in \mathbb{R}^{n_u}$, disturbance $w_t \in \mathbb{R}^{n_w}$, and external input $v_t \in \mathbb{R}^{n_v}$.

Definition 3.8 (Constrained system). A discrete-time system is a *constrained system* if state and/or control inputs are constrained to sets,

$$u_t \in \mathbb{U} \subset \mathbb{R}^{n_u}\ , \tag{3.8}$$

$$x_t \in \mathbb{X} \subset \mathbb{R}^{n_x}\ . \tag{3.9}$$

If the sets are time-varying, this is denoted by $\mathbb{U}_t$ and $\mathbb{X}_t$, respectively.

Assumption 3.9. It is assumed that $\mathbb{U}$ is compact, $\mathbb{X}$ is compact, and both of the sets contain the origin.

Definition 3.10 (Disturbance set). For bounded disturbances w the *disturbance set* $\mathbb{W}$ is defined by

$$w_t \in \mathbb{W} \subset \mathbb{R}^{n_w}\ . \tag{3.10}$$

Assumption 3.11. It is assumed that $\mathbb{W}$ is compact and contains the origin.

Definition 3.12 (Probabilistic constrained system). A discrete-time system is a *probabilistic constrained system* if state and/or control inputs are constrained to sets with a predefined probability,

$$\Pr\left[u_t \in \mathbb{U}\right] \quad \geq \quad 1 - \alpha_u\ , \tag{3.11}$$

$$\Pr\left[x_t \in \mathbb{X}\right] \quad \geq \quad 1 - \alpha_x\ , \tag{3.12}$$

where $\alpha_u \in (0,1)$ and $\alpha_x \in (0,1)$ denote the *probability level of constraint violation* for the input and state constraints, respectively. These probabilistic constraints are also called *chance constraints*.

Definition 3.13 (Individual chance constraint). A (linear) *individual chance constraint* is of the form

$$\Pr\left[G_{(i)}x_t \leq g_{(i)}\right] \quad \geq \quad 1-\alpha_{x,i} \quad \forall i \in \mathbb{N}_1^r \ , \tag{3.13}$$

where $G \in \mathbb{R}^{r\times n_x}$, $g \in \mathbb{R}^r$, $\alpha_{x,i} \in (0,1)$ $\forall i$, and $G_{(i)}$ and $g_{(i)}$ denote the row i of G and g, respectively. This means each row i of the inequality has to be fulfilled individually with the respective probability $1-\alpha_{x,i}$.

Definition 3.14 (Joint chance constraint). A (linear) *joint chance constraint* is of the form

$$\Pr\left[G_{(i)}x_t \leq g_{(i)},\ i \in \mathbb{N}_1^r\right] \quad \geq \quad 1-\alpha_x \ , \tag{3.14}$$

where $G \in \mathbb{R}^{r\times n_x}$, $g \in \mathbb{R}^r$, $\alpha_x \in (0,1)$, and $G_{(i)}$ and $g_{(i)}$ denote the row i of G and g, respectively. This means that all rows i jointly have to be fulfilled with the probability $1-\alpha_x$.

Remark 3.15 (Individual chance constraint and Gaussian uncertainty). Consider the following individual chance constraint

$$\Pr\left[w^T x_t \leq b\right] \quad \geq \quad 1-\alpha \ , \tag{3.15}$$

where $w \in \mathbb{R}^{n_x}$, $b \in \mathbb{R}$ and $w \sim \mathcal{N}(\bar{w}, \Sigma)$. Hence $w^T x_t - b \sim \mathcal{N}(\bar{w}^T x_t - b, x_t^T \Sigma x_t)$ and $\Pr\left[w^T x_t \leq b\right] = \Phi\left(\frac{b-\bar{w}^T x_t}{\sqrt{x_t^T \Sigma x_t}}\right)$. This yields

$$\Pr\left[w^T x_t \leq b\right] \quad \geq \quad 1-\alpha \tag{3.16}$$

$$\Leftrightarrow \qquad b - \bar{w}^T x_t \quad \geq \quad \Phi^{-1}(1-\alpha)\|\Sigma^{1/2}x_t\|_2 \ , \tag{3.17}$$

where Φ is the standard cumulative distribution function and its inverse Φ^{-1} is the quantile function. For a probability of violation $\alpha \in (0, 0.5]$ (i.e. $\Phi^{-1}(1-\alpha) \geq 0$) (3.17) is a second order cone constraint (see Section 3.2). This means for the case of Gaussian uncertainty and probability level $\alpha \in (0, 0.5]$ the chance constraint in (3.15) has a deterministic equivalent in the form of a second order cone constraint.

Definition 3.16 (Positive invariant (PI) set). A set $\mathcal{X} \subset \mathbb{R}^{n_x}$ is a *positive invariant* (PI) set for $x_{t+1} = Ax_t$, if $Ax_t \in \mathcal{X}$ for all $x_t \in \mathcal{X}$.

Definition 3.17 (Robust positive invariant (RPI) set). A set $\mathcal{X} \subset \mathbb{R}^{n_x}$ is a *robust positive invariant* (RPI) set for $x_{t+1} = Ax_t + Ew_t$, if $Ax_t + Ew_t \in \mathcal{X}$ for all $x_t \in \mathcal{X}$ and for all $w_t \in \mathbb{W}$.

Definition 3.18 (Controlled invariant (CI) set). A set $\mathcal{X} \subset \mathbb{R}^{n_x}$ is a *controlled invariant* (CI) set for $x_{t+1} = Ax_t + Bu_t$, $u_t \in \mathbb{U}$, if $\exists\ u_t$ such that $Ax_t + Bu_t \in \mathcal{X}$ and $u_t \in \mathbb{U}$ for all $x_t \in \mathcal{X}$.

Definition 3.19 (Maximum controlled invariant (MCI) set). The *maximum controlled invariant* (MCI) set for $x_{t+1} = Ax_t + Bu_t$ is the set $\mathcal{X} \subset \mathbb{R}^{n_x}$, which is controlled invariant according to Definition 3.18, and furthermore such that every other set that is controlled invariant according to Definition 3.18 is a subset of $\mathcal{X}$.

Definition 3.20 (Robust controlled invariant (RCI) set). A set $\mathcal{X} \subset \mathbb{R}^{n_x}$ is a *robust controlled invariant* (RCI) set of system $x_{t+1} = Ax_t + Bu_t + Ew_t$, if $\exists\ u_t$, such that $Ax_t + Bu_t + Ew_t \in \mathcal{X}$ and $u_t \in \mathbb{U}$ for all $x_t \in \mathcal{X}$ and for all $w_t \in \mathbb{W}$.

Definition 3.21 (Maximum robust controlled invariant (MRCI) set). The *maximum robust controlled invariant* (MRCI) set for $x_{t+1} = Ax_t + Bu_t + Ew_t$ is the set $\mathcal{X} \subset \mathbb{R}^{n_x}$, which is robust controlled invariant according to Definition 3.20, and furthermore such that every other set that is robust controlled invariant according to Definition 3.20 is a subset of $\mathcal{X}$.

3.2 Receding Horizon Control

Receding Horizon Control (RHC) or, interchangeably called, Model Predictive Control (MPC) is an intuitive approach to constrained control that has been successfully applied in many areas over the last decades [Mac02, RM09].

As necessary ingredients, a *model* of the system is needed, most commonly in the form of a discrete-time LTI system

$$x_{t+1} = Ax_t + Bu_t \ , \tag{3.18}$$

as well as the definition of the *constraints*

$$u_t \in \mathbb{U} \tag{3.19}$$

$$x_t \in \mathbb{X} \ . \tag{3.20}$$

At every discrete time instant t, a *measurement* x_t of the state is taken, the system's evolution over a finite *prediction horizon* N is formulated based on the model, and an

optimization problem is solved according to some optimality criterion and subject to the constraints.

In order to distinguish in the following between the *prediction* of a state and the *actual* state, denote with $x_{t+k|t} \in \mathbb{R}^{n_x}$ the prediction for the actual state $x_{t+k} \in \mathbb{R}^{n_x}$ at time t, where $k \in \mathbb{N}_0^N$. Furthermore, vectors (and matrices) that contain all predictions of a variable along the prediction horizon are denoted with bold letters, i.e. $\mathbf{x}_t := \{x_{t|t}, x_{t+1|t}, \ldots, x_{t+N|t}\}$ denotes an ordered collection of the vectors $x_{t+k|t}$, which for ease of notation is considered to be a large stacked-up vector $\mathbf{x}_t \in \mathbb{R}^{(N+1)n_x}$ when used in algebraic expressions. The same notation is adopted for predicted inputs and predicted disturbances throughout this thesis.

The result of the optimization problem is an optimal trajectory of inputs and states into the future satisfying the dynamics and constraints of the system while optimizing the given criterion. The optimal input sequence

$$\mathbf{u}_t^*(x_t) := \{u_{t|t}^*, u_{t+1|t}^*, ..., u_{t+N-1|t}^*\} \tag{3.21}$$

is available, however, only the input of the first time step $u_{t|t}^*$ is applied to the system and the rest is discarded.

Remark 3.22. Instead of optimizing over input sequences one can also optimize over control laws, i.e. functions of previous states or disturbances. The formulation of control laws is also used in this thesis. For ease of notation the basic setup is explained for input sequences here. The formulation with control laws is discussed in Section 3.2.4.

In order to compensate for modeling errors and/or disturbances, a new measurement is taken at the next time step $t+1$ and the whole procedure is repeated with the prediction horizon shifted by one time step. This receding horizon approach is what introduces feedback to the system, since the new finite optimal control problem solved at the beginning of the next time step is a function of the new state at that point in time and hence of any disturbances that have meanwhile acted on the system. The procedure is summarized in the following algorithm.

Algorithm 1 Receding horizon control

1. measure the state x_t at time t
2. obtain $\mathbf{u}_t^*(x_t) := \{u_{t|t}^*, u_{t+1|t}^*, ..., u_{t+N-1|t}^*\}$ by solving an optimization problem with horizon N
3. apply the first element $u_{t|t}^*$ to the system
4. proceed to time step $t+1$
5. go to 1.

3.2.1 MPC for Building Climate Control

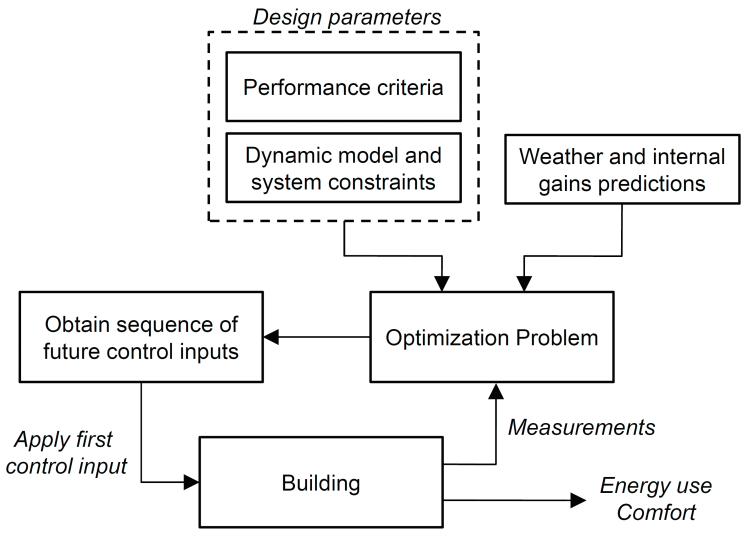

Figure 3.1: MPC scheme for building climate control.

In building control, the procedure is as follows: At the current point in time a heating-/cooling-, etc. plan is formulated for the next several hours to days based on predictions of the upcoming weather conditions, see Figure 3.1. Predictions of any other disturbances (e.g., internal gains), time-dependencies of the control costs (e.g., dynamic electricity prices), or of the constraints (e.g., thermal comfort range) can be readily included in the optimization. The first step of the control plan is applied to the building, determining the setting of all the heating, cooling, and ventilation actuators, then the process is repeated at the next time instant.

A generic MPC framework is given by the following finite-horizon optimal control problem.

Problem 3.23 (Generic MPC problem).

$$J^*(x_t) = \min_{u_{t|t},\dots,u_{t+N-1|t}} \quad V_f(x_{t+N|t}) + \sum_{k=0}^{N-1} l_k(x_{t+k|t}, u_{t+k|t}) \quad \text{Cost function} \tag{3.22}$$

subject to

$$(x_{t+k|t}, u_{t+k|t}) \in \mathbb{X} \times \mathbb{U} \quad \text{Constraints} \tag{3.23}$$

$$x_{t+N|t} \in \mathbb{X}_f \quad \text{Terminal constraint} \tag{3.24}$$

$$x_{t|t} = x_t \quad \text{Current state} \tag{3.25}$$

$$x_{t+k+1|t} = Ax_{t+k|t} + Bu_{t+k|t} \quad \text{Dynamics} \tag{3.26}$$

where N is the prediction horizon, $k \in \mathbb{N}_0^{N-1}$ is the prediction time step, $l_k : \mathbb{R}^{n_x} \times \mathbb{R}^{n_u} \to \mathbb{R}_{+0}$ is the *stage cost*, and $V_f : \mathbb{R}^{n_x} \to \mathbb{R}_{+0}$ is the *terminal cost*.

$$u_{t+k|t} \in \mathbb{U} \subset \mathbb{R}^{n_u} \tag{3.27}$$

$$x_{t+k|t} \in \mathbb{X} \subset \mathbb{R}^{n_x} \ , \tag{3.28}$$

i.e. we have a constrained system according to Definition 3.8, $\mathbb{U}$ and $\mathbb{X}$ satisfy Assumption 3.9, and

$$\mathbb{X}_f \subseteq \mathbb{X} \tag{3.29}$$

denotes some terminal region that contains the origin.

Definition 3.24. The *closed-loop state trajectory* is described by

$$x_{t+1} = Ax_t + Bu^*_{t|t}(x_t) \ , \tag{3.30}$$

where the optimal control input $u^*_{t|t}$ is obtained at each time step by solving MPC Problem 3.23.

The *cost function* and the *constraints* are the main pieces of the MPC design, the *dynamics* of the system have to be modeled to a reasonable precision such that a good control performance is achieved, and the *current state* is used as the initial state for predicting the future system evolution. In the following, a brief explanation of each of the four components in the above MPC formulation is provided with comments on their significance in building control.

Cost function

The cost function describes the desired behavior. This generally serves two purposes:

- *Stability.* The cost function is chosen such that (under some additional assumptions) the optimal cost function $J^*(\cdot)$ in Problem 3.23 is a Lyapunov function and stability can be guaranteed [MRRS00a]. In practice, this requirement is generally relaxed for stable systems with slow dynamics, such as buildings, which leaves the designer free to select the cost strictly on a performance basis.
- *Performance target.* The cost is generally, but not always, used to specify a preference for one closed-loop behavior over another, in building control, e.g., minimizing energy or maximizing comfort.

Several common cost functions are in use, the majority of which are convex, which results in a simple optimization problem to solve. Some common choices, which are also listed in Table 3.1, are:

Table 3.1: Common types of cost functions.

Cost function type	Mathematical description
Quadratic cost	$l_k(x_{t+k\|t}, u_{t+k\|t}) = x_{t+k\|t}^T Q x_{t+k\|t} + u_{t+k\|t}^T R u_{t+k\|t}$
	$V_f(x_{t+N\|t}) = x_{t+N\|t}^T P x_{t+N\|t}$
Linear norm cost	$l_k(x_{t+k\|t}, u_{t+k\|t}) = \|Q x_{t+k\|t}\|_p + \|R u_{t+k\|t}\|_p$
	$V_f(x_{t+N\|t}) = \|Px\|_p,\ p \in \{1, \infty\}$

- *Quadratic cost.* The relative weighting between the states and the inputs, i.e. the choice of the matrices $Q \succeq 0$ and $R \succ 0$ provides a trade-off between regulation quality and input energy. If the system has no constraints, or the constraints are not active, then for a given Q and R this cost is equivalent to the cost of finite-horizon, discrete-time LQR/LQG.

  In the context of building control, such a cost is used if MPC is implemented as a low-level controller for tracking setpoints given by some high-level controller.
- *Linear norm cost.* If one wishes to minimize 'amounts', outliers, or economically motivated signals, then the linear norm cost function is more suitable than the quadratic one. Using a 1-norm cost would also be a common choice for minimizing energy consumption of buildings.

Constraints

The ability to specify constraints in the MPC formulation and have the optimization routine handle them directly is the key strength of the MPC approach. Many different types of constraints are used in practice, an overview of common types suitable for building control is given in Table 3.2.

- *Linear constraint.* This is the most common type of constraint and is used to put upper and/or lower bounds on variables. Linear constraints are the easiest to handle when solving optimization problems and can also be used to approximate any convex constraint to an arbitrary degree of accuracy.
- *Convex quadratic constraint.* This type of constraint is used to bound a variable to lie within an ellipsoid. In building control, this type of constraint would arise, e.g., when formulating a bound on the total input energy produced by several actuators.
- *Chance constraint.* If uncertainty is involved in the problem, this type of constraint is used to formulate that some condition has to be fulfilled with a predefined probability, see also Definitions 3.12-3.14. Since an optimization problem

can only be solved if all variables are deterministic, chance constraints need to be reformulated into deterministic constraints.

- *Second order cone constraint.* Second order cone constraints can - under special circumstances - result from reformulations of chance constraints (see Remark 3.15). For $A = \mathbf{0}$ the constraint collapses to a linear constraint, for $C = \mathbf{0}$ to a convex quadratic constraint.
- *Switched constraint.* This type of constraint comprises a set of constraints, where each one is relevant only if a predefined condition is met. This is a common type of constraint in hybrid systems, i.e. systems that exhibit both continuous and discrete time behavior.
- *Non-linear constraint.* This type of constraint comprises any type of constraint that does not fit into the above categories, where $h(x_{t+k|t})$ can be any nonlinear function. In general, it is very difficult to handle this type of constraint when solving optimization problems.

Table 3.2: Common types of constraints. Note that constraints on the state $x_{t+k|t}$ are listed here for illustrative purposes, but can also be applied to input $u_{t+k|t}$ or as mixed constraints to both state $x_{t+k|t}$ and input $u_{t+k|t}$.

Constraint type	**Mathematical description**
Linear constraint	$Ax_{t+k\|t} \leq b$
Convex quadratic constraint	$(x_{t+k\|t} - \bar{x})^T Q(x_{t+k\|t} - \bar{x}) \leq 1 \ , \ \ Q \succeq 0$
Chance constraint	$\Pr\left[Ax_{t+k\|t} \leq b\right] \geq 1 - \alpha \ , \ \ \alpha \in (0,1)$
Second order cone constraint	$\|Ax_{t+k\|t} + b\|_2 \leq Cx_{t+k\|t} + d$
Switched constraint	if *condition*, then $A_1 x_{t+k\|t} \leq b_1$ else $A_2 x_{t+k\|t} \leq b_2$
Nonlinear constraint	$h(x_{t+k\|t}) \leq 0$

Current state

The system model is initialized with the current (measured or estimated) state of the building and all future predictions begin from the system in this initial state. If some states cannot be measured, but are observable, a Kalman filter would commonly be used for state estimation.

Dynamics

The system model is a critical piece of the MPC controller, since the control performance depends on the quality of the model.

In the following some definitions are given which are useful for discussing properties of MPC formulations.

Definition 3.25 (Feasible set). For an MPC problem, denote with $\mathbb{X}_0 \subseteq \mathbb{X}$ the set of initial states $x_{t|t}$ for which the MPC problem is feasible, i.e.

$$\begin{aligned}\mathbb{X}_0 := \{x_{t|t} \in \mathbb{R}^{n_x} | \ \exists \ \{u_{t|t}, ..., u_{t+N-1|t}\} \text{ such that } x_{t+k|t} \in \mathbb{X}, \ u_{t+k|t} \in \mathbb{U}, \ k \in \mathbb{N}_0^{N-1}, \\ x_{t+N|t} \in \mathbb{X}_f, \text{ where } x_{t+k+1|t} = Ax_{t+k|t} + Bu_{t+k|t}, \ k \in \mathbb{N}_0^{N-1}\} \ . \end{aligned} \tag{3.31}$$

Furthermore, denote with $\mathbb{X}_i$ the set of states $x_{t+i|t}$ at time $t+i$ for which the MPC problem is feasible, i.e.

$$\begin{aligned}\mathbb{X}_i := \{x_{t+i|t}\mathbb{R}^{n_x} | \ \exists \ \{u_{t+i|t}, ..., u_{t+N-1|t}\} \text{ such that } x_{t+k|t} \in \mathbb{X}, \ u_{t+k|t} \in \mathbb{U}, \ k \in \mathbb{N}_i^{N-1}, \\ x_{t+N|t} \in \mathbb{X}_f, \text{ where } x_{t+k+1|t} = Ax_{t+k|t} + Bu_{t+k|t}\} \ . \end{aligned} \tag{3.32}$$

Definition 3.26 (Admissible). A control input, sequence, or law is called *admissible* if it satisfies the input constraints. The elements of an *admissible* disturbance sequence are contained in $\mathbb{W}$.

Definition 3.27 (Strongly feasible). An MPC problem is *strongly feasible* if *from every* feasible state the closed-loop state trajectory *due to any* sequence of feasible solutions and due to *any* admissible disturbances remains within the feasible set.

Definition 3.28 (Least restrictive). A *least-restrictive* strongly feasible MPC problem is one such that there exists no strongly feasible MPC problem with a larger feasible set, for the same system and constraints.

In the following the most important formulations of MPC problems that are relevant for understanding the control options discussed in this thesis are introduced.

3.2.2 Nominal MPC

Consider the following LTI system

$$x_{t+1} = Ax_t + Bu_t \ . \tag{3.33}$$

The aim is to minimize the sum of all stage costs $l_k(\cdot)$ and the terminal cost $V_f(\cdot)$ subject to some polytopic constraints

$$u_t \in \mathbb{U} := \{u \in \mathbb{R}^{n_u} \mid Su \leq s\} \quad \forall t \in \mathbb{N} \tag{3.34}$$

$$x_t \in \mathbb{X} := \{x \in \mathbb{R}^{n_x} \mid Gx \leq g\} \quad \forall t \in \mathbb{N} \ . \tag{3.35}$$

In *Nominal MPC*, there is no disturbance in the system dynamics. It is formulated as follows.

Problem 3.29 (Nominal MPC).

$$J_{\mathrm{n}}^*(x_t) = \min_{u_{t|t},\dots,u_{t+N-1|t}} V_f(x_{t+N|t}) + \sum_{k=0}^{N-1} l_k(x_{t+k|t}, u_{t+k|t}) \tag{3.36}$$

subject to

$$x_{t+k|t} \in \mathbb{X}, \quad u_{t+k|t} \in \mathbb{U} \qquad \forall k \in \mathbb{N}_0^{N-1} \tag{3.37}$$

$$x_{t+N|t} \in \mathbb{X}_f \tag{3.38}$$

$$x_{t+k+1|t} = Ax_{t+k|t} + Bu_{t+k|t} \qquad x_{t|t} = x_t \ . \tag{3.39}$$

Remark 3.30. The terminal constraint set $\mathbb{X}_f$ and the terminal cost $V_f(x_{t+N|t})$ can be chosen such that the constraint satisfaction of the finite-horizon problem ensures the existence of a feasible solution of Problem 3.29 at the next time instant (known as recursive feasibility [RM09]) and hence the constraints can be satisfied for all times as required in (3.34)-(3.35).

The nominal MPC problem (Problem 3.29) is equal to the generic MPC problem (Problem 3.23). In the absence of uncertainty, the optimal control for a given initial state can be either computed by open-loop optimal control or by using dynamic programming, which provides closed-loop control laws [RM09]. The difference between these two options is explained below; it is worth noting that these two solutions coincide in the absence of uncertainty.

3.2.3 Deterministic MPC/ Certainty Equivalence MPC

Consider some additive disturbance in the system, which can originate both from external disturbances or from model inaccuracies, i.e.

$$x_{t+1} = Ax_t + Bu_t + Ew_t \ , \tag{3.40}$$

where $w_t \in \mathbb{R}^{n_w}$ denotes the disturbance. In *Deterministic MPC* (DMPC) or *Certainty Equivalence MPC* the disturbance is simply neglected and the nominal problem in (3.29) is solved, i.e. the nominal prediction is taken as 'equal to certain'.

Remark 3.31. This formulation is computationally very attractive since it has the same number of decision variables as the nominal MPC problem. It is used in the presented investigation in building control as a benchmark.

Whereas for systems with small uncertainties this can be acceptable due to the feedback introduced by the receding horizon approach, for systems with large uncertainties the proper treatment of uncertainties in the controller is important for a good control performance. Traditionally, the most common way to handle uncertainties in the controller is to apply *Robust MPC*.

3.2.4 Robust MPC

In Robust MPC the uncertainty is assumed to be bounded and to lie in some a priori known uncertainty set, $w_t \in \mathbb{W} \subset \mathbb{R}^{n_w}$, and the constraints are tightened in order to achieve constraint satisfaction for all possible realizations of the uncertainty along the horizon. There are three main cost functions which are typically applied: the *nominal cost* as in (3.29), the *min-max cost* (worst case cost) and (less commonly) the *expected value cost*. In the following, the difference between open-loop and closed-loop robust MPC is explained for the frequently applied min-max formulation, but the principle also holds for the other two cost functions.

In min-max robust MPC, the worst-case performance is minimized subject to the satisfaction of constraints for all possible realizations of the disturbance. In open-loop robust MPC the formulation looks as follows.

Problem 3.32 (Open-loop min-max MPC).

$$J_{\mathrm{o}}^*(x_t) := \min_{u_{t|t},\dots,u_{t+N-1|t}} \max_{w_{t|t},\dots,w_{t+N-1|t}} V_f(x_{t+N|t}) + \sum_{k=0}^{N-1} l_k(x_{t+k|t}, u_{t+k|t}) \tag{3.41}$$

subject to

$$x_{t+k|t} \in \mathbb{X}\ , \quad u_{t+k|t} \in \mathbb{U} \qquad \forall k \in \mathbb{N}_0^{N-1} \tag{3.42}$$

$$x_{t+N|t} \in \mathbb{X}_f \tag{3.43}$$

$$x_{t+k+1|t} = Ax_{t+k|t} + Bu_{t+k|t} + Ew_{t+k|t} \qquad x_{t|t} = x_t \tag{3.44}$$

$$w_{t+k|t} \in \mathbb{W} \qquad \forall k \in \mathbb{N}_0^{N-1}\ . \tag{3.45}$$

This formulation is based on open-loop predictions and can be viewed as a zero-sum dynamic game between two players, the controller and the disturbance. The controller plays first and has to choose its action over the whole prediction horizon $\{u_{t|t}, ..., u_{t+N-1|t}\}$, then the controller reveals its plan and the disturbance chooses its actions about the whole prediction horizon $\{w_{t|t}, ..., w_{t+N-1|t}\}$. This means that when choosing its action a priori, the controller has to consider the worst-case disturbance at every future time-step, so the uncertainty quickly grows over the prediction horizon and may lead to infeasibility of the minimization problem, especially for large disturbance sets. To overcome this, feedback should be taken into account, i.e. the controller has a measurement of the state after each control move and can adjust the future actions accordingly, which would be equivalent to playing one move at a time. This behavior is considered in closed-loop min-max MPC, which is formulated with Bellman's recursion as follows.

Problem 3.33 (Closed-loop min-max MPC).

$$J_{\mathrm{c}}^*(k, x_{t+k|t}) := \min_{u_{t+k|t}} J_{\mathrm{c}}(k, x_{t+k|t}, u_{t+k|t}) \tag{3.46}$$

subject to

$$x_{t+k|t} \in \mathbb{X}, \quad u_{t+k|t} \in \mathbb{U} \tag{3.47}$$

$$Ax_{t+k|t} + Bu_{t+k|t} + Ew_{t+k|t} \in \mathbb{X}_{k+1} \tag{3.48}$$

$$w_{t+k|t} \in \mathbb{W} \ , \tag{3.49}$$

where the cost at each step is defined as

$$J_{\mathrm{c}}(k, x_{t+k|t}, u_{t+k|t}) := \max_{w_{t+k|t} \in \mathbb{W}} \ l_k(x_{t+k|t}, u_{t+k|t}) + J_{\mathrm{c}}^*(k+1, Ax_{t+k|t} + Bu_{t+k|t} + Ew_{t+k|t})$$

for $k \in \mathbb{N}_0^{N-2}$ and with boundary conditions $J_{\mathrm{c}}^*(N, x_{t+N|t}) = V_f(x_{t+N|t})$ and $\mathbb{X}_N = \mathbb{X}_f$.

Remark 3.34. If we have a time-invariant state constraint set $\mathbb{X}$, $\mathbb{X}_{k+1} = \mathbb{X} \ \forall \ k \in \mathbb{N}_0^{N-1}$ and $\mathbb{X}_{k+1} = \mathbb{X}_f$ for $k = N-1$ to ensure that the final state is in the terminal set.

Remark 3.35. If future uncertainties were perfectly known, i.e. a perfect prediction of future uncertainties were given and hence no uncertainties left, this problem would result in a nominal MPC problem (with adjusted predictions), which could be solved and would give a bound on the performance. However, such information is non-causal, therefore Problem 3.33 constitutes a theoretical benchmark. This benchmark, also called *performance bound*, is used in the presented investigations in building control as a measure of how far away from the (theoretical) optimal solution a given controller is. More specifically, it is used to compute the controller performance that would be achievable if a perfect weather prediction was available.

The above dynamic programming problem can also be formulated in the usual MPC notation using *policies* instead of open loop control sequences as optimization variables. The first state $x_t = x_{t|t}$ is measured, however, the predicted states $x_{t+1|t}, ..., x_{t+N|t}$ are uncertain. The goal is to address this uncertainty in the MPC formulation. To do this, consider for predicted control inputs $u_{t+1|t}$ to $u_{t+N|t}$ a causal state feedback controller, or equivalently, a causal disturbance feedback controller, which takes into account feedback of the predicted states up to prediction time step k or feedback of the predicted disturbances up to prediction time step $k-1$,

$$u_{t+k|t} = \phi_{t+k|t}(x_{t+1|t}, ..., x_{t+k|t}) = \mu_{t+k|t}(w_{t|t}, ..., w_{t+k-1|t}) \ . \tag{3.50}$$

Remark 3.36. The feedback controller is called *causal* since it strictly depends on the states (or disturbances) that have already been realized at the time when the corresponding predicted control input will be applied.

Remark 3.37. It is equivalent to consider feedback of states and feedback of disturbances if the states can be measured, since the disturbances can be straightforwardly computed with given states and known inputs and the other way around. Note that for this to hold, feedback of the states from prediction time step 1 to k is considered but feedback of the disturbances from prediction time step 0 to $k-1$.

When using disturbance feedback, the min-max problem can be written as follows.

Problem 3.38 (Min-max MPC with policies).

$$J_{\mathrm{p}}^*(x_t) := \min_{\boldsymbol{\mu}} \max_{w_{t|t},\dots,w_{t+N-1|t}} V_f(x_{t+N|t}) + \sum_{k=0}^{N-1} l_k(x_{t+k|t}, u_{t+k|t}) \tag{3.51}$$

subject to

$$x_{t+k|t} \in \mathbb{X}\ , \quad u_{t+k|t} \in \mathbb{U} \qquad \forall k \in \mathbb{N}_0^{N-1} \tag{3.52}$$

$$x_{t+N|t} \in \mathbb{X}_f \tag{3.53}$$

$$u_{t+k|t} = \mu_{t+k|t}(w_{t|t}, \dots, w_{t+k-1|t}) \qquad \forall k \in \mathbb{N}_1^{N-1} \tag{3.54}$$

$$x_{t+k+1|t} = Ax_{t+k|t} + Bu_{t+k|t} + Ew_{t+k|t} \qquad x_{t|t} = x_t \tag{3.55}$$

$$w_{t+k|t} \in \mathbb{W} \qquad \forall k \in \mathbb{N}_0^{N-1}\ , \tag{3.56}$$

where $\boldsymbol{\mu} := [u_{t|t}^T \ \ \mu_{t+1|t}(w_{t|t})^T \ \ \dots \ \ \mu_{t+N-1|t}^T(w_{t|t}, \dots, w_{t+N-2|t})]^T$ is the optimization variable. From this formulation one can clearly see that in open-loop robust MPC it is optimized over control *sequences*, whereas in closed-loop robust MPC, it is optimized over control *laws*. In the above formulation, the optimization is defined over an infinite dimensional function space, which is generally not tractable (and solving the dynamic programming problem can also quickly lead to problems in higher dimensions). This can be addressed by restricting the policies to a finite-dimensional subspace [GKM06, BTGGN04, LÖ3, vHB02] and solving the resulting MPC problem. Consider the control input parameterization

$$u_{t+k|t} := \sum_{i=1}^{k} L_{(t+k,t+i)|t} x_{t+i|t} + g_{t+k|t}\ , \tag{3.57}$$

where the matrix $L_{(t+k,\,t+i)|t}$ is a short-hand notation for the matrix $L_{t+k|t,\,t+i|t}$. Unfortunately, when using this input parameterization, the set of admissible L, g is non-convex in general. The parameterization in (3.57) can however be equivalently rewritten as

$$u_{t+k|t} := \sum_{i=0}^{k-1} M_{(t+k,\,t+i)|t} w_{t+i|t} + h_{t+k|t}\ , \tag{3.58}$$

where the matrix $M_{(t+k,\,t+i)|t}$ is a short-hand notation for the matrix $M_{t+k|t,\,t+i|t}$ and the set of admissible M and h is convex [GKM06].

Tube MPC

A variant of the closed-loop robust MPC strategy, the so-called *Tube MPC* uses a feedback policy of the form $u_{t+k|t} = K(x_{t+k|t} - \bar{x}_{t+k|t}) + c_{t+k|t}$, where $\bar{x}$ denotes the nominal state [RM09]. The idea is to steer the system to the origin through a tube with a cross section $\mathcal{Z}$, which is a positive invariant set of the system $x_{t+1} = (A+BK)x_t+w_t$, by optimizing over c. This formulation is well-suited for very fast and small-scale systems since the invariant sets are computed a priori, so the online computation effort is comparatively small. The drawbacks are that it is not obvious how to choose K in order to avoid conservatism and, especially for large-scale systems, the computation of the robust invariant sets might be problematic.

3.2.5 Chance Constrained Stochastic MPC

The advantages of robust control lie in the guarantees on stability and recursive feasibility that can be given for all admissible disturbances. Which disturbances are admissible, i.e. the admissible disturbance set $\mathbb{W}$, needs to be determined before controller design. If the realizations of the disturbances lie outside of the a priori determined disturbance set, no statements about stability and recursive feasibility can be made. If the disturbance bounds are, however, determined to be very wide, the performance degrades. Therefore the use of *Stochastic MPC* was suggested, which can provide a tradeoff between performance and constraint satisfaction. In stochastic MPC, the hard constraints are softened by replacing them with chance constraints. Chance constraints were first introduced by [CCS58, MW65, Pre70] and have been extensively studied in the field of stochastic programming, e.g., [Pre95, KM05, BL97]. A formulation of a stochastic MPC problem as used in this thesis is given as follows.

Problem 3.39 (Stochastic MPC).

$$J_{\mathrm{s}}^*(x_t) := \min_{\boldsymbol{\mu}} \quad \mathrm{E}\left[V_f(x_{t+N|t}) + \sum_{k=0}^{N-1} l_k(x_{t+k|t}, u_{t+k|t})\right] \tag{3.59}$$

subject to

$$\Pr\left[x_{t+k|t} \in \mathbb{X}\right] \geq 1-\alpha_x, \quad u_{t+k|t} \in \mathbb{U} \qquad \forall k \in \mathbb{N}_0^{N-1} \tag{3.60}$$

$$\Pr\left[x_{t+N|t} \in \mathbb{X}_f\right] \geq 1-\alpha_x \tag{3.61}$$

$$u_{t+k|t} = \mu_{t+k|t}(w_{t|t}, ..., w_{t+k-1|t}) \qquad \forall k \in \mathbb{N}_1^{N-1} \tag{3.62}$$

$$x_{t+k+1|t} = Ax_{t+k|t} + Bu_{t+k|t} + Ew_{t+k|t} \qquad x_{t|t} = x_t \tag{3.63}$$

$$w_{t+k|t} \in \mathbb{W} \qquad \forall k \in \mathbb{N}_0^{N-1}\ , \tag{3.64}$$

where $\alpha_x \in (0,1)$ denotes the level of constraint violation.

One major problem with chance constraints is that their feasible set is generally non-convex. The traditional way to deal with chance constraints in the field of stochastic programming is to use a scenario-based approach where one assumes a discrete distribution of the uncertainty or one creates scenarios from Monte Carlo samples and reformulates the chance constraint such that the (hard) constraints are fulfilled for all scenarios. This is efficiently solvable if the constraints are convex for a particular drawn sample and the sampling size is not too large. This approach is addressed in [CC05, CC06, Cal10]. However, these approaches can be computationally very demanding for larger sampling sizes and especially for the large-scale problems which are of interest here.

Recently, different approaches have been proposed for stochastic MPC. In [BB09], the authors consider a scenario-based approach that considers discrete multiplicative disturbances and solve a QCQP. In [CKRC10] stochastic tubes for MPC with probabilistic constraints are considered for bounded disturbances. Performance bounds for linear stochastic control which are computed by solving a semidefinite program are presented in [WB09].

Part II

Computationally Efficient MPC under Uncertainty

4 Tractable Approximations of Chance Constrained Stochastic MPC

4.1 Introduction

This chapter is concerned with solving a *Model Predictive Control* (MPC) problem for the class of discrete-time linear systems subject to stochastic disturbances. The aim is to provide a method for efficiently finding control policies given a set of polytopic input constraints and *chance constraints* on the state, which is computationally tractable to be applicable to large-scale systems.

One example of a control problem, which naturally leads to probabilistic constraints and which is the primary motivation for this work, originates from building climate control. Based on European building standards, it is required that the room temperature is kept within a comfort range with a predefined probability [EN 07]. The control problem is to minimize energy while satisfying this chance constraint (and some additional hard constraints, e.g., on control inputs). Problems of uncertain linear systems with chance constraints can also be found in other areas as for example in finance, physics, aeronautics, etc. [PDED04]. In order to be tractable for large-scale systems, it is desirable to formulate the problem such that it retains the original structure, i.e. an LP remains an LP, a QP remains a QP, etc.

4.1.1 Main Idea and Outline

The goal of the *Stochastic MPC* formulation is to reduce the conservatism of traditional robust solutions by staying closer to the constraints and hence achieving a better control performance (reduction in input (energy) usage); this is obtained by using Affine Disturbance Feedback and by exploiting the fact that the constraints are given as chance constraints and hence may be violated from time to time. The presented material offers a comparison and analysis of different formulations on a small-scale example. The proposed method is also tested on a large-scale building example which is presented in detail in Chapter 7.

Section 4.2 states the problem setting and formulates the *Stochastic Finite Horizon Optimal Control Problem* (SFHOCP) that is going to be approximated. In Section 4.3 the Affine Disturbance Feedback formulation is presented heading to the formulation of the *Stochastic MPC Problem with Chance Constraints*. Section 4.4 deals with three chance constraint reformulations, one being equivalent and leading to *Second Order Cone* (SOC) constraints and the other being approximations. In Section 4.5 a small example for demonstrating the properties of the different formulations is given. Finally, in Section 4.6, conclusions are drawn.

4.1.2 Dealing with Uncertainty

In the presence of disturbances, it is generally preferable instead of finding the optimal open-loop input sequence to optimize over closed-loop policies, i.e. to formulate the predicted control inputs as state feedback controller (or, equivalently, a disturbance feedback controller). The predicted control input at time t for prediction time step $t+k$, $u_{t+k|t}$, is formulated as a function of the states from time t up to time $t+k$, or, equivalently, as a function of the disturbances that have happened from time t up to time $t+k-1$, see Section 3.2.4 in Chapter 3.

Formulating such closed-loop policies is also known as recourse, multi-stage problem, or sequential decision making. There exist two extreme cases to this problem, the first one is to ignore the uncertainty and solve the deterministic MPC problem, this is also called *Certainty Equivalence MPC*. Making no use of information about the uncertainty (e.g., from some a priori known distribution of the disturbance), this can be argued to give a lower bound on the performance. The other extreme is a non-causal controller that has perfect information about the uncertainties and hence gives an upper bound on the performance, but is obviously not applicable; this is referred to in the following as *Performance Bound*.

Finding optimal closed-loop policies involves the optimization over an infinite dimensional function space and is not tractable except for very special cases. To overcome this, an alternative approach is to restrict the optimization to a finite dimensional subspace of the policies, i.e. to choose a control parameterization and optimize over its parameters.

A popular approach is to use a fixed feedback gain [Bem98, CRZ01, KM03], where the predicted control inputs $u_{t+k|t}$ for the predicted time step $t+k$ are parameterized as $u_{t+k|t} = Kx_{t+k|t} + c_{t+k|t}$, with K being a stabilizing linear feedback control law which is determined offline and the perturbation sequence $c_{t+k|t}$ being the optimization variable. This is computationally attractive since the online computation is restricted to the optimization of the $c_{t+k|t}$. It is however not obvious how to select the linear

control law a priori. A natural improvement is to simultaneously optimize over both the feedback gain and the perturbation sequence. However, in general, with this approach the predicted state and input sequences are nonlinear functions of the sequence of state feedback gains and hence this results in a non-convex set of feasible decision variables.

Inspired from results in optimization theory on robust optimization problems, in particular on so-called *Adjustable Robust Counterpart (ARC)* [BTGGN04] problems, where optimization variables correspond to decisions that can be adjusted as soon as the realization of the uncertain variable is available, the authors in [Lö3, vHB02] proposed to parameterize the control inputs to be an affine function of the disturbances, which leads to a convex set of feasible decision variables. This *Affine Disturbance Feedback* parameterization is shown to be equivalent to the *Affine State Feedback* parameterization in [GKM06] in the sense that it leads to the same control inputs. A more general approach is that of nonlinear disturbance feedback, where the decision variables are the coefficients of a linear combination of nonlinear basis functions of the disturbance [HCL09]. In this work it is investigated how the use of Affine Disturbance Feedback can be extended to the stochastic setting.

4.1.3 Definition of Constraints

For problems where hard constraints can be relaxed for some time, the formulation of chance constraints can be beneficial in terms of performance, since it allows to formulate the tradeoff between performance and constraint satisfaction [BS06]. Chance constraints were first introduced by [CCS58] and have been studied extensively in the field of *Stochastic Programming*, e.g., [Pre95, KM05, BL97]. The standard approach in stochastic programming is to consider discrete distributions and then to look at different scenarios, which can be computationally very demanding, in particular for large-scale problems, which are of interest here.

A number of different approaches have been proposed for stochastic MPC. In [BB09], the authors consider a scenario-based approach that considers discrete multiplicative disturbances and solve a *quadratically constrained quadratic program* (QCQP). In [CKRC10] stochastic tubes for MPC with probabilistic constraints are considered for bounded disturbances. Performance bounds for linear stochastic control computed by solving a semidefinite program are presented in [WB09].

In this work linear *individual chance constraints* are considered as introduced in Definition 3.13. This means that each row of the inequality has to be fulfilled individually with the respective probability.

4.2 Problem Setting

Consider the following discrete-time LTI system

$$x_{t+1} = Ax_t + Bu_t + Ew_t \ , \tag{4.1}$$

with system state $x_t \in \mathbb{R}^{n_x}$, control input $u_t \in \mathbb{R}^{n_u}$ and stochastic disturbance $w_t \in \mathbb{R}^{n_w}$.

Assumption 4.1. (A, B) is stabilizable and at each sample instant a measurement of the state is available.

Assumption 4.2. The disturbances are assumed to be independent and identically distributed (i.i.d.) and to follow a multivariate standard normal distribution, $w_t \sim \mathcal{N}(\mathbf{0}_{\{n_w \times 1\}}, \mathbf{I}_{\{n_w\}})$.

Remark 4.3. Having a non-zero mean disturbance would add a constant to the system dynamics making them affine. All results in this work still hold in this case. In case of the covariance being different from identity, one can reformulate, such that the covariance matrix is part of E. So, it can be assumed that $w \sim \mathcal{N}(\mathbf{0}_{\{n_w \times 1\}}, \mathbf{I}_{\{n_w\}})$ without loss of generality.

The system is subject to polytopic constraints on the input and linear individual chance constraints on the state

$$Su_{t+k|t} \leq s \tag{4.2}$$

$$\Pr\left[G_{(j)}x_{t+k|t} \leq g_{(j)}\right] \geq 1 - \alpha_{x,j} \ , \quad \forall\, j \in \mathbb{N}_1^r \ , \tag{4.3}$$

where $S \in \mathbb{R}^{q \times n_u}$, $s \in \mathbb{R}^q$, $G \in \mathbb{R}^{r \times n_x}$, $g \in \mathbb{R}^r$ and $\alpha_{x,j} \in (0, 1)$ denotes the level of constraint violation for row j of the constraints on $x_{t+k|t}$. The chance constraints are considered row-wise, i.e. each row j of a chance constraint has to be fulfilled individually with the corresponding violation level $\alpha_{x,j}$.

Remark 4.4. The constraints on states and input can also be time-varying, e.g., for introducing time varying temperature constraints (setbacks), which is not indicated by a separate index here for notational convenience.

In the following predictions about the system's evolution over a finite planning horizon are used in order to define suitable control policies. Consider the prediction horizon $N \in \mathbb{N}_+$ and define

$$\mathbf{x}_t := \left[x_{t|t}^T \dots x_{t+N|t}^T\right]^T \in \mathbb{R}^{n_x(N+1)} \tag{4.4}$$

$$\mathbf{u}_t := \left[u_{t|t}^T \dots u_{t+N-1|t}^T\right]^T \in \mathbb{R}^{n_u N} \tag{4.5}$$

$$\mathbf{w}_t := \left[w_{t|t}^T \dots w_{t+N-1|t}^T\right]^T \in \mathbb{R}^{n_w N} \ . \tag{4.6}$$

Let furthermore prediction dynamics matrices $\mathbf{A}$, $\mathbf{B}$ and $\mathbf{E}$ (see Appendix A) be such that

$$\mathbf{x}_t = \mathbf{A}x_t + \mathbf{B}\mathbf{u}_t + \mathbf{E}\mathbf{w}_t \ . \tag{4.7}$$

Consequently, the constraints on input $\mathbf{u}_t$ and states $\mathbf{x}_t$ over the prediction horizon N are given as

$$\mathbf{S}\mathbf{u}_t \leq \mathbf{s} \tag{4.8}$$

$$\Pr\left[\mathbf{G}_{(j)}\mathbf{x}_t \leq \mathbf{g}_{(j)}\right] \geq 1 - \alpha_{\mathbf{x},j} \ , \quad \forall j \in \mathbb{N}_1^{r(N+1)} \tag{4.9}$$

where $\mathbf{S} \in \mathbb{R}^{qN \times n_u N}$, $\mathbf{s} \in \mathbb{R}^{qN}$, $\mathbf{G} \in \mathbb{R}^{r(N+1) \times n_x (N+1)}$, $\mathbf{g} \in \mathbb{R}^{r(N+1)}$, and $\alpha_{\mathbf{x},j} \in (0,1)$ denotes the probability level of constraint violation for row j of the constraints on the states $\mathbf{x}_t$.

The first state $x_{t|t}$ is measured, however, the predicted states $x_{t+1|t}, ..., x_{t+N|t}$ are uncertain. This uncertainty should be addressed in the MPC formulation. For this, consider for predicted control inputs $u_{t+1|t}$ to $u_{t+N|t}$ a causal state feedback controller, or equivalently, a causal disturbance feedback controller, which takes into account feedback of the predicted states up to prediction time step $t+k$ or feedback of the predicted disturbances up to prediction time step $t+k-1$,

$$u_{t+k|t} = \phi_{t+k|t}(x_{t+1|t}, ..., x_{t+k|t}) = \mu_{t+k|t}(w_{t|t}, ..., w_{t+k-1|t}) \ . \tag{4.10}$$

Remark 4.5. The feedback controller is called *causal* since it strictly depends on the states (or disturbances) that have already been realized at the time when the corresponding predicted control input will be applied.

Remark 4.6. It is equivalent to consider feedback of states and feedback of disturbances, since the disturbances can be straightforwardly computed with given states and known inputs and the other way around. Note that for this to hold, feedback of the states from time step 1 to k is considered but feedback of the disturbances from time step 0 to $k-1$.

The aim is to solve the following *Stochastic Finite Horizon Optimal Control Problem* (SFHOCP).

Problem 4.7 (SFHOCP).

$$J^*(x_t) := \min_{\boldsymbol{\mu}_t} \mathrm{E}\left[\sum_{k=0}^{N-1} l_k(x_{t+k|t}, u_{t+k|t}) + l_N(x_{t+N|t})\right] \tag{4.11}$$

subject to

$$\mathbf{S}\mathbf{u}_t \leq \mathbf{s} \tag{4.12}$$

$$\Pr\left[\mathbf{G}_{(j)}\mathbf{x}_t \leq \mathbf{g}_{(j)}\right] \geq 1 - \alpha_{\mathbf{x},j} \qquad \forall j \in \mathbb{N}_1^{r(N+1)} \tag{4.13}$$

$$\mathbf{x}_t = \mathbf{A}x_t + \mathbf{B}\mathbf{u}_t + \mathbf{E}\mathbf{w}_t \tag{4.14}$$

$$\mathbf{w}_t \sim \mathcal{N}(\mathbf{0}_{\{n_w N \times 1\}}, \mathbf{I}_{\{n_w N\}}) \tag{4.15}$$

$$u_{t+k|t} = \mu_{t+k|t}(w_{t|t}, ..., w_{t+k-1|t}) \qquad k \in \mathbb{N}_1^{N-1}\ , \tag{4.16}$$

for some stage cost $l_k(x_{t+k|t}, u_{t+k|t})$ and some terminal cost $l_N(x_{t+N|t})$. The decision variable is

$$\boldsymbol{\mu}_t = [u_{t|t}^T \quad \mu_{t+1|t}^T(w_{t|t}) \quad \ldots \quad \mu_{t+N-1|t}^T(w_{t|t}, ..., w_{t+N-2|t})]^T\ . \tag{4.17}$$

Note that in Problem 4.7 the aim is not to find an optimal control input *sequence*, but to find an optimal control *policy* as defined in (4.10) taking into account that there is recourse/feedback at every future time step/stage. This SFHOCP can easily lead to an intractable problem, since it depends on the control policies and involves the optimization over an infinite-dimensional function space. This problem is approximated here by restricting the policies to a finite-dimensional subspace. Furthermore, the above problem involves probabilistic constraints, that should be reformulated such that they can be efficiently handled in the optimization problem. The next two sections deal with approximations and reformulations in order to turn Problem 4.7 into a tractable MPC problem. First Affine Disturbance Feedback is introduced and then, three reformulations of the chance constraints are considered.

4.3 Affine Disturbance Feedback for Stochastic MPC

In order to restrict the control policies to a finite-dimensional subspace, we choose to apply *Affine Disturbance Feedback*. Affine Disturbance Feedback is a control input parameterization that has been successfully applied in robust control [GKM06, BTGGN04, LÖ3, vHB02], see also discussion in Section 3.2.4 of Chapter 3. In this work, its use is extended to stochastic MPC. The formulation is given as follows.

Definition 4.8 (Affine Disturbance Feedback). Define $\mu_{t+k|t} : \mathbb{R}^{n_w N} \to \mathbb{R}^{n_u}$

$$\mu_{t+k|t}(\mathbf{w}_t) := \sum_{j=0}^{k-1} M_{(t+k,\, t+j)|t} w_{t+j|t} + h_{t+k|t}\ , \quad k \in \mathbb{N}_0^{N-1}\ , \tag{4.18}$$

with $M_{(t+k,\,t+j)|t} \in \mathbb{R}^{n_u \times n_w}$ and $h_{t+k|t} \in \mathbb{R}^{n_u}$ using the short-hand notation introduced in Section 3.2.4.

Let $\mu_t(\mathbf{w}_t) := [u_{t|t}^T \;\; \mu_{t+1|t}^T(\mathbf{w}_t) \;\; \dots \;\; \mu_{t+N-1|t}^T(\mathbf{w}_t)]^T$. Note that the first predicted input is the optimization variable $u_{t|t}$, whereas the predicted control inputs of future steps $t+k$ depend on the disturbances that have meanwhile acted on the system, i.e. the predicted disturbances up to $t+k-1$. Therefore, applying such a control policy is also called *closed-loop prediction* MPC. Defining

$$\mathbf{M}_t := \begin{bmatrix} \mathbf{0} & \dots & \dots & \mathbf{0} \\ M_{(t+1,\,t)|t} & \mathbf{0} & \ddots & \mathbf{0} \\ \vdots & \ddots & \ddots & \vdots \\ M_{(t+N-1,\,t)|t} & \cdots & M_{(t+N-1,\,t+N-2)|t} & \mathbf{0} \end{bmatrix} , \quad \mathbf{h}_t := \begin{bmatrix} h_{t|t} \\ \vdots \\ \vdots \\ h_{t+N-1|t} \end{bmatrix} , \tag{4.19}$$

one can write $\boldsymbol{\mu}_t(\mathbf{w}_t) = \mathbf{M}_t\mathbf{w}_t + \mathbf{h}_t$.

Remark 4.9. Note that due to the structure of $\mathbf{M}_t$ for the computation of the control input at time step $t+k$ only the disturbances up to time $t+k-1$ are taken into account. Also note that the very first control input is not a function of the disturbance, but $u_{t|t} = h_{t|t}$.

Consider the minimization of a quadratic cost function.

Definition 4.10. $J : \mathbb{R}^{n_x(N+1)} \times \mathbb{R}^{n_u N \times n_w N} \times \mathbb{R}^{n_u N} \times \mathbb{R}^{n_w N} \to \mathbb{R}_{+0}$

$$J(\mathbf{x}_t, \mathbf{M}_t, \mathbf{h}_t, \mathbf{w}_t) := \mathrm{E}\left[\mathbf{x}_t^T\mathbf{Q}\mathbf{x}_t + (\mathbf{M}_t\mathbf{w}_t + \mathbf{h}_t)^T\mathbf{R}(\mathbf{M}_t\mathbf{w}_t + \mathbf{h}_t)\right] , \tag{4.20}$$

where $\mathbf{Q} = \mathbf{Q}^T \succeq 0$ and $\mathbf{R} = \mathbf{R}^T \succ 0$.

With $\mathrm{E}[\mathbf{w}_t] = \mathbf{0}$ and $\mathrm{E}[\mathbf{w}_t\mathbf{w}_t^T] = \mathbf{I}$ and using (4.7) the cost function of the ADF MPC problem $J_N : \mathbb{R}^{n_x} \times \mathbb{R}^{n_u N \times n_w N} \times \mathbb{R}^{n_u N} \to \mathbb{R}_{+0}$ can be expressed as

$$\begin{aligned} &J_N(x_t, \mathbf{M}_t, \mathbf{h}_t) = x_t^T\mathbf{A}^T\mathbf{Q}\mathbf{A}x_t + \mathrm{Tr}[\mathbf{E}^T\mathbf{Q}\mathbf{E}] + ... \\ &\mathbf{h}_t^T(\mathbf{B}^T\mathbf{Q}\mathbf{B} + \mathbf{R})\mathbf{h}_t + 2\mathbf{h}_t^T\mathbf{B}^T\mathbf{Q}\mathbf{x}_t + ... \\ &\mathrm{Tr}[\mathbf{M}_t^T\mathbf{B}^T\mathbf{Q}\mathbf{B}\mathbf{M}_t + \mathbf{M}_t^T\mathbf{R}\mathbf{M}_t + 2\mathbf{M}_t^T\mathbf{B}^T\mathbf{Q}\mathbf{E}] \; . \end{aligned} \tag{4.21}$$

Proposition 4.11 *The cost function in (4.20) is a convex quadratic function of the decision variables* $\mathbf{M}_t$ *and* $\mathbf{h}_t$.

Proof:
The convexity of the quadratic cost function is preserved due to the policies being affine

and under expectation. ■

Note that the disturbances $w_{t+k|t}$ have an infinite support and the inputs $\mu_{t+k|t}$ are, except for the very first input $u_{t|t}$, a function of the disturbances (see Remark 4.9). Therefore, it is only possible to define a hard constraint on the first input $u_{t|t}$ (see also Remark 4.13).

Now an approximation of the SFHOCP in Problem 4.7 can be stated by using the Affine Disturbance Feedback formulation.

Problem 4.12 (Approximate SFHOCP using ADF).

$$(\mathbf{M}_t^*(x_t), \mathbf{h}_t^*(x_t)) := \arg \min_{(\mathbf{M}_t, \mathbf{h}_t) \in \Pi(x_t)} J_N(x_t, \mathbf{M}_t, \mathbf{h}_t) \tag{4.22}$$

For state x_t the set of admissible Affine Disturbance Feedback policies $(\mathbf{M}_t, \mathbf{h}_t)$ is given by the set

$$\Pi_t(x_t) := \left\{ (\mathbf{M}_t, \mathbf{h}_t) \left| \begin{array}{l} (\mathbf{M}_t, \mathbf{h}_t) \text{ satisfies (4.18)} \\ \Pr\ [\mathbf{S}_{(i)}(\mathbf{M}_t \mathbf{w}_t + \mathbf{h}_t) \leq \mathbf{s}_{(i)}] \geq 1 - \alpha_{\mathbf{u},i} \quad \forall i \in \mathbb{N}_1^{qN} \\ \Pr\ [\mathbf{G}_{(j)}(\mathbf{A}x_t + \mathbf{B}\mathbf{h}_t + \mathbf{B}\mathbf{M}_t \mathbf{w}_t + \mathbf{E}\mathbf{w}_t) \leq g_{(j)}] \geq 1 - \alpha_{\mathbf{x},j} \quad \forall j \in \mathbb{N}_1^{r(N+1)} \\ \mathbf{w}_t \sim \mathcal{N}(\mathbf{0}_{n_w N \times 1}, \mathbf{I}_{n_w N}) \end{array} \right. \right\}.$$

Remark 4.13. Since the aim is to impose hard constraints on the control inputs, it makes sense to choose a violation level for $\alpha_{\mathbf{u},i}$, which is small in order to fulfill the hard constraint with a high probability. Note that the input constraints are actually never violated when this strategy is applied in closed loop (if a feasible solution can be found) due to the structure of $\mathbf{M}_t$, i.e. on the first predicted state, which is applied, a hard constraint is imposed (see also Remark 4.9). Hence, $\alpha_{\mathbf{u},i}$ is a tuning parameter and needs to be chosen considering the tradeoff between a realistic prediction of the future input constraints and turning the problem infeasible.

Problem 4.12 is hard to solve for general distributions, because each predicted state and input is a function of the sum of i.i.d. disturbances, hence in general, in order to compute the distribution of the predicted states and inputs one needs to compute the convolution of the density functions of multivariate random variables. However, for the case of Gaussian variables this is much simpler, since the sum of two Gaussian variables is again a Gaussian variable and hence all predicted states and inputs follow a Gaussian distribution. Therefore, only a deterministic reformulation of a chance constraint involving a random Gaussian variable needs to be found. The next section proposes three reformulations of Problem 4.12, one being equivalent leading to a SOC problem, the other two being linear approximations.

4.4 Chance Constraint Reformulations

All chance constraint reformulations are shown for the chance constraints on the states. They can be applied to the chance constraints on the inputs accordingly, which is omitted here.

4.4.1 Quantile Function

Note that the functions describing the constraints in Problem 4.12 are bi-affine in the decision variables and the disturbances. If the disturbance is normally distributed, the functions are bi-affine in the decision variables and the disturbances, and $\alpha_{\mathbf{x},j} \in (0, 0.5]$, then individual chance constraints can be equivalently formulated as deterministic second order cone constraints [Pre95] as follows

$$\Pr \left[\mathbf{G}_{(j)} \left(\mathbf{A}x_t + \mathbf{B}\mathbf{h}_t + \mathbf{B}\mathbf{M}_t\mathbf{w}_t + \mathbf{E}\mathbf{w}_t\right) - \mathbf{g}_{(j)} \leq 0\right] \geq 1 - \alpha_{\mathbf{x},j} \tag{4.23}$$

$$\Leftrightarrow \quad \mathbf{G}_{(j)}(\mathbf{A}x_t + \mathbf{B}\mathbf{h}_t) \leq \mathbf{g}_{(j)} - \Phi^{-1}(1 - \alpha_{\mathbf{x},j})\|\mathbf{G}_{(j)}(\mathbf{B}\mathbf{M}_t + \mathbf{E})\|_2 \tag{4.24}$$

where Φ is the standard Gaussian cumulative distribution function and its inverse Φ^{-1} is the *quantile function* (QF), see also Remark 3.15. The inequalities (4.24) are SOC constraints that are convex in the decision variables $\mathbf{M}_t$ and $\mathbf{h}_t$. This reformulation of the chance constraints can be used to restate Problem 4.12.

Problem 4.14 (ADF with QF).

$$(\mathbf{M}_t^*(x_t), \mathbf{h}_t^*(x_t)) := \arg \min_{(\mathbf{M}_t, \mathbf{h}_t) \in \Pi_{QF}(x_t)} J_N(x_t, \mathbf{M}_t, \mathbf{h}_t) \tag{4.25}$$

For initial state x_t the set of admissible Affine Disturbance Feedback policies $(\mathbf{M}_t, \mathbf{h}_t)$ when using the quantile functions is given by

$$\Pi_{\mathrm{QF}}(x_t) := \left\{ (\mathbf{M}_t, \mathbf{h}_t) \left| \begin{array}{l} (\mathbf{M}_t, \mathbf{h}_t) \text{ satisfies (4.18)} \\ \mathbf{S}_{(i)}\mathbf{h}_t \leq \mathbf{s}_{(i)} - \Phi^{-1}(1 - \alpha_{\mathbf{u},i})\|\mathbf{S}_{(i)}\mathbf{M}_t\|_2 \quad \forall i \in \mathbb{N}_1^{qN} \\ \mathbf{G}_{(j)}(\mathbf{A}x_t + \mathbf{B}\mathbf{h}_t) \leq \mathbf{g}_{(j)} \ - \Phi^{-1}(1 - \alpha_{\mathbf{x},j})\|\mathbf{G}_{(j)}(\mathbf{B}\mathbf{M}_t + \mathbf{E})\|_2 \\ \forall j \in \mathbb{N}_1^{r(N+1)} \end{array} \right. \right\}.$$

The set of admissible initial states is given by

$$\mathcal{X}_{\mathrm{QF}} := \{x_t \mid \exists (\mathbf{M}_t, \mathbf{h}_t) \in \Pi_{\mathrm{QF}}(x_t)\}. \tag{4.26}$$

Theorem 4.15 (ADF with QF)
For Problem 4.14 the following statements hold:
(1) *The solution of Problem 4.14 is equal to the solution of Problem 4.12.*
(2) *Problem 4.14 is convex.*

Proof:
(1) Follows from (4.24) and the reformulation of the input constraints as in (4.24).
(2) Second order cone constraints are by definition convex, therefore $\Pi_{\mathrm{QF}}(x_t)$ is convex. This together with the cost function of Problem 4.14 being convex according to Proposition 4.11 establishes the assertion. ■

We then follow the standard MPC procedure; the optimal control input $u^*_{t|t}(x_t)$ is given by

$$u^*_{t|t}(x_t) = h^*_{t|t}(x_t) \tag{4.27}$$

and the closed-loop trajectory evolves according to

$$x_{t+1} = Ax_t + Bu^*_{t|t}(x_t) + Ew_t \ . \tag{4.28}$$

4.4.2 Bounds on the Disturbance Set

The reformulation of the chance constraints in the previous section led to an SOC problem, this can however be time consuming to compute for large-scale systems. This section deals with a linear approximation of the chance constraints.

Let us consider the chance constraints on the states in (4.3) more closely; the same procedure can be applied also to the input constraints in a similar fashion:

$$\Pr\left[\mathbf{G}_{(j)}\left(\mathbf{A}x_t + \mathbf{B}\mathbf{h}_t + \mathbf{B}\mathbf{M}_t\mathbf{w}_t + \mathbf{E}\mathbf{w}_t\right) - \mathbf{g}_{(j)} \leq 0\right] \geq 1 - \alpha_{\mathbf{x},j} \ . \tag{4.29}$$

We propose to replace the chance constraint in (4.29) with the following robust constraint

$$\begin{aligned} &\mathbf{G}_{(j)}\left(\mathbf{A}x_t + \mathbf{B}\mathbf{h}_t + \mathbf{B}\mathbf{M}_t\mathbf{w}_t + \mathbf{E}\mathbf{w}_t\right) - \mathbf{g}_{(j)} \leq 0, \quad \forall \mathbf{w}_t \in \mathbb{W}^N \ , \\ &\mathbb{W}^N := \{w_t \in \mathbb{R}^{n_w N} |\ \|\mathbf{w}_t\|_\infty \leq \Omega_{\mathbf{x},j}\} \ , \end{aligned} \tag{4.30}$$

where $\Omega_{\mathbf{x},j}$ is chosen according to Theorem 4.16, which is directly derived by some algebraic reformulations of (4.29) and use of Theorem 2b of [BS06], see Appendix B. The idea of this replacement is that the robust constraint is chosen such that the original chance constraint is fulfilled. The advantage of this is that the resulting robust optimization problem is easier to solve. The property that the robust constraint satisfies the original chance constraint is stated in the following theorem.

Theorem 4.16 (Probability bound)
For $\mathbf{w_t} \sim \mathcal{N}(\mathbf{0}, \mathbf{I})$ and for $\Omega_{\mathbf{x},j} > 1$ the following probability bound of infeasibility holds:

$$\Pr\left[\mathbf{G}_{(j)}\left(\mathbf{A}x_t + \mathbf{B}\mathbf{h}_t + \mathbf{B}\mathbf{M}_t\mathbf{w}_t + \mathbf{E}\mathbf{w}_t\right) - \mathbf{g}_{(j)} > 0\right] \leq \sqrt{e} \cdot \Omega_{\mathbf{x},j} \cdot \exp\left(-\frac{\Omega^2_{\mathbf{x},j}}{2}\right) \ .$$

Proof: See Appendix B. ■

This theorem gives us a performance guarantee in the following sense:

Corollary 4.17 *If $\Omega_{\mathbf{x},j}$ is chosen according to Theorem (4.16), i.e. such that $\alpha_{\mathbf{x},j} \geq \sqrt{e} \cdot \Omega_{\mathbf{x},j} \cdot \exp\left(-\frac{\Omega^2_{\mathbf{x},j}}{2}\right)$ and the constraint in (4.30) is applied, then the chance constraint in (4.29) is satisfied.*

As a result, this approximation can be used to solve a classic robust optimization problem. Now a tractable approximation of Problem 4.7 can be stated, which is an approximation with *Bounds on the Disturbance Set* (BDS).

Problem 4.18 (ADF with BDS).

$$(\mathbf{M}_t^*(x_t), \mathbf{h}_t^*(x_t)) := \arg \min_{(\mathbf{M}_t, \mathbf{h}_t) \in \Pi_{\mathrm{BDS}}(x_t)} J_N^{\mathrm{ADF}}(x_t, \mathbf{M}_t, \mathbf{h}_t) \tag{4.31}$$

For state x_t the set of admissible Affine Disturbance Feedback policies $(\mathbf{M}_t, \mathbf{h}_t)$ with Bounds on the Disturbance Set is given by

$$\Pi_{\mathrm{BDS}}(x_t) := \left\{ (\mathbf{M}_t, \mathbf{h}_t) \left| \begin{array}{l} (\mathbf{M}_t, \mathbf{h}_t) \text{ satisfies (6.7.4)} \\ \mathbf{S}_{(i)}\mathbf{h}_t \leq \mathbf{s}_{(i)} - \max_{\|\mathbf{w}_t\|_\infty \leq \Omega_{\mathbf{u},i}} \mathbf{S}_{(i)}\mathbf{M}_t\mathbf{w}_t \quad \forall i \in \mathbb{N}_1^{qN} \\ \mathbf{G}_{(j)}(\mathbf{A}x_t + \mathbf{B}\mathbf{h}_t) \leq \mathbf{g}_{(j)} \ - \max_{\|\mathbf{w}_t\|_\infty \leq \Omega_{\mathbf{x},j}} \mathbf{G}_{(j)}(\mathbf{B}\mathbf{M}_t\mathbf{w}_t + \mathbf{E}\mathbf{w}_t) \\ \forall j \in \mathbb{N}_1^{r(N+1)} \end{array} \right. \right\}.$$

The set of admissible initial states is given by

$$\mathcal{X}_{\mathrm{BDS}} := \{x_t \mid \exists (\mathbf{M}_t, \mathbf{h}_t) \in \Pi_{\mathrm{BDS}}(x_t)\}. \tag{4.32}$$

The computation of Problem 4.18 by means of solving a standard QP is shown in Appendix C.

Theorem 4.19 (ADF with BDS)

For Problem 4.18 the following statements hold:

(1) *It is a conservative approximation of Problem 4.12 in the sense that the level of constraint violation is strictly smaller than α.*

(2) *It is convex.*

Proof:

(1) The statement follows from Theorem 4.16 and Corollary 4.17. It can also be seen from the fact, that linear constraints are used for inner approximations of SOC constraints.

(2) $\Pi_{BDS}(x_0)$ is convex from (14) in Appendix C. This together with the cost function of Problem 4.18 being convex according to Proposition 4.11 establishes the assertion.■

4.4.3 Fixed Feedback

The two previous presented formulations have advantages and disadvantages: Problem 4.14 uses an equivalent deterministic reformulation of the chance constraints, but leads to an SOC problem, whereas Problem 4.18 leads to linear constraints, which are computationally more tractable, but uses an approximation of the chance constraints.

In this section, the above advantages are combined in a third formulation, *Fixed Feedback* (FF). This formulation is motivated by the insight that Problem 4.14 involves a SOC constraint due to the use of Affine Disturbance Feedback as introduced in Section 4.3. More specifically, the optimization variables in the feedback matrix $\mathbf{M}_t$ make the constraints SOC constraints, whereas using a fixed feedback matrix (i.e. a matrix where the entries are no optimization variables but fixed values) would lead to linear constraints. In order to benefit from the advantages of the feedback but still have a computationally tractable problem, we suggest to fix the feedback matrix a priori and optimize over the amount of feedback that is considered, i.e. to optimize over a scaling factor that multiplies the fixed feedback matrix.

The fixed feedback $\bar{\mathbf{M}}$ is computed by taking the average over some number $n_{\mathbf{M}}$ of optimal feedback matrices $\mathbf{M}_l^*(x_l)$ that were already obtained and stored previously after solving the SOC problem at time l for the corresponding measured state x_l, i.e.

$$\bar{\mathbf{M}} := \frac{1}{n_{\mathbf{M}}} \sum_{l=1}^{n_{\mathbf{M}}} \mathbf{M}_l^*(x_l) \ . \tag{4.33}$$

A scalar decision variable $\gamma \in [0,1]$ is introduced that is used to optimize how much feedback is taken into account ranging from none (i.e. open-loop prediction, $\mathbf{M} = \mathbf{0}$) to the full pre-optimized feedback $\bar{\mathbf{M}}$. This yields the following approximation.

Problem 4.20 (ADF with FF).

$$(\gamma_t^*(x_t), \mathbf{h}_t^*(x_t)) := \arg \min_{(\gamma_t, \mathbf{h}_t) \in \Pi_{\mathrm{FF}}(x_t)} J_N^{\mathrm{ADF}}(x_t, \gamma_t \bar{\mathbf{M}}, \mathbf{h}_t) \tag{4.34}$$

For state x_t the set of admissible $(\gamma, \mathbf{h}_t)$ when using the fixed feedback is given by

$$\Pi_{\mathrm{FF}}(x_t) := \tag{4.35}$$
$$\left\{ (\gamma, \mathbf{h}_t) \left| \begin{array}{l} \mathbf{S}_{(i)}\mathbf{h}_t \leq \mathbf{s}_{(i)} - \Phi^{-1}(1-\alpha_{\mathbf{u},i}) \|\mathbf{S}_{(i)}\gamma_t \bar{\mathbf{M}}\|_2 \quad \forall i \in \mathbb{N}_1^{qN} \\ \mathbf{G}_{(j)}(\mathbf{A}x_t + \mathbf{B}\mathbf{h}_t) \leq \mathbf{g}_{(j)} \ - \Phi^{-1}(1-\alpha_{\mathbf{x},j}) \|\mathbf{G}_{(j)}(\mathbf{B}\gamma_t \bar{\mathbf{M}} + \mathbf{E})\|_2 \\ \forall j \in \mathbb{N}_1^{r(N+1)} \\ \gamma_t \in [0,1] \end{array} \right. \right\} .$$

Hence, Problem 4.20 involves SOC constraints, but has much fewer decision variables. The set of admissible initial states is given by

$$\mathcal{X}_{\mathrm{FF}} := \{x_t \mid \exists (\mathbf{M}_t, \mathbf{h}_t) \in \Pi_{\mathrm{FF}}(x_t)\} \ . \tag{4.36}$$

Theorem 4.21 (ADF with FF)
Problem 4.20 is convex.

Proof:
Second order cone constraints are by definition convex, therefore $\Pi_{\mathrm{FF}}(x_t)$ is convex. This together with the cost function of Problem 4.14 being convex according to Proposition 4.11 establishes the assertion. ■

4.5 Numerical Example

To test the proposed three strategies a simplified version of the building example in [GT05] is examined. The system dynamics are given in the form of (4.1), but with an external input to account for the weather forecast:

$$x_{t+1} = Ax_t + Bu_t + Vv_t + Ew_t \ . \tag{4.37}$$

Let $x_t = [x_{t,(1)} \ \ x_{t,(2)} \ \ x_{t,(3)}]^T$ denote the state, where $x_{t,(1)}$ is the room temperature, $x_{t,(2)}$ the temperature in the wall connected with another room, and $x_{t,(3)}$ the temperature in the wall connected to the outside. There is a prediction for the external input $v_t = [v_{t,(1)} \ \ v_{t,(2)} \ \ v_{t,(3)}]^T$, the outside temperature $v_{t,(1)}$, the solar radiation $v_{t,(2)}$, and the internal heat gains (people, appliances etc.) $v_{t,(3)}$. The predictions of internal gains are assumed to be perfect in this example, i.e. the realization is equal to the prediction. However, for the weather variables, the realization is equal to the prediction plus some random noise $w_{t,(1)}$ and $w_{t,(2)}$, respectively. The noise is assumed to consist of i.i.d. Gaussian random variables. The control objective is to keep the room temperature above 21 °C with minimum energy. The single available input $u_{t,(1)}$ is the heating per floor area, which is constrained to $0 \leq u_1 \leq 45$ [W/m^2]. The time step is 1 h. The system matrices are given as

$$\begin{aligned} A &= \begin{bmatrix} 0.8511 & 0.0541 & 0.0707 \\ 0.1293 & 0.8635 & 0.0055 \\ 0.0989 & 0.0032 & 0.7541 \end{bmatrix} \quad B = \begin{bmatrix} 0.070 \\ 0.006 \\ 0.004 \end{bmatrix} \\ V &= \begin{bmatrix} 0.02221 & 0.00018 & 0.0035 \\ 0.00153 & 0.00007 & 0.0003 \\ 0.10318 & 0.00001 & 0.0002 \end{bmatrix} \quad E = \begin{bmatrix} 0.4 & 0.014 \\ 0.028 & 0.006 \\ 1.857 & 0.001 \end{bmatrix} \ . \end{aligned} \tag{4.38}$$

An extract of three days of the predicted disturbances can be found in Figure 4.1. Five control strategies were compared:
CLP-QF: Closed-loop prediction MPC with use of Quantile Function. This is the

strategy formulated in Problem 4.14.
OLP-QF: Open-loop prediction MPC with use of Quantile Function. This is the strategy formulated in Problem 4.14, but with $\mathbf{M} = 0$.
CLP-BDS: Closed-loop prediction MPC with Bounds on the Disturbance Set. This is the strategy formulated in Problem 4.18.
OLP-BDS: Open-loop prediction MPC with Bounds on the Disturbance Set. This is the strategy formulated in Problem 4.18, but with $\mathbf{M} = 0$.
FF-QF: Closed-loop prediction MPC with Fixed Feedback. This is the strategy formulated in Problem 4.20. $\bar{\mathbf{M}}$ is computed by averaging over all feedback matrices that were stored in CLP-QF. In a real implementation, there would be only some feedback matrices of a priori trials available. Since it can be expected that the performance improves with the number of feedback matrices considered (at least for a small number of feedback matrices), the performance in this investigation constitutes an upper bound on the performance of this controller.

Three investigations were carried out:
Investigation 1: The weather was kept constant at $v_{t,(1)} = 10.6\,°\mathrm{C}$, $v_{t,(2)} = 18.38\,\mathrm{W/m^2}$, and $v_{t,(3)} = 18\,\mathrm{W/m^2}$. The random noise was set to its mean value, $w_{t,(1)} = w_{t,(2)} = 0$, $\alpha_{\mathbf{u},i} = 0.0003$ in order to have a high probability to fulfil the (hard) input constraints, and $\alpha_{\mathbf{x},j}$ was varied.
Investigation 2: The weather was following the prediction. The random noise was set to its mean value, $w_{t,(1)} = w_{t,(2)} = 0$, $\alpha_{\mathbf{u},i} = 0.0003$, and $\alpha_{\mathbf{x},j}$ was varied.

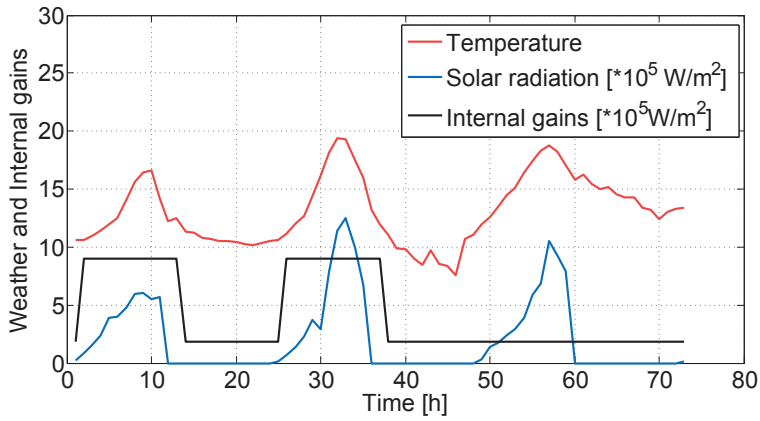

Figure 4.1: Outside temperature, solar radiation, and internal heat gains. The outside temperature fluctuates. The internal heat gains are comprised of a constant part and a part that is changing with the daytime. This is because in office buildings people being are assumed to be absent during the nights and on weekends. Solar radiation is equal to zero at night.

Investigation 3: The weather was kept constant at $v_{t,(1)} = 10.6\,°\mathrm{C}$, $v_{t,(2)} = 18.38\,\mathrm{W/m^2}$, and $v_{t,(3)} = 18\,\mathrm{W/m^2}$. The random noise following a standard Gaussian distribution was applied to the system in a randomized study with 70 samples. $\alpha_{\mathbf{u},i} = 0.0003$, and $\alpha_{\mathbf{x},j}$ was varied.

All investigations were carried out for three days = 72 h, with a prediction horizon of $N = 6$. In the cost function only the control inputs were penalized, i.e. the cost function in (4.20) was used, but with $\mathbf{Q} = \mathbf{0}$, reflecting the goal to minimize energy while keeping the states within the comfort range.

Investigation 1

In Figure 4.2(a) the control performance in terms of energy use of the five investigated strategies for different levels of $\alpha_{\mathbf{x},j}$ is depicted. OLP-BDS uses by far the most energy. Considering instead the closed-loop prediction formulation (CLP-BDS) clearly improves the performance. OLP-QF uses even less energy than CLP-BDS and again, using the closed-loop formulation further improves the performance (CLP-QF). To summarize, closed-loop prediction improves the performance and using QF is better than BDS. Since CLP-QF is the best strategy, but can lead to problems with the computational tractability for large-scale problems, also the FF-QF is compared with. Figure 4.2(a) shows that the performance of CLP-QF and FF-QF is almost identical. Figure 4.3(a) shows the room temperature profile of the same investigation. As expected, OLP-BDS is very conservative and stays very far away from the constraint. The other controllers are less conservative. CLP-QF is the least conservative. Figure 4.4(a) depicts the corresponding heating input that was applied. Note that for longer prediction horizons N, no feasible solution for OLP-BDS could be found.

Investigation 2

In Figure 4.2(b) the control performance in terms of energy use of the five investigated strategies for different levels of $\alpha_{\mathbf{x},j}$ is depicted. The results are very similar to the one of Investigation 1, i.e. QF is superior to BDS and CLP is better than OLP. The applied energy is less in this investigation since additional heat gains were introduced due to the outside temperature, solar radiation, and internal gains. Figure 4.3(b) and Figure 4.4(b) show the room temperature profile and the heating input respectively. Here, the effect of the varying outside weather conditions can clearly be seen. Again, the behavior of the controllers is qualitatively similar to the ones of Investigation 1.

Investigation 3

In Figure 4.5 the result of the randomized simulations is plotted. The comparison of the control performance in terms of energy use versus $\alpha_{\mathbf{x},j}$ is similar to the results

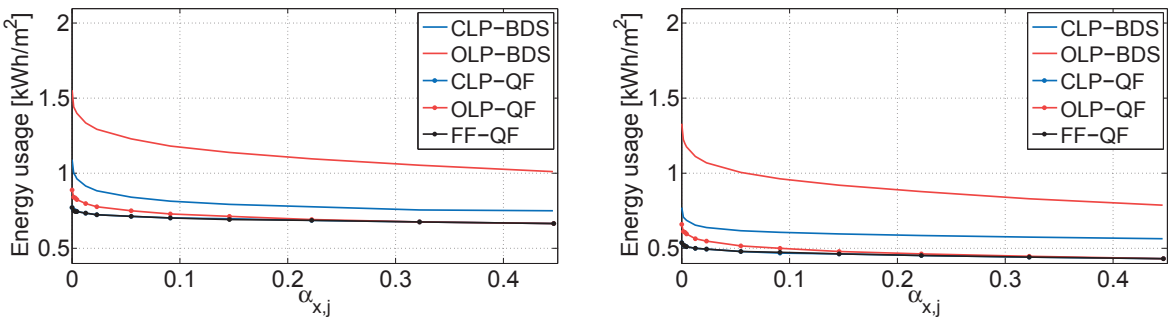

(a) Investigation 1 (b) Investigation 2

Figure 4.2: Energy use [Wh/m^2] versus $\alpha_{\mathbf{x},j}$.

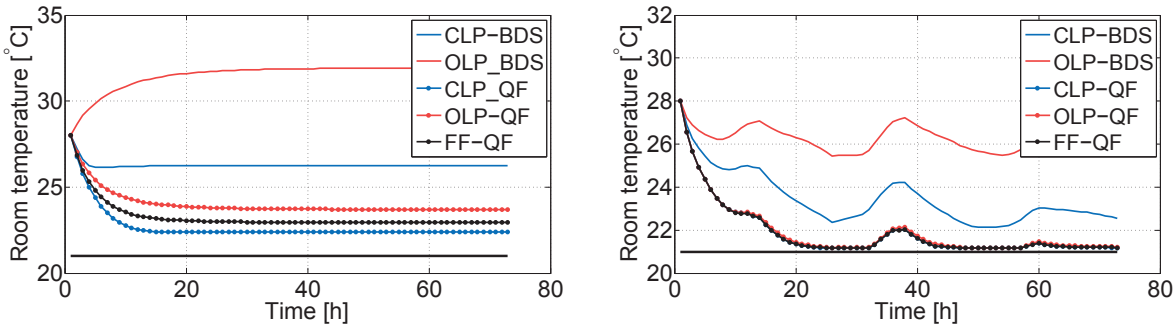

(a) Investigation 1 with $\alpha_{\mathbf{x},j} = 0.0003$ (b) Investigation 2 with $\alpha_{\mathbf{x},j} = 0.32$

Figure 4.3: Room temperature profile [°C].

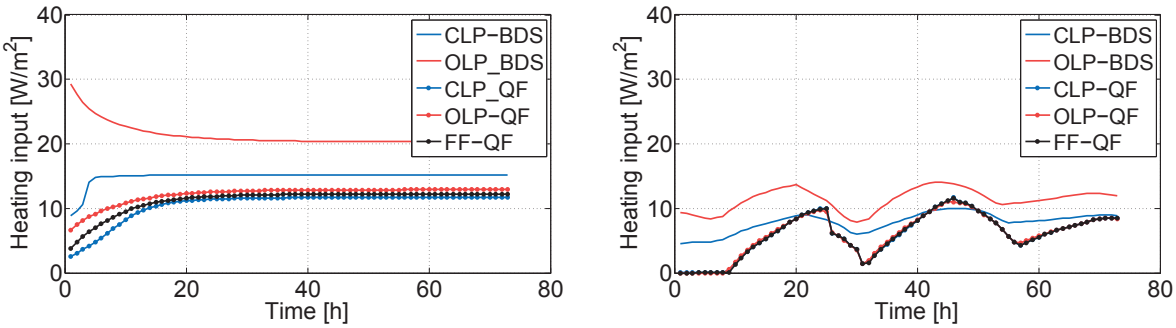

(a) Investigation 1 with $\alpha_{\mathbf{x},j} = 0.0003$ (b) Investigation 2 with $\alpha_{\mathbf{x},j} = 0.32$

Figure 4.4: Heating input [W/m^2].

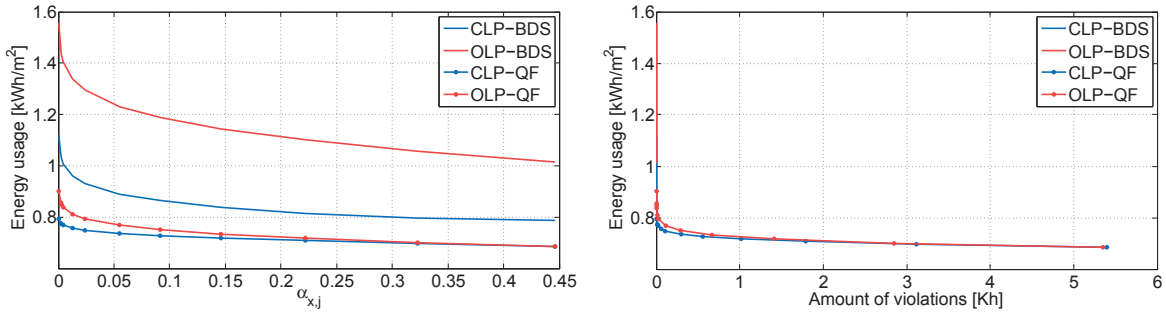

(a) Energy use [Wh/m^2] versus $\alpha_{\mathbf{x},j}$.

(b) Energy use [Wh/m^2] versus amount of violations.

Figure 4.5: Relation of energy use and probability of violations (predicted and realized).

from the first two investigations: QF is better than BDS and the closed-loop controllers outperform the open-loop controllers (Figure 4.5(a)). In Figure 4.5(b), the energy use is plotted against the average resulting amount of violations from the randomized study. For BDS, there was no violation at all, whereas for QF there were up to 7 Kh[1].

From the results, it can be concluded, that the QF formulation can be expected to outperform BDS, whereas with the FF-QF formulation, almost a similar performance as CLP-QF can be achieved, but it is computationally more tractable. Furthermore, it can be seen that the parameter α can be used as a tuning parameter in order to change the resulting amount of violations, which cannot a priori be determined. Therefore, FF-QF was further investigated and analyzed on a large-scale building example as described in Chapter 7.

4.6 Conclusions

A stochastic MPC formulation involving chance constraints was presented that is tractable for large-scale systems such as buildings. This formulation combines the use of Affine Disturbance Feedback with a tractable reformulation of the chance constraints. Three different reformulations of the chance constraints were proposed, one being exact and leading to second order cone constraints and the other two being approximations that are computationally less expensive. The proposed formulations were compared and analyzed on a small-scale example.

[1] 1 Kh denotes the violation by one Kelvin for one hour

5 Blocking Parameterization of Affine Disturbance Feedback MPC

5.1 Introduction

This chapter is concerned with solving a robust MPC problem for the class of constrained discrete-time linear systems subject to additive, but bounded disturbances. The MPC formulation uses the Affine Disturbance Feedback formulation already employed in Chapter 4, which shows a good performance. The computational complexity is, however, increased compared to open-loop prediction, because of a significant increase in the number of decision variables. The motivation for this chapter is to reduce the number of degrees of freedom of the Affine Disturbance Feedback parameterization for the purpose of reducing the computational complexity of the resulting MPC problem, and furthermore to investigate how to reduce the degrees of freedom in such a way as to maintain high control performance, but to guarantee strong feasibility.

5.1.1 Blocking for Reducing Computational Complexity

In order to reduce the computational complexity, it is common practice in nominal MPC to reduce the number of decision variables by fixing the input or its derivatives to be constant over several prediction steps [CGKM07]. Although this alleviates the computational burden, it renders terminal constraints incapable of enforcing strong feasibility and stability and often leads to sub-optimality. In [CGKM07] the authors propose to employ a time-varying blocking strategy such that stability can be guaranteed. In [GIK09, GI10] strong feasibility is guaranteed with a time-invariant blocking matrix by constraining the state at the first prediction step to a controlled invariant feasible set. In contrast to [CGKM07], this method is guaranteed to be least-restrictive. In order to simplify the computation of the controlled invariant feasible set, the approach from [GI10] is used, where a controlled invariant set is taken and the state constraints of the prediction problem are relaxed so as to render the controlled invariant set a controlled invariant feasible set.

5.1.2 Main Idea and Outline

The idea is to impose a structure on the disturbance feedback matrix in such a way that the resulting loss in performance is small. Furthermore, the method in [GI10] is extended to the robust case to guarantee strong feasibility.

In Section 5.2 the problem setting is given, the Affine Disturbance Feedback parameterization is formulated, and the MPC problem with an expectation-based cost function is stated. Section 5.3 introduces the concept of blocking for the Affine Disturbance Feedback matrix and explains how strong feasibility can be enforced. The proposed method is demonstrated in an illustrative example in Section 5.4 and a conclusion is given in Section 5.5.

5.2 Problem Setting

Consider the discrete-time linear time-invariant system

$$x_{t+1} = Ax_t + Bu_t + Ew_t \tag{5.1}$$

with state $x_t \in \mathbb{R}^{n_x}$, control input $u_t \in \mathbb{R}^{n_u}$, and disturbance $w_t \in \mathbb{R}^{n_w}$.

Assumption 5.1. The pair (A, B) is stabilizable.

Control input u and state x must satisfy constraints

$$u_t \in \mathbb{U} \subset \mathbb{R}^{n_u} \quad \forall\, t \in \mathbb{N} \tag{5.2}$$

$$x_t \in \mathbb{X} \subset \mathbb{R}^{n_x} \quad \forall\, t \in \mathbb{N}\ . \tag{5.3}$$

Assumption 5.2. Disturbances satisfy $w_t \in \mathbb{W} \subset \mathbb{R}^{n_w} \quad \forall\, t \in \mathbb{N}$.

Assumption 5.3. Constraint sets $\mathbb{X}$, $\mathbb{U}$ and $\mathbb{W}$ have non-empty interiors and are polytopic, time-invariant, and known.

5.2.1 Affine Disturbance Feedback Input Parameterization

Define $\mathbf{x}_t$, $\mathbf{u}_t$ and $\mathbf{w}_t$ as in (4.4)-(4.6) and prediction dynamics matrices $\mathbf{A}$, $\mathbf{B}$ and $\mathbf{E}$ such that

$$\mathbf{x}_t = \mathbf{A}x_t + \mathbf{B}\mathbf{u}_t + \mathbf{E}\mathbf{w}_t\ . \tag{5.4}$$

Assumption 5.4.

$$\begin{aligned} \mathbf{w}_t &\in \mathbb{W}^N && (5.5)\\ \mathrm{E}\left[\mathbf{w}_t\right] &:= \bar{\mathbf{w}}_t \in \mathbb{R}^{n_w N} && (5.6)\\ \mathrm{E}\left[(\mathbf{w}_t - \bar{\mathbf{w}}_t)(\mathbf{w}_t - \bar{\mathbf{w}}_t)^{\mathrm{T}}\right] &:= \Sigma_t = \Sigma_t^{\mathrm{T}} \in \mathbb{R}^{n_w N \times n_w N} \ . && (5.7) \end{aligned}$$

Note that the predicted disturbance trajectories $\mathbf{w}_t$ as well as their stochastic properties $\bar{\mathbf{w}}_t$ and Σ_t may change from one time step to the next. The stochastic properties are assumed known, the disturbances themselves not. The constraint set $\mathbb{W}^N$ is time-invariant and known by Assumption 5.3.

In Affine Disturbance Feedback MPC [GKM06, OJM08] the control input trajectory $\mathbf{u}$ is parameterized such that

$$u_{t+k|t}(\mathbf{w_t}) := \sum_{i=0}^{k-1} M_{(t+k,\,t+j)|t} w_{t+j|t} + h_{t+k|t} \ , \quad k \in \mathbb{N}_0^{N-1} \ , \tag{5.8}$$

with $M_{(t+k,\,t+i)|t} \in \mathbb{R}^{n_u \times n_w}$ and $h_{t+k|t} \in \mathbb{R}^{n_u}$. Using (4.19) we can write

$$\mathbf{u}_t = \mathbf{M}_t \mathbf{w}_t + \mathbf{h}_t \ . \tag{5.9}$$

Consider the quadratic cost function

$$J(x_t, \mathbf{M}_t, \mathbf{h}_t, \mathbf{w}_t) := \mathbf{x}_t^{\mathrm{T}} \mathbf{Q} \mathbf{x}_t + (\mathbf{M}_t \mathbf{w}_t + \mathbf{h}_t)^{\mathrm{T}} \mathbf{R} (\mathbf{M}_t \mathbf{w}_t + \mathbf{h}_t) \ , \tag{5.10}$$

where $\mathbf{Q} \in \mathbb{R}^{n_x(N+1) \times n_x(N+1)}$, $\mathbf{Q} = \mathbf{Q}^{\mathrm{T}} \succeq 0$ and $\mathbf{R} \in \mathbb{R}^{n_u N \times n_u N}$, $\mathbf{R} = \mathbf{R}^{\mathrm{T}} \succ 0$ contain all stage and terminal costs, and further consider state and input constraints

$$\begin{aligned} \mathbf{u}_t &\in \mathbb{U}^N && (5.11)\\ \mathbf{x}_t &\in \mathbb{X}^{N+1} \ . && (5.12) \end{aligned}$$

For state x_t the set of admissible Affine Disturbance Feedback policies $(\mathbf{M}_t, \mathbf{h}_t)$ is then given by the set

$$\Pi(x_t) := \left\{ (\mathbf{M}_t, \mathbf{h}_t) \middle| \begin{array}{l} \mathbf{M}_t \text{ satisfies (4.19)}, \\ \mathbf{A} x_t + \mathbf{B} \mathbf{h}_t + (\mathbf{B} \mathbf{M}_t + \mathbf{E}) \mathbf{w}_t \in \mathbb{X}^{N+1} \\ \mathbf{M}_t \mathbf{w}_t + \mathbf{h}_t \in \mathbb{U}^N \quad \forall \mathbf{w}_t \in \mathbb{W}^N \end{array} \right\} . \tag{5.13}$$

The objective in this chapter is to apply a blocking parameterization of the decision variables to reduce the computational complexity of the MPC problem (Section 5.3). Terminal costs and constraints can be chosen such that the closed-loop system resulting from a non-blocking Affine Disturbance Feedback MPC controller is input-to-state

stable [GKM06]. Unfortunately, a priori stability guarantees are lost when employing blocking parameterizations. The emphasis of this work is on guaranteeing strong feasibility of the MPC problem. Strong feasibility is independent of the cost function and depends only on the system dynamics and constraints. Constraints to enforce strong feasibility are developed in Section 5.3.2. Next, the MPC problem is formulated.

5.2.2 Expectation Based Disturbance Feedback MPC Problem

The optimal control input is determined by solving MPC Problem 5.5.

Problem 5.5 (Expectation based ADF MPC).

$$\left(\mathbf{M}_t^*(x_t), \mathbf{h}_t^*(x_t)\right) := \arg \min_{(\mathbf{M}_t, \mathbf{h}_t) \in \Pi(x_t)} \mathrm{E}\left[J(x_t, \mathbf{M}_t, \mathbf{h}_t, \mathbf{w}_t)\right]$$

Remark 5.6. The expectation $\mathrm{E}\left[J\right]$ of the quadratic cost is employed as the optimization objective. Thus the stochastic properties $(\bar{\mathbf{w}}_t, \Sigma_t)$ of disturbance trajectory $\mathbf{w}_t$ are taken into account, even though they do not appear explicitly in MPC Problem 5.5. More commonly the nominal cost is used, which is equivalent to the expectation with $\bar{\mathbf{w}}_t = 0 \wedge \Sigma_t = 0$.

The optimal control input $u_{t|t}^*(x_t)$ is given by

$$u_{t|t}^*(x_t) = h_{t|t}^*(x_t)$$

and the closed-loop state trajectory evolves according to

$$x_{t+1} = Ax_t + Bu_{t|t}^*(x_t) + Ew_t \ .$$

MPC Problem 5.5 can be reformulated into a standard QP problem, where the optimization variables are the vector $\mathbf{h}_t$ of offsets and a vector $\bar{\mathbf{m}}_t \in \mathbb{R}^{\frac{n_u n_w N(N-1)}{2}}$, which contains all decision variables of disturbance feedback matrix $\mathbf{M}_t$.

Remark 5.7. The number of decision variables of the MPC problem with Affine Disturbance Feedback is of order N^2 due to disturbance feedback matrix $\mathbf{M}_t$. The number of decision variables for open-loop prediction MPC is only of order N.

Remark 5.8. An open-loop prediction MPC problem can easily be derived from MPC Problem 5.5 by forcing $\mathbf{M}_t = 0$ in both the cost function J and the constraints Π. A consequence of this is that the set of feasible solutions of the open-loop prediction MPC problem is a subset (usually a strict subset) of the set of feasible solutions of the Affine Disturbance Feedback MPC problem. Thus closed-loop prediction MPC is expected to outperform open-loop prediction MPC. However, no statements about closed-loop performance can be made until after controller verification.

5.3 Complexity Reduction via Blocking

5.3.1 Blocking Parameterization

To reduce the computational complexity of MPC Problem 5.5, the number of decision variables is reduced by employing a method called *blocking*. Traditionally, a method called *move-blocking* is used in controller design, where the predicted control input trajectory is restricted to be constant over sets of multiple prediction steps (and hence blocking control moves) [CGKM07]. In this work the term *blocking* is used to mean that a vector of decision variables is parameterized by a lower-dimensional vector of decision variables in combination with a so-called *blocking matrix*, which forces some structure upon the original vector of decision variables.

Let $\bar{\mathbf{m}}_t$ denote a vector that contains the decision variables of $\mathbf{M}_t$, and let $\bar{\mathbf{m}}_t$ be parameterized by blocking matrix Λ and a vector $\tilde{\mathbf{m}}_t$ according to:

$$\bar{\mathbf{m}}_t = \Lambda \tilde{\mathbf{m}}_t \tag{5.14}$$

$$\tilde{\mathbf{m}}_t \in \mathbb{R}^{\nu} \qquad \Lambda \in \{0,1\}^{\frac{n_u n_w N(N-1)}{2} \times \nu} \tag{5.15}$$

$$\nu \in \mathbb{N} \qquad \nu \leq \frac{n_u n_w N(N-1)}{2} \ . \tag{5.16}$$

Blocking matrix Λ and dimension ν are design parameters and can be manipulated to affect the complexity of the blocked MPC problem. In this work only the disturbance feedback matrix $\mathbf{M}_t$ is parameterized, as opposed to the offset vector $\mathbf{h}_t$ also. One reason for this is that $\mathbf{M}_t$ has the most decision variables, in general. Furthermore, by parameterizing $\mathbf{M}_t$ only, the set of feasible solutions of the blocked MPC problem is still guaranteed to be a superset (usually strict superset) of the set of feasible solutions of the open-loop prediction MPC problem, (see Remark 5.8).

Remark 5.9. Based on numerical trials it appears that an effective blocking strategy in many instances is to let $\mathbf{M}_t$ have the same sub-matrix blocks $M_{(t+k,\,t+j)|t}$ along the diagonals, such that $M_{(t+k+1,\,t+j+1)|t} = M_{(t+k,\,t+j)|t}$. Each of the $n_u n_w$ elements within the block is a decision variable. This reduces the total number of decision variables of $\mathbf{M}_t$ to $n_u n_w (N-1)$. This diagonal structure implies that the disturbance feedback policy is time-invariant with respect to prediction time k.

5.3.2 Prediction Constraint Relaxation

The purpose of this section is to apply the method proposed in [GI10] for designing nominal, least-restrictive (see Definition 3.28), strongly feasible (see Definition 3.27) blocking MPC problems to the robust Affine Disturbance Feedback setting. In non-

blocking MPC problems, Affine Disturbance Feedback or not, strong feasibility is usually enforced by constraining the state $x_{t+N|t}$ of the final prediction step to a robust controlled invariant set [Bla99,GKM06,MRRS00b]. This assumes that the shifted solution from the previous step is an admissible solution for the current step, up to but not including the final control move, and that subsequently the existence of the final control move is guaranteed by the robust invariant terminal constraints. When employing blocking this assumption no longer holds, firstly because due to the structure imposed on disturbance feedback matrix $\mathbf{M}_t$ the shifted solution from the previous step may not be an admissible solution at the current step. Secondly, even if it were, the final control move may not be free to be chosen, as it may be dependent on the previous control moves, depending on the particular blocking matrix Λ selected.

The outline of the proposed procedure is as follows. To enforce strong feasibility of the MPC problem its constraints must directly enforce that the state at the next step remains within the feasible set, recursively. Thus the state $x_{t+1|t}$ of the first prediction step is explicitly constrained to a it robust controlled invariant (RCI) set (see Definition 3.20), as it is then known that an admissible control input trajectory which recursively satisfies these constraints exists. However, feasibility of the blocked MPC problem is not guaranteed for each element of a robust controlled invariant set, because due to the blocking scheme the predicted state constraints may no longer be satisfiable. Therefore the prediction state constraints of steps beyond the first prediction step are relaxed, i.e. expanded, in a minimal way so as to admit a feasible solution to the MPC problem for each element of the robust controlled invariant set. Despite the relaxed prediction state constraints the constraints on the first prediction step enforce constraint satisfaction of the closed-loop state trajectory.

Denote by $\mathcal{X} \subset \mathbb{X}$ a robust controlled invariant (RCI) set for system (5.1) subject to constraints (5.2)-((5.3)) and with $\mathcal{X}^* \subset \mathbb{X}$ the *maximum* robust controlled invariant (MRCI) set (see Definition 3.21).

It is implied throughout this work that disturbance constraint set $\mathbb{W}$ is small enough such that $\mathcal{X}^* \neq \emptyset$. If this does not hold then any attempt at controller design is futile. Furthermore, $\mathcal{X}^*$ is convex and bounded under Assumption 5.3. Thus, if $\mathcal{X}^*$ is not a polytope then it can be inner-approximated arbitrarily closely by a polytope. To facilitate a computationally viable controller design procedure make Assumption 5.10.

Assumption 5.10 (MRCI set is polytope). MRCI set $\mathcal{X}^*$ has been determined and is given by the polytope

$$\mathcal{X}^* := \{x \in \mathbb{R}^{n_x} | Yx \leq y\} \ , \tag{5.17}$$

the number of vertices of $\mathcal{X}^*$ is $\kappa \in \mathbb{N}_+$, and vertices $\mathscr{V}_j \in \mathbb{R}^{n_x}$ $\forall j \in \mathbb{N}_1^\kappa$ have been computed.

Remark 5.11. The set $\mathcal{X}^*$ is employed to design strongly feasible MPC problems which contain blocking parameterizations. In fact the employed set need not be MRCI set $\mathcal{X}^*$, *any* robust controlled invariant set suffices. However, use of $\mathcal{X}^*$ results in a *least-restrictive*, strongly feasible MPC problem. If the particular control problem at hand permits a restrictive controller then a non-maximum robust controlled invariant set can replace $\mathcal{X}^*$. In such cases subsequent results on least-restrictiveness do not apply. Subsequent results on strong feasibility do apply.

Let $\mathbb{X} := \{x \in \mathbb{R}^{n_x} | Gx \leq g\}$, $G \in \mathbb{R}^{r \times n_x}$, $g \in \mathbb{R}^r$, i.e. prediction state constraints (5.12) are stated explicitly as

$$Gx_{t+k|t} \leq g \quad \forall k \in \mathbb{N}_0^N \ . \tag{5.18}$$

The aim is to compute the minimal prediction constraint relaxations $\zeta_k \in \mathbb{R}^r \wedge \zeta_k \geq 0 \ \forall k \in \mathbb{N}_2^N$ such that when the prediction state constraints enforced in the MPC problem are

$$Yx_{t+1|t} \leq y \tag{5.19}$$

$$Gx_{t+k|t} \leq g + \zeta_k \quad \forall k \in \mathbb{N}_2^N \ , \tag{5.20}$$

then the resulting MPC problem is feasible for every element x_t of the MRCI set $\mathcal{X}^*$. Robust controlled invariant constraint (5.19) directly enforces recursive constraints satisfaction of the actual closed-loop state trajectory. State constraints for prediction steps $k \in \mathbb{N}_2^N$ can be relaxed arbitrarily. To maintain good cost performance it is desirable to relax the prediction state constraints in a minimal way. Here, minimality is with respect to the 2-norm. Let

$$\zeta_{t+k} := \left[\zeta_{t+k,2}^{\mathrm{T}}, \ldots, \zeta_{t+k,N}^{\mathrm{T}}\right]^{\mathrm{T}} \in \mathbb{R}^{r(N-1)} \tag{5.21}$$

$$\mathbb{X}_{t+k} := \{x \in \mathbb{R}^{n_x} | Gx \leq g + \zeta_{t+k}\} \quad \forall k \in \mathbb{N}_2^N \tag{5.22}$$

$$\mathscr{X} := \mathbb{X} \times \mathcal{X}^* \times \mathbb{X}_{t+2} \times \cdots \times \mathbb{X}_{t+N} \ , \tag{5.23}$$

where $\mathbb{X}_k$ denotes the relaxed prediction state constraint set for prediction step k, and $\mathscr{X}$ is the resulting constraint set for the entire predicted state trajectory $\mathbf{x}_t$. The minimal relaxation ζ^* is given by the solution of QP Problem 5.12.

Problem 5.12 (Minimal constraint relaxation).

$$\zeta^* := \arg \min_{\zeta \in \mathbb{R}^{r(N-1)}} \zeta^{\mathrm{T}} \zeta \tag{5.24}$$

subject to

$$\forall j \in \mathbb{N}_1^{\kappa} \quad \exists (\tilde{\mathbf{m}}_t, \mathbf{h}_t) \quad \text{subject to} \tag{5.25}$$

$$Y\left(A\mathscr{V}_j + Bh_{t|t} + Ew_t\right) \leq y \tag{5.26}$$

$$\mathbf{A}\mathscr{V}_j + \mathbf{B}\mathbf{h}_t + (\mathbf{B}\mathbf{M}_t + \mathbf{E})\mathbf{w}_t \in \mathscr{X} \tag{5.27}$$

$$\mathbf{M}_t\mathbf{w}_t + \mathbf{h}_t \in \mathbb{U}^N \qquad \forall \mathbf{w}_t \in \mathbb{W}^N \ , \tag{5.28}$$

where $\mathbf{M}_t$ results from $\tilde{\mathbf{m}}_t$ and blocking strategy (5.14).

The constraints of Problem 5.12 enforce that for each vertex $\mathscr{V}_j$ of MRCI set $\mathcal{X}^*$ there exists an admissible blocked feedback policy $(\tilde{\mathbf{m}}_t, \mathbf{h}_t)$. Problem 5.12 can be reformulated as a QP problem.

Note that finding ζ^* requires simultaneous optimization over each vertex $\mathscr{V}_j$ of $\mathcal{X}^*$. Thus Problem 5.12 is very large for a large number of vertices. An *outer-approximation* can be determined at much lower computational cost by finding a minimal relaxation ζ for each vertex $\mathscr{V}_j$ in turn, then *maximizing* over those solutions. Note that under-approximations of ζ^* are not suitable. Also note that all further results hold when employing outer-approximations.

Theorem 5.13 *Problem 5.12 admits a feasible solution.*

Proof:
Constraint (5.26) implies robust controlled invariance. As the pair (Y, y) describes MRCI set $\mathcal{X}^*$ the existence of a suitable $h_{t|t}$ is guaranteed trivially. Next, because disturbance trajectory constraint set $\mathbb{W}^N$ is bounded the predicted state trajectory $\mathbf{x}_t$ from *any* vertex $\mathscr{V}_j$, for *any* disturbance sequence $\mathbf{w}_t \in \mathbb{W}^N$ and for *any* feedback policy $(\mathbf{M}_t, \mathbf{h}_t)$, is bounded. Thus starting from vertex $\mathscr{V}_j$ there exists a ζ satisfying $\zeta^{\mathrm{T}}\zeta < \infty$ such that $\mathbf{x}_t \in \mathscr{X}$ $\forall j \in \mathbb{N}_1^{\kappa}$. ■

Let $\mathscr{X}^*$ be the minimally relaxed constraint set for predicted state trajectory $\mathbf{x}_t$, analogously as in ((5.23)). Incorporating prediction constraint relaxations the set $\tilde{\Pi}$ of admissible blocked disturbance feedback policies is given by

$$\tilde{\Pi}(x_t) := \left\{ (\tilde{\mathbf{m}}_t, \mathbf{h}_t) \middle| \begin{array}{l} \mathbf{A}x_t + \mathbf{B}\mathbf{h}_t + (\mathbf{B}\mathbf{M}_t + \mathbf{E})\mathbf{w}_t \in \mathscr{X}^* \\ Y(Ax_t + Bh_{t|t} + Ew_t) \leq y \\ \mathbf{M}_t\mathbf{w}_t + \mathbf{h}_t \in \mathbb{U}^N \quad \forall \mathbf{w}_t \in \mathbb{W}^N \end{array} \right\} \tag{5.29}$$

where $\mathbf{M}_t$ results from $\tilde{\mathbf{m}}_t$ and blocking strategy (5.14).

The set $\tilde{\mathcal{X}}_0$ for which an admissible blocked affine disturbance feedback policy $(\tilde{\mathbf{m}}, \mathbf{h})$ exists is given by

$$\tilde{\mathcal{X}}_0 := \left\{ x \in \mathbb{R}^{n_x} | \tilde{\Pi}(x) \neq \emptyset \right\} \ . \tag{5.30}$$

The MPC problem with constraint relaxations is given by MPC Problem 5.14, where the only difference is the set of the admissible blocked disturbance feedback policies. The prediction cost function remains unchanged.

Problem 5.14 (Blocking parameterization of ADF MPC).

$$\left(\tilde{\mathbf{m}}_t^*(x_t), \mathbf{h}_t^*(x_t)\right) := \arg \min_{(\tilde{\mathbf{m}}_t, \mathbf{h}_t) \in \tilde{\Pi}(x_t)} \mathrm{E}\left[J(x_t, \mathbf{M}_t, \mathbf{h}_t, \mathbf{w}_t)\right] \tag{5.31}$$

where $\mathbf{M}_t$ results from $\tilde{\mathbf{m}}_t$ and blocking strategy (5.14).

Theorem 5.15 *The following statements hold:*
(1) $\tilde{\mathcal{X}}_0 = \mathcal{X}^*$
(2) *MPC Problem 5.14 is strongly feasible.*
(3) *MPC Problem 5.14 is a least-restrictive MPC problem for system* (5.1) *subject to constraints* (5.3).

Proof:
(1) A formal proof is omitted, but this follows from the convexity of $\mathcal{X}^*$, $\mathbb{U}$, $\mathbb{X}$, $\mathbb{W}$, and from linearity of system (5.1). We first show that $\tilde{\mathcal{X}}_0 \supseteq \mathcal{X}^*$. Any $x \in \mathcal{X}^*$ can be written as a convex combination of the vertices $\mathscr{V}_j$ of $\mathcal{X}^*$. Problem 5.12 determines the relaxation ζ^* such that a feedback policy $(\tilde{\mathbf{m}}_t, \mathbf{h}_t)$ which satisfies the prediction constraints exists $\forall j \in \mathbb{N}_1^\kappa$. For all states $x \in \mathcal{X}^*$ there then exists a convex combination of these feedback policies which is admissible. We next show that $\tilde{\mathcal{X}}_0 \subseteq \mathcal{X}^*$. Constraint (5.26) explicitly forces $\tilde{\mathcal{X}}_0$ to be a robust controlled invariant set. Thus clearly it must be a subset of maximum controlled invariant (MCI) set $\mathcal{X}^*$.
(2) For any initial state $x_t \in \mathcal{X}^*$ the constraint set $\mathscr{X}^*$ directly enforces that $x_{t+1|t} \in \mathcal{X}^*$ for any admissible feedback policy $(\tilde{\mathbf{m}}_t, \mathbf{h}_t) \in \tilde{\Pi}(x_t)$ and despite any admissible disturbance $\mathbf{w}_t \in \mathbb{W}^N$. By induction this holds recursively.
(3) By the definition of MRCI set $\mathcal{X}^*$ a strongly feasible MPC problem with a feasible set larger than $\mathcal{X}^*$ cannot exist. Thus, due to Theorem 5.15 (1) above, MPC Problem 5.14 is least-restrictive. ■

Remark 5.16. The proposed method is especially beneficial for long prediction horizons N, since the computational complexity of Affine Disturbance Feedback grows with the order of N^2 whereas the computation of the robust controlled invariant set does not depend on N and moreover has to be performed just once and offline.

5.3.3 Reduction of Computational Complexity

As mentioned previously, the Affine Disturbance Feedback MPC is computationally demanding for a large number of inputs n_u, disturbances n_w, but most importantly for long prediction horizons N, since the number of decision variables depends on N^2. For the proposed procedure in contrast, the computation of the robust controlled invariant feasible set is done offline and only once before the actual control phase starts.

Hence the computational complexity is not so critical in this case. Furthermore, the robust controlled invariant set is computed before and independently of the constraint relaxation procedure. Thus, the offline computation is tractable also for large prediction horizons N, since the computation of the robust controlled invariant set does not depend on the horizon length.

In order to compare the online computational complexity, one has to also look at the constraints. Blocking of Affine Disturbance Feedback MPC can, depending on the blocking scheme, lead to a significant reduction in decision variables. For the proposed procedure, there are, however, constraints added to ensure that the first predicted state is constrained to the robust controlled invariant feasible set. A more complex polytopic description of the robust controlled invariant feasible set hence leads to more constraints and increases again the computational complexity. The complexity of the robust controlled invariant feasible set, however, does not depend on N, n_u or n_w, but just on the dimension of the state and the dynamics.

This means that for systems with small and medium state dimensions, the computational complexity can be reduced especially for large prediction horizons N. If the state dimensions are large it can happen with certain dynamics that the resulting polytope describing the robust controlled invariant feasible set is complex and hence one would need to introduce a lot of constraints to require the first predicted state to lie within the robust controlled invariant feasible set. In this case, however, one could solve the problem by not taking the maximum robust control invariant feasible set but an robust controlled invariant feasible set lying inside of the maximum one with a simpler representation.

5.4 Numerical Example

This example is originally made up by R. Gondhalekar [OGJM09] and is used here to illustrate the proposed blocking strategies. A man of mass $m_1 = 70\,\text{kg}$ is walking his dog of mass $m_2 = 10\,\text{kg}$ along a $3\,\text{m}$ wide sidewalk. To the right of the sidewalk is a road, to the left a muddy field. In the field, $6\,\text{m}$ from the edge of the sidewalk, is a cat. The dog notices the cat and attempts to attack it. Luckily for the cat, the dog's leash is shorter than the distance from the edge of the field to the cat. The dog is pulling on the leash in order to get to the cat. However, the man does not want to get muddy shoes, therefore pulls the dog back in order to avoid being pulled into the field. He cannot pull back too far as he must avoid entering the road to the rear.

A model of this problem is depicted in Figure 5.1. The man's position is denoted by x. A position $x > x_{\max} = 9$ m implies the man is on the road, whereas $x < x_{\min} = 6$ m

implies he is in the field. Any position $x_{\min} \leq x \leq x_{\max}$ is acceptable. Furthermore, any speed $|\dot{x}| \leq 1$ m s^{-1} is allowed. The force the man exerts on himself is denoted by u, and must satisfy $|u| \leq 0.5 m_1 g$, with $g = 9.81$ m s^{-2}, i.e. the man can exert a force of half his body weight in either direction. The desire of the dog to attack the cat is denoted by the linear spring with $\kappa = 2m_2 g / x_{\min} = 32.73$ N m^{-1}, i.e. when the man is at the edge of the sidewalk the dog is able to exert a steady state force of twice her body weight on the man. In addition to this steady state force the dog is able to exert an unpredictable disturbance force w, which is bounded by $0 \leq w \leq m_2 g$, i.e. positive and less than the body weight of the dog. The continuous-time dynamics are given by

$$\begin{bmatrix} \dot{x} \\ \ddot{x} \end{bmatrix} = \begin{bmatrix} 0 & 1 \\ \frac{-\kappa}{m_1} & 0 \end{bmatrix} \begin{bmatrix} x \\ \dot{x} \end{bmatrix} + \begin{bmatrix} 0 \\ \frac{-1}{m_1} \end{bmatrix} u + \begin{bmatrix} 0 \\ \frac{-1}{m_1} \end{bmatrix} w \tag{5.32}$$

and are discretized with a step-size of 0.1 s.

The objective is to design a robust MPC controller for the force input u the man applies to himself using $R = 1$ and $Q = 0.1 \cdot \mathbf{I}_{\{2\}}$. This implies the man is mostly interested in using a low amount of energy, but does make some effort to move towards the cat. The cat remains seated at the origin throughout the entire course of events.

The MCI and MRCI sets for this problem are shown in Figure 5.2 and 5.3 by the lighter and darker sets, respectively.

Six control laws were considered. For each a horizon of $N = 15$ was employed.

<u>ADF:</u> Affine Disturbance Feedback. This is the standard affine disturbance feedback closed-loop MPC strategy. The feedback policy $(\mathbf{M}, \mathbf{h})$ is optimized. There are $n_u N + \frac{n_u n_w N(N-1)}{2}$ optimization variables. No prediction state constraint relaxations are applied. The terminal state is constrained to the maximum robust controlled invariant set.

<u>OLP:</u> Open-loop prediction. This is the standard robust open-loop MPC strategy. The predicted control input trajectory $\mathbf{u}$ is directly optimized. There are $n_u N$ optimization variables. No prediction state constraint relaxations are applied. The terminal state is constrained to the maximum robust controlled invariant set.

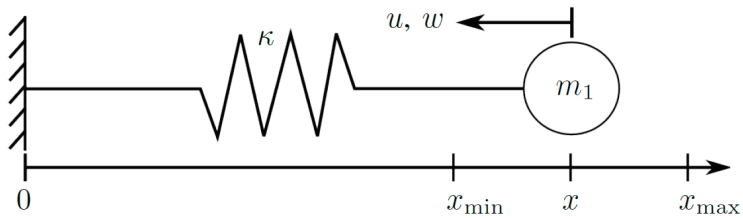

Figure 5.1: Dog walking schematic.

ADF-R: Relaxed Affine Disturbance Feedback. This is the proposed non-standard affine disturbance feedback closed-loop MPC strategy proposed. It is equivalent to setting blocking matrix $\Lambda = I$. The feedback policy $(\mathbf{M}, \mathbf{h})$ is optimized. There are $n_u N + \frac{n_u n_w N(N-1)}{2}$ optimization variables. Prediction state constraint relaxations are applied. The state of the first prediction step is constrained to the maximum robust controlled invariant set.

ADF-D: Diagonally blocked Affine Disturbance Feedback. This is the proposed non-standard Affine Disturbance Feedback closed-loop MPC strategy. It employs the diagonal blocking strategy mentioned in Remark 5.9. The feedback policy $(\tilde{\mathbf{m}}, \mathbf{h})$ is optimized. There are $n_u N + n_u n_w (N-1)$ optimization variables. Prediction state constraint relaxations are applied. The state of the first prediction step is constrained to the maximum robust controlled invariant set.

ADF-1: One degree of freedom blocked Affine Disturbance Feedback. This is the proposed non-standard Affine Disturbance Feedback closed-loop MPC strategy. It employs a blocking matrix $\Lambda = [1, \ldots, 1]^{\mathrm{T}}$, i.e. $\nu = 1$. This implies that each decision variable of $\mathbf{M}$ is forced to be the same. The feedback policy $(\tilde{\mathbf{m}}, \mathbf{h})$ is optimized. There are $n_u N + 1$ optimization variables. Prediction state constraint relaxations are applied. The state of the first prediction step is constrained to the maximum robust controlled invariant set.

ADF-0: Zero degree of freedom blocked Affine Disturbance Feedback. This is the proposed non-standard Affine Disturbance Feedback closed-loop MPC strategy. It employs a blocking matrix $\Lambda = 0$. This implies $\mathbf{M} = 0$, i.e. open-loop prediction. Only the offset vector $\mathbf{h}$ is optimized. There are $n_u N$ optimization variables. Prediction state constraint relaxations are applied. The state of the first prediction step is constrained to the maximum robust controlled invariant set.

Note that each of these strategies has the same number of prediction state and input constraints. Further note that the structure of {OLP, ADF} and {ADF-R, ADF-D, ADF-1, ADF-0} are different. In the former the terminal state, in the latter the state of the first prediction step, is constrained to the MRCI set. State constraint relaxations are applied for all strategies in the latter.

Plotted in Figure 5.2 are six state trajectories, one for each of the six control strategies, from initial state $x_0 = (7, 1)$. These simulations were performed without noise. This is to check the nominal performance of the controllers. Denote by $\bar{x}$ and $\bar{u}$ the steady state and control input, respectively, reached after 500 steps. Denote by T the average computation time per iteration, averaged over the 500 simulation steps. Further denote by V/V_{ADF} the ratio of steady state cost of the particular controller

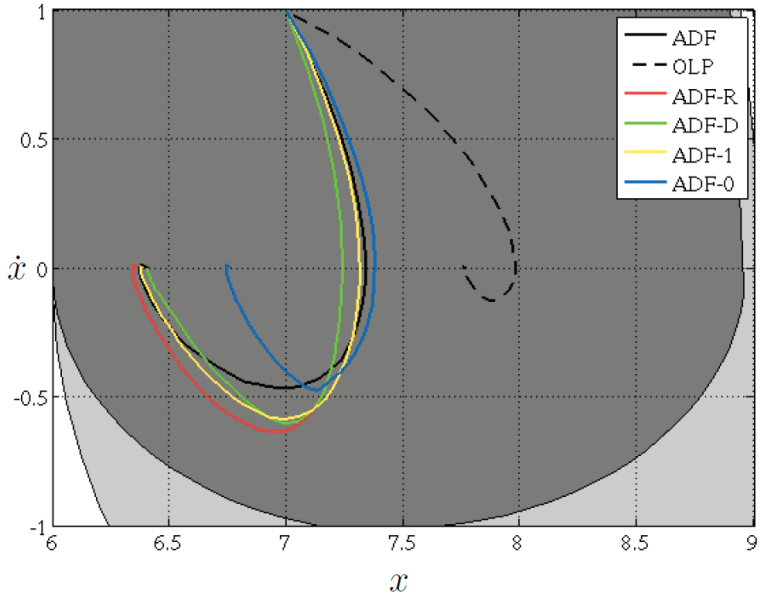

Figure 5.2: Nominal trajectories with proposed controllers. The MCI and MRCI sets for this problem are shown by the lighter and darker areas, respectively.

w.r.t. the steady state cost of the ADF controller. The obtained results are given in Table 5.1.

In Figure 5.3 all settings are kept the same except for the fact that a predefined disturbance sequence is applied. Here no steady state is reached since there is a persistent disturbance. All trajectories stay within the MRCI set.

5.5 Conclusions

It was shown that by employing blocking the computational complexity of Affine Disturbance Feedback can be reduced, especially for long prediction horizons, while retaining good performance and guaranteeing strong feasibility. Strong feasibility is guaranteed by enforcing the first predicted state to lie within a robust controlled invariant feasible set. For this an existing method was extended to the robust case and adapted for using with Affine Disturbance Feedback. Furthermore, it was shown that by imposing a structure on the feedback matrix the number of decision variables is reduced and so is subsequently the computational effort. For a small example it was shown that even with the limited degree of freedom, the performance achieved by blocked Affine Disturbance Feedback is still remarkably good and close to the unblocked case.

Table 5.1: Comparison of blocking schemes.

	$\bar{x}$	$\bar{u}$	T	V/V_{ADF}
ADF:	6.40	-209.6	0.710	1.000
OLP:	7.76	-254.1	0.571	1.470
ADF-R:	6.36	-208.2	0.611	0.986
ADF-D:	6.41	-209.7	0.585	1.001
ADF-1:	6.38	-209.0	0.578	0.994
ADF-0:	6.75	-221.1	0.572	1.113

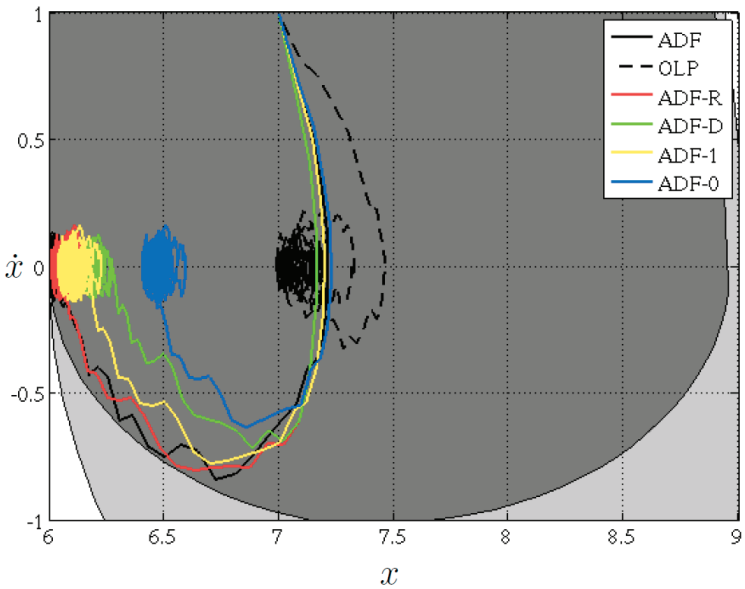

Figure 5.3: Disturbed trajectories with proposed controllers. The MCI and MRCI sets for this problem are shown by the lighter and darker areas, respectively.

Part III

Investigations in Building Climate Control

6 Simulation Environment

6.1 Introduction

Within the OptiControl project, large-scale simulation studies were carried out in close collaboration of Siemens Building Technologies, EMPA, MeteoSwiss, Gruner AG, and ETH Zurich. In the first part of this chapter (Sections 6.2 - 6.6) the modeling approach as well as the definitions, terminology, and simulations setups are introduced. These were determined within the project and are used in the simulations throughout this thesis. Note that the definitions, data collections (in particular of the weather and building parameters), and coding work are the result of a joint work of all project partners, which is also documented in more detailed form in [GE09]. The purpose of this part is to provide the reader of this thesis with the necessary background to understand the subsequent simulation studies. In the second part of this chapter (Sections 6.7 and 6.8) all control strategies and benchmarks are explained in detail and the implementation of MPC for building climate control is described. Section 6.9 provides a summary of all available simulation settings.

In the OptiControl project, the focus was on IRA, i.e. the integrated control of HVAC, blind positioning, and electric lighting of a room or building zone. The control task in IRA is to keep the room temperature-, illuminance-, and CO_2- levels within predefined comfort ranges while minimizing energy consumption. In IRA, there are both high energy cost actuators (e.g., chillers, gas boilers, conventional radiators) and low energy cost actuators (e.g., blind operation and evaporative cooling) available for heating and cooling. The aim is to exploit the use of the low energy cost actuators by making use of the thermal storage capacity of the building. Furthermore, IRA typically involves diverse technical equipment and hence results in a complex control task, where the use of MPC can be expected to provide large benefits compared to current control practice.

Concerning the building type, the focus was on office buildings for three reasons: first, they are the main building type equipped with IRA; second, they typically employ very energy-intensive HVAC systems and hence increasing the energy efficiency is of great importance; and third, they have relatively high internal gains that need to be handled appropriately.

IRA is concerned with the control of individual zones. A zone may be a single room or several rooms which are grouped and jointly actuated. In order to formulate a model, the approach in design tools like, e.g., SIA 382 [SIA] was followed and the focus was on an individual zone neglecting any interconnection or coordination with other zones. In order to determine the boundary conditions of the modeled zone, it was assumed that the neighboring zones are identical to the modeled zone. In the following, when it is referred to a building, a building zone is meant.

The model to be used for the presented simulations was required to be detailed enough on the one hand to represent the building dynamics, the energy usage, and all control relevant processes. On the other hand, the model was required not to be too complex, since it was supposed to be used both as a simulation model and in the MPC controller as a controller model for carrying out large-scale simulation studies. In [EN 09] a linear dynamic model is described, which is used for design and energy demand calculations of buildings. It is given as a simple 3-node thermal *resistance-capacitance* (RC) network. This model was however found to be not detailed enough for the described purposes. In contrast, the building models used in existing building simulation softwares (e.g., TRNSYS [sof11c], EnergyPlus [sof11b]) are very detailed, but cannot be readily used for control purposes. Therefore, a new model was developed that is detailed enough to be used as a simulation model and can also be used as a controller model.

The model is a lumped-parameter model, which assumes nodes in the room as well as in the walls, floor, and ceiling describing the respective temperatures. The heat transfer rate between two nodes ϑ_i and ϑ_e is then given by

$$\underbrace{\frac{dQ}{d\vartheta_i}}_{C_i} \cdot \frac{d\vartheta_i}{dt} = \underbrace{A \cdot U_{ie}}_{1/R_{ie}} (\vartheta_e - \vartheta_i) \ , \tag{6.1}$$

where t denotes the time, Q is thermal energy, and C_i denotes the thermal capacitance of layer i, A is the cross-sectional area, U_{ie} the heat transmission coefficient, and R_{ie} is the resistance between node i and e.

In Figure 6.1 the thermal RC network model is depicted. The influence of the actuators is modeled according to their heat transfer properties (e.g., the heating input from the radiator goes directly into the room node, whereas floor heating affects the room with some delay and therefore the control input from floor heating goes into the node in the floor). Note that for illustration purposes all considered subsystems are shown simultaneously in Figure 6.1. Control inputs are given in red, disturbances in blue. In the center, the room node ϑ_r is depicted, to its left the floor/ceiling slab with several resistances R and capacitances C. To its right, on top a facade wall with integrated windows and at the bottom, an internal wall representing all walls

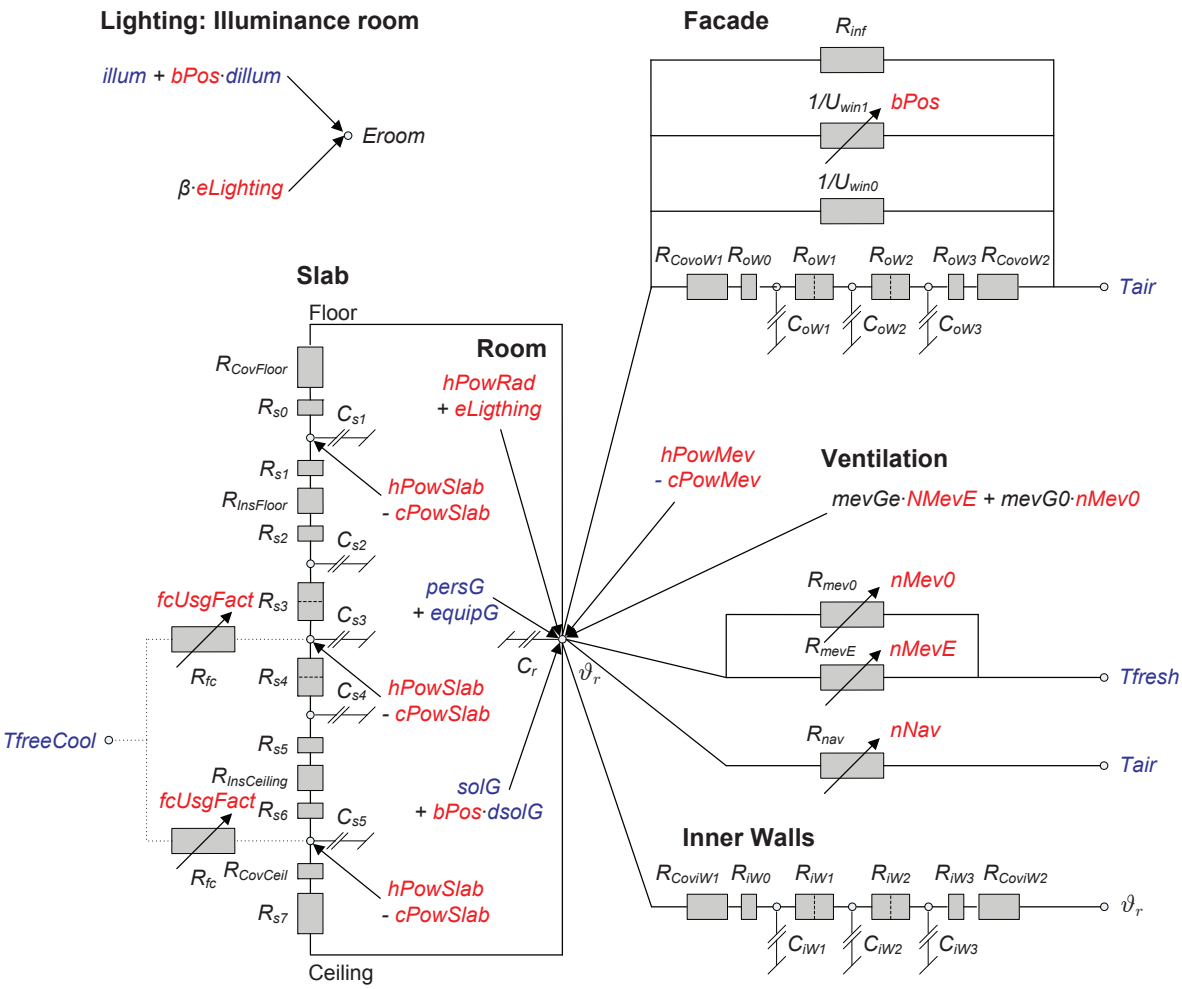

Figure 6.1: Thermal RC network model. ϑ_r denotes the room temperature. Control inputs are given in red and are explained in Section 6.3, disturbances are given in blue and are explained in Section 6.5, constants (and names) are given in black. Resistances are denoted with R, capacitances are denoted with C. Note that for illustration all considered subsystems are shown simultaneously.

to neighboring rooms. Neighboring rooms are assumed to have identical boundary conditions. Hence, there is no influence from neighboring rooms to the modeled room. Furthermore, the mechanical ventilation and the room illuminance are depicted in Figure 6.1. Note that the arrows at the resistances in the picture denote that the heat transmission coefficient is multiplied with a control input $\in [0, 1]$, i.e. the heat transmission coefficient is scaled to lie between 0 (resistance $= \infty$) and its full value.

In the following, all parameters and the parts of the model are detailed, i.e. the building types, that are leading to different resistances in the model (Section 6.2), the HVAC systems (Section 6.3), the control settings (Section 6.4), and the disturbances (Section 6.5).

6.2 Building Types

The building types considered in this study varied in terms of four parameters: *building standard* $\in$ {swiss average(sa), passive house(pa)}, *construction type* $\in$ {heavy(h), light(l)}, *window area fraction* $\in$ {high(wh), low(wl)}, and *facade orientation* $\in$ {North (N), South(S), South+East(SE), South+West(SW)}. Two example cases are shown in Figure 6.2.

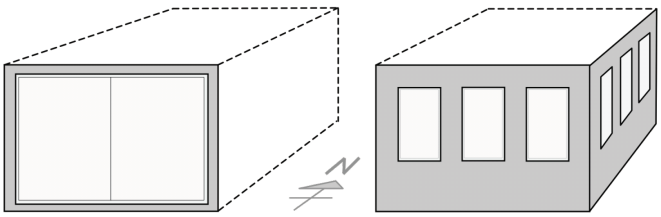

Figure 6.2: From: [LWD+09]. Schematic representation of two building zones. Left: window area fraction high, facade orientation South (normal office); right: window area fraction low, facade orientation South+West (corner office).

Let B :=(building standard, construction type, window area fraction, facade orientation) denote a particular combination of parameters, and let $\mathbb{B}$ denote the set of all possible combinations, with $\mathbb{B}$:= {(sa,h,wh,N), (pa,h,wh,N), (sa,l,wh,N,), (pa,l,wh,N),...}. An overview of the different building types is given in Table 6.1.

6.3 HVAC Systems

IRA deals with heating, ventilation, air-conditioning, blind positioning, and electric lighting of a building zone or room. In this section the various HVAC subsystems that are the actuators in the model depicted in Figure 6.1 are detailed, and five different HVAC systems, i.e. combinations of subsystems, that are considered in the simulation studies are presented (see Table 6.2).

Table 6.1: Building types differ in terms of four parameters.

Parameter	Value	Identifier
Building standard	Swiss average	sa
	Passive house	pa
Construction type	Heavy	h
	Light	l
Window area fraction	Low	wl
	High	wh
Facade orientation	North (normal office)	N
	South (normal office)	S
	South+East (corner office)	SE
	South+West (corner office)	SW

Blinds (bPos)

Blinds can be continuously controlled between fully closed and fully open (bPos $\in [0, 1]$). Physically this is achieved by pulling up and down the blinds or by rotating the slats. For corner offices, it is assumed that both windows have the same blind position. The blind positioning affects both the illuminance in the room as well as the heat transfer between the room and the outside. For this, the solar gains and solar illuminance are split into two parts (solG, illum) for closed blinds and (dSolG, dillum) for open blinds. For closed blinds (bPos = 0), only (solG, illum) are considered, whereas with open blinds (bPos = 1) additionally (dsolG, dillum) are considered, see Figure 6.1

Electric lighting (eLighting)

Electric lighting has primarily an effect on the illuminance in the room; the resulting illuminance is proportional to the power demand of the electric lighting ($\beta = 70\,\mathrm{lm/W}$). Besides, electric lighting also provides some heat gains into the room.

Mechanical ventilation with energy recovery (NMevE,NMev0), heating (hPowMev), cooling (cPowMev)

Mechanical ventilation is used to provide the room with fresh air and to guarantee indoor air quality (IAQ). The controlled variable is the air change rate, which describes the number of times that the air volume of the room is replaced per hour. Two modes of operation are considered. IAQoff: non-IAQ controlled ventilation with constant lower bound on the air change rate; IAQon: IAQ controlled ventilation with variable lower bound on the air change rate depending on occupancy (CO_2-level). For IAQoff, the

system is operated based on a the fixed working hour time schedule. Ventilation starts 1 h before working time and ends 1 h after. For IAQon, the ventilation depends on the occupancy profile. In both cases, the air change rate is limited to $n = 4.0\,\mathrm{h}^{-1}$ in order to prevent draft. Mechanical ventilation can also be used for heating (hPowMev) and cooling (cPowMev) and can be operated with (NMevE) or without (NMev0) energy recovery, i.e. preconditioning supply air with exhaust air via a heat exchanger.

Natural ventilation, night-time only (nNav)

Natural ventilation denotes the ventilation between room and outside air when the window is open. In this setup, natural ventilation is only used during night-time and is thermally driven. During occupancy hours, mechanical ventilation is used. This mixture of mechanical ventilation during day-time and natural ventilation during night-time is called hybrid ventilation.

Cooled ceiling (cPowSlab)

Cooled ceilings are capillary tube systems embedded in a gypsum layer and are directly mounted to the ceiling surface. Since they are thermally connected to the building structure, a considerable part is transferred to the building mass and released to the room with some delay.

Free cooling with wet cooling tower (fcUsgFact)

Free cooling with a wet cooling tower works by evaporative cooling and hence its efficiency depends on the wetbulb temperature. As can be seen from Figure 6.1, free cooling can be used continuously between fully or none (fcUsgFact $\in [0, 1]$). The distribution to the room is done either via the cooled ceiling or via TABS. Free cooling is not free of cost as the name suggests, but it uses less power than a conventional chiller.

Radiator heating (hPowRad)

For radiator heating a direct power input to the room node is assumed and no distribution system is considered.

Floor heating (hPowSlab)

Floor heating is slower than radiator heating, i.e. it is released to the room with a delay. This is modeled as direct power input into the first node in the floor, see Figure 6.1.

TABS: Thermally activated building system for heating (hPowSlab) and cooling (cPowSlab)

TABS are a generic term for systems which incorporate the building mass as thermal energy storage. It consists of a tube-system situated in the slabs and functions for both heating and cooling by pumping a heated or cooled medium through the slabs by which the storage is activated. In Figure 6.1 the TABS is entering the middle node in the slab. Note that also the cooled ceiling and floor heating can be seen as TABS systems and are modeled likewise.

Concerning the IRA application, five different variants with different automated subsystems were considered, an overview can be found in Table 6.2. All HVAC systems have automated blinds and electric lighting. *System 2* (S2) has mechanical ventilation, cooled ceiling, free cooling, and radiator heating. *System 1* (S1) is the same as System 2, but without mechanical ventilation. *System 3* (S3) is the same as System 2, but only with mechanical ventilation. *System 4* (S4) has mechanical and natural ventilation as well as floor heating and *System 5* (S5) has mechanical ventilation, free cooling, and TABS. Let $\mathbb{S}$ denote the set of available HVAC systems, with $\mathbb{S} := \{\mathrm{S1}, \mathrm{S2}, \mathrm{S3}, \mathrm{S4}, \mathrm{S5}\}$. A more detailed description of the different HVAC systems can be found in [LWC+09]. The dimensioning of the HVAC systems was based on calculations from the Swiss building standards, details can be found in Appendix A of [GE09].

Table 6.2: Five HVAC systems and their automated subsystems.

	HVAC system				
Automated subsystems	**S1**	**S2**	**S3**	**S4**	**S5**
Blinds	✓	✓	✓	✓	✓
Electric lighting	✓	✓	✓	✓	✓
Mech. ventilation, heating, cooling	-	✓	✓	✓	✓
Natural ventilation heating/cooling (night-time only)	-	-	-	✓	-
Cooled ceiling (capillary tube system)	✓	✓	-	-	-
Free cooling with wet cooling tower	✓	✓	-	-	✓
Radiator heating	✓	✓	-	-	-
Floor heating	-	-	-	✓	-
Thermally activated building systems for heating/cooling	-	-	-	-	✓

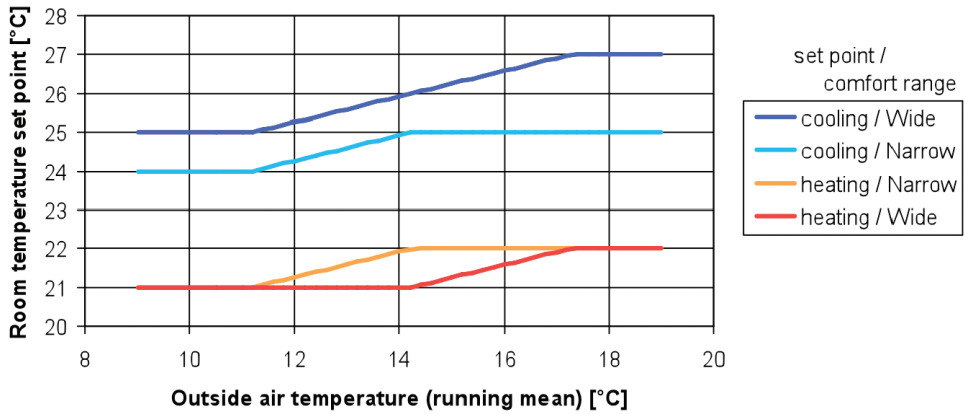

Figure 6.3: From: [LWD+09]. Room temperature set points for heating and cooling, and for the temperature comfort ranges narrow and wide.

6.4 Control Settings

In this section the control settings are defined, i.e. the control costs as well as the comfort constraints resulting from the allowed room temperature range, definition of setbacks, and ventilation.

Control Costs

In the simulations, energy was solely considered in the form of electrical energy. Two options for the cost were considered in the formulation of the MPC problem: First, the minimization of the *Non-Renewable Primary Energy* (NRPE) usage; and second, the minimization of the monetary cost. In order to describe these, as a first step the delivered energy was computed, which depends on the efficiency of the distribution subsystem as well as the energy generation/conversion system. The delivered energy for one time step is given by $\xi^T u_t \in \mathbb{R}$, where $u_t \in \mathbb{R}^{n_u}$ is a vector containing the energy uses of each actuator and $\xi \in \mathbb{R}^{n_u}$ is a scaling vector that takes into account the different efficiencies. Note that the delivered energy was assumed to depend linearly on the actuator use. As a second step, the delivered energy was then multiplied either with a conversion factor $c_{\text{NRPE}} \in \mathbb{R}$ in order to determine the NRPE usage or with $c_{\text{el},t} \in \mathbb{R}$, which is the price for electricity at time step t (possibly time-varying as for the investigation in Chapter 9) in order to determine the monetary cost. Hence, the *control costs* are $\in \{c_{\text{NRPE}}, c_{\text{el},t}\}$. Details of the computation of the control cost can be found in Appendix C of [GE09].

Table 6.3: Control settings.

Parameter	Value	Identifier
Control costs	NRPE	c_{NRPE}
	Monetary	$c_{\mathrm{el},k}$
Room temperature range	Narrow	nar
	Wide	wid
Setback	Setbacks on	SBon
	Setbacks off	SBoff
Ventilation	IAQ-controlled	IAQon
	Non-IAQ-controlled	IAQoff

Room Temperature Range

The room temperature is typically constrained to lie within the so-called *comfort range*, which is defined by a minimum and a maximum temperature. Two different options for the comfort range are used, *comfort range* $\in \{\text{narrow(nar)}, \text{wide(wid)}\}$. To determine the minimum and maximum temperatures, the temperature set points for heating and cooling were used, similar to [SIA06a]. The actual range at a given time instant was determined as a function of the exponentially weighted running mean of the past measured outside air temperature values, see Figure 6.3. The running mean was calculated similarly as in [EN 07], with the exception that hourly mean values were used instead of daily mean values.

Setback

For temperature, the two comfort ranges narrow and wide could be used with or without *setbacks*, i.e. a relaxation of the comfort constraints during non-working hours (widened comfort range of 12°C - 35°C during nights and weekends), hence *setbacks* $\in \{\text{setbacks on (SBon)}, \text{setbacks off (SBoff)}\}$. These setback definitions only apply for temperature constraints.

For illuminance, a lower bound of 500 lux was defined. This bound was only active during working hours. No upper bound was defined, instead, it was assumed that the user would be able to adjust an internal blind for glare protection in case of excessive solar radiation.

Ventilation

Two options were considered: First, *ventilation* is operated based on a time schedule

(IAQoff); second, ventilation is IAQ-controlled, i.e. the air change rate is adapted dynamically depending on the occupancy (IAQon). Hence, *ventilation* $\in$ {IAQon, IAQoff}. See also the description of mechanical ventilation.

In Table 6.3 an overview of the control settings is given. Let $A :=$ (control costs, room temperature range, setback, ventilation} denote a particular choice of parameters. And let $\mathbb{A}$ denote the set of all possible choices, with $\mathbb{A} := \{(c_{\mathrm{NRPE}}, \mathrm{nar}, \mathrm{SBon}, \mathrm{IAQon}), (c_{\mathrm{el},k}, \mathrm{nar}, \mathrm{SBon}, \mathrm{IAQon}), (c_{\mathrm{NRPE}}, \mathrm{wid}, \mathrm{SBon}, \mathrm{IAQon}), ...\}$.

6.5 Disturbances

A building is subject to a wide range of disturbances, amongst them the influence of neighboring rooms, weather, internal gains due to occupants and equipment, as well as occupant behavior. For the case of IRA, it is reasonable to assume that the user cannot directly change the actuators, but instead would communicate any requests to the control system via an interface. Therefore, the occupant behavior was not considered in this study. For the disturbances the focus was on weather and internal gains due to persons and equipment, which is detailed next.

Table 6.4: Sites for the weather measurements with a short description of the ambient weather and climate and their geographical heights.

Country	Site name	Abbrev.	Weather & climate	Height
Switzerland	Zurich-Fluntern	SMA	Swiss plateau climate with characteristic inversion conditions	556 m
	Lugano	LUG	Representative for the Swiss climate south of the Alps	273 m
France	Marseille Marignane	MSM	Mediterranean climate with total inflow from the Mediterranean Sea	5 m
Austria	Wien Hohe Warte	WHW	Plain with continental climate	209 m

6.5.1 Weather

The three weather variables that were considered in this study are: air temperature (equal to Tair and Tfresh in the model given in Figure 6.1), wet bulb temperature (equal to TfreeCool in the model), and solar radiation (used to compute solG, dsolG, illum, dillum in the model, for details see [LWD+09, LWC+09]). MeteoSwiss provided historical data (i.e. archived weather predictions of the COSMO-7 numerical weather prediction model [SDS+03b] operated by MeteoSwiss) as well as the respective measurements of the year 2007. At the time of the analysis, COSMO-7 delivered hourly weather predictions for the next three days with an update cycle of 12 hours and a horizontal grid mesh size of 6.6 km [SSS09]. For this study, four meteorological measurement sites in different European countries were chosen in order to represent different climatic zones in Europe. The list can be found in Table 6.4. The *weather location* $\in \{\text{Zurich(SMA)}, \text{Lugano(LUG)}, \text{Marseille(MSM)}, \text{Vienna(WHW)}\}$.

Note that throughout this thesis it is distinguished between weather *forecast*, which is the information about the future weather as given by MeteoSwiss and weather *prediction*, which is the information about the weather that the controller takes into account.

For control purposes the following data was used as weather predictions:

- The forecast that is delivered by MeteoSwiss, which is termed *weather forecast*.
- The measurements that are delivered by MeteoSwiss, which means that it is assumed that a perfect weather prediction is available (realization = prediction); this is termed *perfect weather prediction* and is used to estimate the consequences of the uncertainty in the weather predictions.

Table 6.5: Values for internal gains levels.

Parameter	**Unit**	**Internal gains level**	
		low	**high**
Floor area per person	m^2	14	7.8
Internal gains due to occupants	W/m^2	5	9
Internal gains due to equipment	W/m^2	7	15
CO_2-production	$m^3/(h\ m^2)$	1.1e-3	1.9e-3

6.5.2 Internal Gains

The heat gains that are due to either occupants (people) or equipment (e.g., computers, printers) are called *internal gains*. Two levels for internal gains were considered in the

simulations: *internal gains level* ∈ {high(ih),low(il)}. These levels were based on the Swiss standard SIA 2024 [SIA06b] for cellular offices. The values are given in Table 6.5. The assumed profiles from SIA 2024 are shown in Figure 6.4. During weekends internal gains due to occupants were assumed to be zero and internal gains due to equipment were set to the weekday's night-time values.

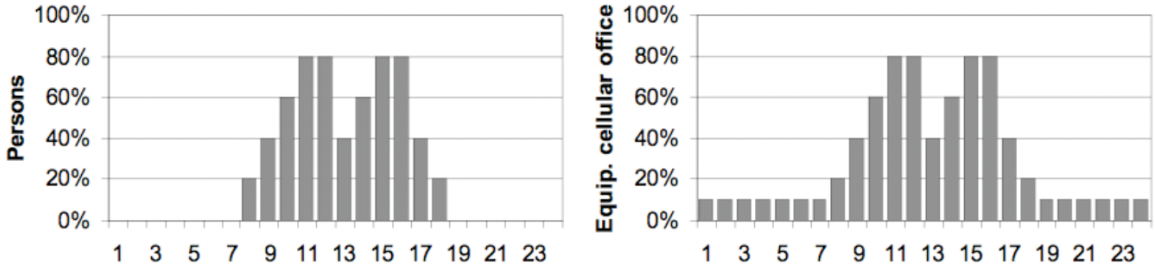

Figure 6.4: From: SIA 2024 [SIA06b]. Example of diurnal occupancy profiles for weekdays. Data are mean values over the hour indicated. Time labeling is for local wintertime.

In Table 6.6 an overview of all disturbance parameters is given.

Table 6.6: Disturbance parameters.

Parameter	Value	Identifier
Weather location	Zurich	SMA
	Lugano	LUG
	Marseille	MSM
	Vienna	WHW
Internal gains level	High	ih
	Low	il

6.6 Simulation Software

Within the project BACLab (Building Automation and Control Laboratory), a Matlab-based building simulation software, was developed. It comprises a database of building parameters and HVAC systems such that the building models described above can be generated, furthermore a database of historical weather predictions and corresponding measurements, and different control strategies. This software was used for the here presented simulation studies.

6.7 Control Strategies and Benchmarks for Building Climate Control

In this section the different control strategies are presented that are compared in the investigations: *Rule-Based Control* (RBC), *Performance Bound* (PB), *Deterministic MPC* (DMPC) and *Stochastic MPC* (SMPC). RBC is the current control practice and is therefore used as a benchmark. A second benchmark is given by PB, which is defined as optimal control with perfect information (see also Section 3.2.4), in particular with a perfect weather prediction, i.e. the prediction is equal to the realization. The control strategies under investigation are DMPC, which is the standard approach in MPC (see also Section 3.2.3), and SMPC, which is a newly developed MPC strategy for the purpose of building climate control that can explicitly take into account uncertainties and was introduced and developed in Chapter 4. All control strategies are described below. The definition of the costs and constraints for the MPC strategies as well as the computation of PB are detailed in Section 6.8. To start with, the control problem is classified in order to better understand the requirements.

6.7.1 Classification of Control Problem

The time step of the building model was chosen to be one hour, since this was considered to be sufficient for a good estimate of the yearly energy consumption. This hourly time step provides the controller with enough time for computing control inputs even for a large-scale problem.

The model is bilinear (in input and state as well as in input and disturbance). In order to use linear MPC methods, it is necessary to linearize the model at each time step around some nominal trajectory.

The model comprises an additive uncertainty due to the weather prediction errors. This uncertainty has a high impact on the building, in particular the uncertainty resulting from the prediction of solar radiation. The constraints on room temperature can be understood as chance constraints, which gives the controller additional flexibility, since the controller can choose when to violate the constraints.

6.7.2 Rule Based Control

The current control practice in Integrated Room Automation is RBC. RBC determines all control inputs based on a series of rules of the form "if *condition*, then *action*". The conditions and actions are usually associated with numerical parameters (e.g., threshold

values) that have to be chosen. A good performance of RBC critically depends on a good choice of rules and associated parameters. More complex HVAC systems make it increasingly hard to define rules that ensure an energy efficient control.

An extract of an RBC controller for blind positioning is given as an example in Algorithm 2. Threshold values and parameters are written in italics. More details on the RBC controller can be found in [GTG09].

Algorithm 2 Example: rule-based blind positioning (extract)

```
if( solar gains < threshold value )
    open blinds fully
else
    if( room is not occupied )
        close blinds fully
    else
        close blinds to predefined position that attempts to maintain luminance setpoint
    end
end
```

6.7.3 Deterministic MPC

DMPC is the standard MPC approach that is used in virtually all commercial MPC applications. It takes the real (imperfect, uncertain) weather prediction (as defined in Section 6.5.1) and makes its control decision by assuming that the predictions are correct (i.e. equal to certain). Therefore, it is also often called Certainty Equivalence.

DMPC has in all presented simulation studies (unless stated otherwise) an hourly time step and a prediction horizon of 24, which corresponds to one day.

6.7.4 Chance Constrained Stochastic MPC

Chance-constrained Stochastic MPC (SMPC) as introduced in Chapter 4 is a class of Stochastic MPC that is very well suited for the purpose of building control. This is due to the strategy's two key elements: First, the strategy directly accounts for the uncertainty in the weather forecast; and second, it allows to formulate so-called chance constraints, i.e. to enforce constraints to be fulfilled with a predefined probability, similarly as it is required in the building standards for room temperature constraints [EN 07].

The importance of these two elements for building control is explained in the next two sections.

Affine Disturbance Feedback

SMPC uses Affine Disturbance Feedback, which was introduced in Section 4.3. This means that the uncertainty in the weather can be accounted for in the controller, and hence a better control performance can be expected. The main benefit of using this Affine Disturbance Feedback formulation is that the resulting problem can be formulated as a convex robust optimization problem, so that it can be efficiently solved, while providing very good performance [GKM06, OJM08].

The main limitation of this formulation is the added computational complexity of optimizing over $M_{(t+k,t+i)|t}$ and $h_{t+k|t}$ rather than just the inputs $u_{t+k|t}$. This can however be mitigated by, e.g., restricting the degrees of freedom of the matrices $M_{(t+k,t+i)|t}$ (i.e. blocking, see Chapter 5) or by optimizing over weighted sums of a small number of pre-computed matrices (approximation with Fixed Feedback, see Section 4.4.3 of Chapter 4). These techniques have been shown to be effective in building control while significantly reducing the computational effort [OGJM09, Par09].

Chance Constraints

A chance-constrained formulation according to Definition 3.12 is employed in which it is required that the predicted states of the building satisfy the constraints only with a given probability. This formulation has significant benefits for building control:

- The European standards specify that comfort bounds on room temperature do not need to be guaranteed at all times, but may be violated for a small fraction of time during the year, for example in extreme weather situations [EN 07]. By using chance constraints, a similar behavior can be encoded directly in the controller.
- When combined with Affine Disturbance Feedback, it is possible to formulate the resulting optimization as a second order cone problem. Such problems are convex and can be readily solved by existing codes, although they can be fairly computationally expensive at larger scales. To cope with the computational complexity, one can also use approximate formulations, see Chapter 4.

For the remainder of this thesis, the Stochastic MPC approach in which comfort bounds are expressed as chance constraints and future control input signals are parameterized in terms of an Affine Disturbance Feedback is referred to as SMPC.

6.7.5 Performance Bound

PB is defined as optimal control with perfect knowledge of both the system dynamics as well as all future disturbances affecting the system. For analysis purposes, it is possible to formulate such a controller for a given building and a given year after the

weather has been recorded and hence is known. Its performance is better than that of any other realistic controller that only has imperfect information. PB is itself not an (applicable) controller, but rather a concept that can serve as a benchmark.

If all disturbances were known, one could in principle solve the optimal control problem for the whole simulation horizon by solving a single optimization problem. However, due to the bilinear system dynamics the resulting optimization problem is non-convex. The problem is therefore approximated by using a form of sequential linear programming (explained in detail in Section 6.8), which means that the model is linearized at each time step and the problem is solved for a prediction horizon of 168 or seven days (iteratively until a convergence criterion is met), then one moves forward by the control horizon (i.e. the number of time steps that control inputs are applied in open-loop) of 72 or three days, and finally a new measurement is taken and the procedure is repeated. The receding horizon formulation is used for limiting the error due to solving an approximate (linearized) problem. The choice of the control horizon of three days is based on the tradeoff between achieving a low computation time and having a good performance. To summarize, for computing PB the nominal MPC is used, but with perfect weather predictions (as defined in Section 6.5.1), a prediction horizon of seven days, and a control horizon of three days.

6.8 Implementation of MPC for Building Climate Control

In this section it is outlined how the various inputs to the controller (weather predictions, local weather and building measurements, building model data, etc.) are translated to a mathematical structure that can be processed by standard optimization software. An overview is given in Figure 6.5. This picture is also used as an outline for this section. Note that this description is based on the assumptions and definitions given so far in this chapter.

6.8.1 Step 1: Weather Prediction at Building Site

(a) Weather Forecast

The weather predictions were given by archived forecasts of the (deterministic) numerical weather prediction model COSMO-7 operated by MeteoSwiss [SDS+03b]. The forecast data comprised the outside air temperature, the wetbulb temperature, and the incoming solar radiation. At the time of the analysis, COSMO-7 delivered hourly pre-

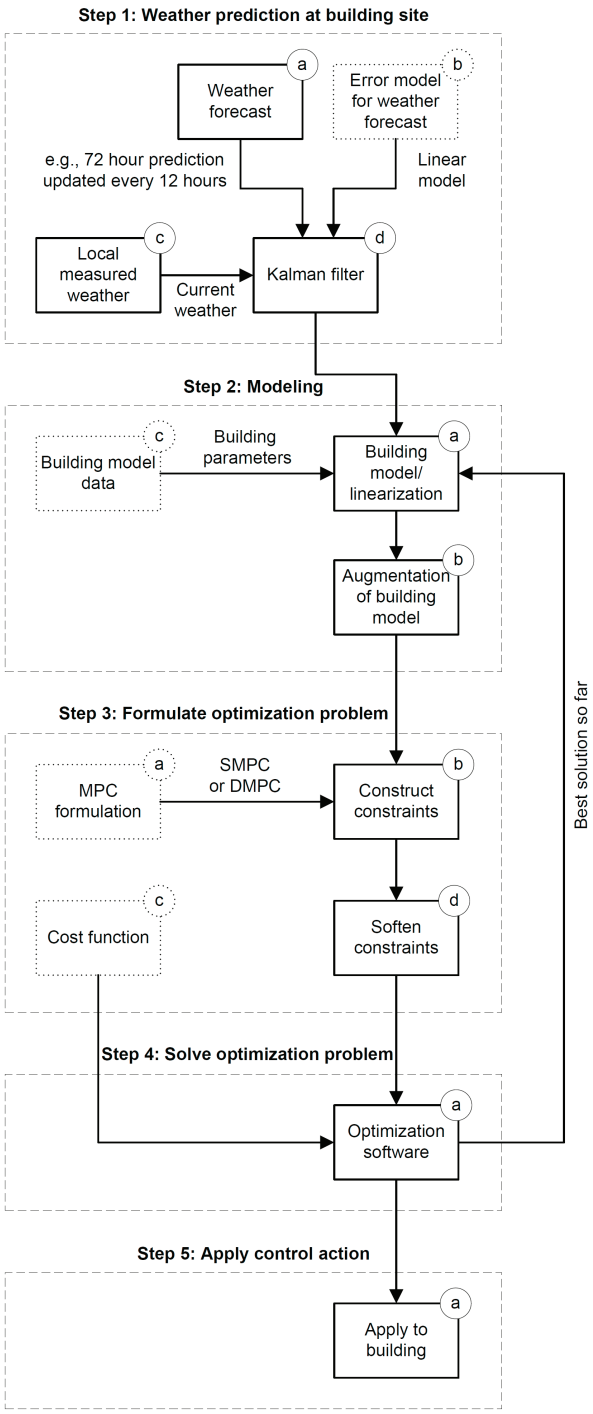

Figure 6.5: Decision flow of the MPC strategy for building control. The parts that have to be designed a priori are in dotted boxes. The letters indicate the corresponding paragraph in the text.

dictions for the next three days with an update cycle of 12 hours and a horizontal grid mesh size of 6.6 km [SSS09]. For this study, four meteorological measurement sites in different European countries were chosen in order to represent different climatic zones in Europe. The list can be found in Table 6.4.

(b) Error Model for Weather Forecast

The major challenge from a control point of view with using numerical weather forecasts lies in their inherent uncertainty due to the stochastic nature of atmospheric processes, the imperfect knowledge of the weather model's initial conditions, as well as modeling errors. The actual weather disturbance acting on the building can be decomposed as

$$v_k = \bar{v}_k + \tilde{v}_k \ , \tag{6.2}$$

where $\bar{v}_k$ is the COSMO-7 weather forecast and $\tilde{v}_k$ is the prediction error at each time step k. In order to improve the estimation of future disturbances acting on the building, the following autoregressive model driven by Gaussian noise was identified based on the archived weather forecasts and corresponding in-situ measurements

$$\tilde{v}_{k+1} = F\tilde{v}_k + Kw_k \ . \tag{6.3}$$

The noise w_k is assumed to follow a Gaussian distribution, $w_k \sim \mathcal{N}(\mathbf{0}, \mathbf{I})$. Testing the randomness of residuals showed that the goodness of fit was satisfactory for all investigated cases, i.e. autocorrelation coefficients for the residuals did not differ significantly from zero.

(c) Local Measured Weather

For the local measured weather, archived measurements of the same sites as given in Table 6.4 were used. Having the sites for the weather forecasts and the local measured weather coincide means that there is no spatial error between the building and the weather station.

(d) Kalman Filter

In this setup, a Kalman filter is used to update the predictions arriving every 12 hours on an hourly basis with the incoming new measurements. In a realistic setting the use of a Kalman filter would also be beneficial in order to eliminate the systematic error due to the fact that the building is not situated directly at the weather station site as well as due to the environment of the building itself (shadow from other buildings,

trees etc.). Furthermore, a Kalman filter would be used if not all system states could be measured. In this study the focus is on the potential of advanced control strategies, i.e. the performance these strategies can achieve at best compared to the state of the art. Therefore, the question of how to obtain state measurements and for which states to do state estimation is not addressed, but it is assumed that all states are measured (precisely).

For the presented simulation study, a standard Kalman filter is implemented as described, e.g., in [AM79] for the purpose of updating the weather predictions arriving every 12 hours on an hourly basis. It is used for solar radiation, outside temperature, and wetbulb temperature with the following adaptations for solar radiation:

- The Kalman filter is only applied during daytime, since solar radiation is equal to zero at night.
- It is enforced that the prediction is always non-negative.

The Kalman filter is applied only for DMPC and SMPC, but not for PB, since the latter has perfect weather predictions available.

6.8.2 Step 2: Modeling

(a) Building Model/ Linearization

There is a large amount of computer-aided modeling tools (e.g., TRNSYS [sof11c], EnergyPlus [sof11b]), however, these are designed mainly for estimating the energy usage of a building and cannot be readily used for control. Instead, for the studies of the OptiControl project, a building model was newly developed. A scheme of this newly developed building model is given in Figure 6.1 of Section 6.1.

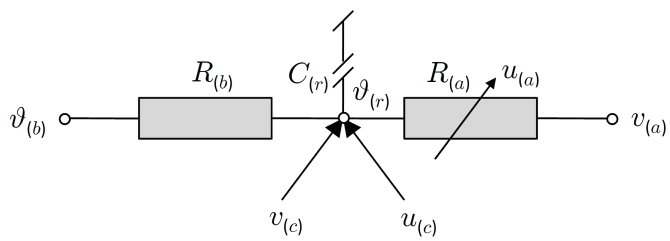

Figure 6.6: Simple example model to demonstrate how to construct the differential equation describing the temperature in each node.

From the RC model in Figure 6.1 one can read off a differential equation for each node based on the equation for heat transfer. This is explained for a small example

here. Given the highly simplified model in Figure 6.6, the differential equation for node r reads

$$C_{(r)} \cdot \frac{\partial \vartheta_{(r)}}{\partial t} = \frac{1}{R_{(a)}} \cdot u_{(a)}(v_{(a)} - \vartheta_{(r)}) + \frac{1}{R_{(b)}} \cdot (\vartheta_{(b)} - \vartheta_{(r)}) + u_{(c)} + v_{(c)} \ , \tag{6.4}$$

with $C_{(r)}$ denoting the thermal capacitance of node r, $\vartheta_{(r)}$ and $\vartheta_{(b)}$ denoting the temperatures at their respective nodes in the building, $v_{(a)}$ denoting a disturbance (e.g., outside temperature), $R_{(a)}$ and $R_{(b)}$ denoting resistances, and $u_{(a)} \in [0, 1]$ and $u_{(c)}$ denoting control inputs.

Remark 6.1. Illuminance and CO_2 concentration were modeled by instantaneous responses since the time constants involved were much smaller than the hourly time step employed for the modeling and simulations. Details can be found in [GE09].

Remark 6.2. Note that the scaling of the heat transfer coefficient $\frac{1}{R_{(a)}}$ to lie between 0 and its maximum value by choosing $u_{(a)}$ results in a product of $u_{(a)}$ and $v_{(a)}$, and $u_{(a)}$ and $\vartheta_{(r)}$, which causes the resulting model to be bilinear. Such a bilinearity arises in the model given in Figure 6.1 due to the blinds (the heat transfer between the room and the outside depends on the control input for the blinds), the cooling tower (the cooling power depends on the control input and the wetbulb temperature), as well as the ventilation (depends on control input and outside temperature).

If a model with one of the HVAC systems in Table 6.2 is to be constructed, then the differential equations for all nodes in the model of Figure 6.1 with the particular HVAC subsystems of choice are formulated as shown above for one example. Hence a state space model with

$$\vartheta := [\vartheta_{(1)} \quad \vartheta_{(2)} \quad \dots \quad \vartheta_{(n_\vartheta)}]^T \ , \tag{6.5}$$

$$u := [u_{(1)} \quad u_{(2)} \quad \dots \quad u_{(n_u)}]^T \ , \tag{6.6}$$

$$v := [v_{(1)} \quad v_{(2)} \quad \dots \quad v_{(n_v)}]^T \tag{6.7}$$

can be formulated, where n_ϑ denotes the number of nodes in the model, n_u denotes the number of actuators, and n_v denotes the number of disturbance inputs. The state space model is then discretized and results in a bilinear model of the following form

$$\begin{aligned} \vartheta_{t+1} &= A_{(\vartheta)}\vartheta_t + B_{(u)}u_t + [B_{(\vartheta,u_1)}\vartheta_t \quad B_{(\vartheta,u_2)}\vartheta_t \quad \dots \quad B_{(\vartheta,u_{nu})}\vartheta_t] \cdot u_t + ... \\ &\quad ... + [B_{(v,u_1)}v_t \quad B_{(v,u_2)}v_t \quad \dots \quad B_{(v,u_{nu})}v_t] \cdot u_t + B_{(v)}v_t \\ y_t &= C_{(\vartheta)}\vartheta_t + D_{(u)}u_t + [D_{(v,u_1)}v_t \quad D_{(v,u_2)}v_t \quad \dots \quad D_{(v,u_{nu})}v_t] \cdot u_t + D_{(v)}v_t \ , \end{aligned} \tag{6.8}$$

where t denotes the time step, $\vartheta_t \in \mathbb{R}^{n_\vartheta}$ denotes the states, i.e. the temperatures at the different nodes, $u_t \in \mathbb{R}^{n_u}$ denotes the control inputs, $v_t \in \mathbb{R}^{n_v}$ denotes the disturbances

(weather and internal gains), and y_t denotes the output, furthermore, $A_{(\vartheta)} \in \mathbb{R}^{n_\vartheta \times n_\vartheta}$, $B_{(\vartheta,u_i)} \in \mathbb{R}^{n_\vartheta \times n_\vartheta}$ $\forall i \in \mathbb{N}_1^{n_u}$, $B_{(v,u_i)} \in \mathbb{R}^{n_\vartheta \times n_v}$ $\forall i \in \mathbb{N}_1^{n_u}$, and $B_{(v)} \in \mathbb{R}^{n_\vartheta \times n_v}$, $C_{(\vartheta)} \in \mathbb{R}^{n_y \times n_\vartheta}$, $D_{(u)} \in \mathbb{R}^{n_y \times n_u}$, $D_{(v)} \in \mathbb{R}^{n_y \times n_v}$, and $D_{(v,u_i)} \in \mathbb{R}^{n_y \times n_v}$ $\forall i \in \mathbb{N}_1^{n_u}$.

Since the dynamic behavior of the building is bilinear between inputs, states and disturbances, the dynamic equations of the MPC problem result in a non-convex optimization, which can be difficult to solve.

The bilinearity between inputs and disturbances is treated differently from the one between inputs and states. In general the model will be used for predicting the future behavior of the building, so $\vartheta_{t+k|t}$ and $v_{t+k|t}$ are predicted states and disturbances, respectively.

For the bilinearity between inputs and disturbances, we assume that the disturbances will take the values of their prediction (weather and internal gains prediction), i.e. $v_{t+k|t} = \bar{v}_{t+k|t}$. By fixing the disturbance to its prediction in the bilinear part of (6.8), this part becomes linear in the predicted input $u_{t+k|t}$.

Remark 6.3. Note that it is assumed that the disturbances will take the values of their *prediction*. For MPC, this means that the values of the weather forecast are applied. When computing PB, this means, that the values of the measurements are applied.

For the bilinearity between inputs and states the situation is more complicated, since the aim is to linearize around some fixed state and to use the resulting linear model in the optimization problem; however, the optimization in turn tries to find the optimal future states. The approach that we take is a form of Sequential Linear Programming (SLP) for solving non-linear problems in which the model is iteratively linearized around the current solution, the problem is solved and this is repeated until a convergence condition is met [GS61]. Denote by $\bar{\vartheta}_t$ the solution for the state that is linearized around. This yields

$$\begin{aligned} \vartheta_{t+1} &= A_{(\vartheta)}\vartheta_t + \Big[B_{(u)} + [B_{\vartheta,u_1)}\bar{\vartheta}_t \quad B_{(\vartheta,u_2)}\bar{\vartheta}_t \quad \dots \quad B_{(\vartheta,u_{nu})}\bar{\vartheta}_t] + \dots \\ &\quad \dots + [B_{(v,u_1)}\bar{v}_t \quad B_{(v,u_2)}\bar{v}_t \quad \dots \quad B_{(v,u_{nu})}\bar{v}_t]\Big] \cdot u_t + B_{(v)}v_t \\ &= A_{(\vartheta)}\vartheta_t + B_{(u|t)}u_t + B_{(v)}v_t \ , \end{aligned} \tag{6.9}$$

where $B_{(u|t)}$ denotes the matrix which contains all input matrices. Note, that $B_{(u|t)}$ is time-dependent since at each time-step t a new linearization is performed. Similarly, for the output equation this yields

$$y_t = C_{(\vartheta)}\vartheta_t + D_{(u|t)}u_t + D_{(v)}v_t \ , \tag{6.10}$$

where $D_{(u|t)}$ denotes the matrix which contains all input matrices of the output equation and is time-varying. Using (6.2) yields

$$\vartheta_{t+1} = A_{(\vartheta)}\vartheta_t + B_{(u|t)}u_t + B_{(v)}\bar{v}_t + B_{(v)}\tilde{v}_t \tag{6.11}$$

$$y_t = C_{(\vartheta)}\vartheta_t + D_{(u|t)}u_t + D_{(v)}\bar{v}_t + D_{(v)}\tilde{v}_t \ . \tag{6.12}$$

(b) Augmentation of Building Model with Uncertainty Model

The building model in (6.12) is augmented with the error model of the weather forecast in (6.3). This yields

$$\underbrace{\begin{bmatrix}\vartheta_{t+1}\\ \tilde{v}_{t+1}\end{bmatrix}}_{x_{t+1}} = \underbrace{\begin{bmatrix}A_{(\vartheta)} & B_{(v)}F\\ \mathbf{0} & F\end{bmatrix}}_{A}\underbrace{\begin{bmatrix}\vartheta_t\\ \tilde{v}_t\end{bmatrix}}_{x_t} + \underbrace{\begin{bmatrix}B_{(u|t)}\\ \mathbf{0}\end{bmatrix}}_{B_t}u_t + \underbrace{\begin{bmatrix}B_{(v)}\\ \mathbf{0}\end{bmatrix}}_{H}\bar{v}_t + \underbrace{\begin{bmatrix}B_{(v)}K\\ K\end{bmatrix}}_{E}w_t \tag{6.13}$$

$$y_t = \underbrace{\begin{bmatrix}C_{(\vartheta)} & D_{(v)}F\end{bmatrix}}_{C}\underbrace{\begin{bmatrix}\vartheta_t\\ \tilde{v}_t\end{bmatrix}}_{x_t} + \underbrace{D_{(u|t)}}_{D_t}u_t + \underbrace{D_{(v)}}_{V}\bar{v}_t + \underbrace{D_{(v)}K}_{W}w_t \tag{6.14}$$

$$\Rightarrow x_{t+1} = Ax_t + B_tu_t + H\bar{v}_t + Ew_t \tag{6.15}$$

$$y_t = Cx_t + D_tu_t + V\bar{v}_t + Ww_t \ . \tag{6.16}$$

Note that B_t and D_t are time-varying, hence, the overall model is a time-varying linear model with the weather and internal gains prediction $\bar{v}_t$ as external input and uncertainty w_t.

With $\mathbf{x}, \mathbf{u}, \mathbf{w}$ as defined in (4.4)-(4.6) of Chapter 4 and

$$\bar{\mathbf{v}} := \begin{bmatrix}\bar{v}_0^T & \dots & \bar{v}_{N-1}^T\end{bmatrix}^T \in \mathbb{R}^{n_vN} \tag{6.17}$$

$$\mathbf{y} := \begin{bmatrix}y_0^T & \dots & y_{N-1}^T\end{bmatrix}^T \in \mathbb{R}^{n_yN} \tag{6.18}$$

one can write

$$\mathbf{x} = \mathbf{A}x_0 + \mathbf{B}\mathbf{u} + \mathbf{H}\bar{\mathbf{v}} + \mathbf{E}\mathbf{w} \tag{6.19}$$

$$\mathbf{y} = \mathbf{C}x_0 + \mathbf{D}\mathbf{u} + \mathbf{V}\bar{\mathbf{v}} + \mathbf{W}\mathbf{w} \ , \tag{6.20}$$

where matrices $\mathbf{A}$, $\mathbf{B}$, $\mathbf{H}$, $\mathbf{E}$, $\mathbf{C}$, $\mathbf{D}$, $\mathbf{V}$, and $\mathbf{W}$ can be found in Appendix A.

(c) Building Model Data

One problem to get such a model as in (6.8) is to get the parameters such that one can set up the equations as in (6.4). These parameters can be either determined from

the construction plan according to the materials used and their tabular values or, alternatively, the parameters can be determined via estimation methods. For this investigation, only simulation models needed to be constructed; therefore, tabular values for the materials were used. This is detailed in [LWC+09].

6.8.3 Step 3: Formulate Optimization Problem

In this section it is reported on how to formulate the optimization problem. As a first step, an appropriate MPC formulation is chosen; then, according to this, constraints are constructed, the cost function is formulated, and constraints are softened in order to prevent infeasibility of the problem.

(a) MPC Formulation

In the following, the choices for the two principle MPC formulations are detailed: DMPC and SMPC. For SMPC we apply the approximation with Fixed Feedback as introduced in Section 4.4.3 of Chapter 4. This means that we optimize over the average of a small number of pre-computed matrices, which are determined by solving the problem described in Section 4.4.1 of Chapter 4.

(b) Construct Constraints

Two types of constraints are to be enforced: First, all inputs are constrained to be between zero and some upper bound, which can be written as

$$\mathbf{S}\mathbf{u}_t \quad \leq \quad \mathbf{s} \ , \tag{6.21}$$

where $\mathbf{S} \in \mathbb{R}^{qN \times n_u}$, and $\mathbf{s} \in \mathbb{R}^{qN}$; and second, the room temperature, illuminance, and CO_2 are constrained to lie in their respective comfort range. For room temperature it is required to fulfill the comfort constraint with a predefined probability, i.e.

$$\Pr\left[\mathbf{G}_{(j)}\mathbf{y}_t \leq \mathbf{g}_{(j)}\right] \quad \geq \quad 1 - \alpha_{\mathbf{y},j} \tag{6.22}$$

$$\Leftrightarrow \quad \Pr\left[\mathbf{G}_{(j)}(\mathbf{C}x_0 + \mathbf{D}\mathbf{u}_t + \mathbf{V}\bar{\mathbf{v}}_t + \mathbf{W}\mathbf{w}_t) \leq \mathbf{g}_{(j)}\right] \quad \geq \quad 1 - \alpha_{\mathbf{y},j} \ , \tag{6.23}$$

where $\alpha_{\mathbf{y},j} \in (0,1)$, $\mathbf{G} \in \mathbb{R}^{rN \times n_y}$, and $\mathbf{g} \in \mathbb{R}^{rN}$.

Remark 6.4. Note that the constraints on illuminance and CO_2 are given as hard constraints. Due to the fact that they are modeled with instantaneous responses and that there is enough input power available, the hard constraints can always be met. For lighting, it could theoretically be possible to violate the constraints due to the

uncertainty in the weather prediction. It is however assumed in the simulation that the illuminance level gets adjusted (by the user) to the actual need and, therefore, constraints are always met. For CO_2 there is no uncertainty involved since the occupancy levels are always perfectly predicted. For these reasons, the constraints on illuminance and CO_2 are not further considered, but the focus is on the room temperature constraints.

Deterministic MPC

When applying DMPC in this setting, the idea is to assume that the uncertainty from the weather takes its expected value, i.e. $\mathbf{w}_t = \mathbf{0}$. With this, the constraints are formulated as follows:

$$\mathbf{S}\mathbf{u}_t \leq \mathbf{s} \tag{6.24}$$

$$\mathbf{G}\mathbf{C}x_t + \mathbf{G}\mathbf{D}\mathbf{u}_t + \mathbf{G}\mathbf{V}\bar{\mathbf{v}}_t \leq \mathbf{g}\ . \tag{6.25}$$

The primary limitation of DMPC is the fact that, if the uncertainty does not take the expected value, then the above constraints may be violated. This is most often dealt with by artificially tightening the upper and lower bounds, which provides a buffer zone and can be effective for small variances. The cost to be paid is the additional energy required to be conservative and hold the room temperature further away from the bounds than strictly required.

Performance Bound

For PB we take the same formulation for the constraints as in (6.24) and (6.25). However, since we have perfect weather predictions available, $\mathbf{w}_t$ actually takes its expected value, i.e. $\mathbf{w}_t = \mathbf{0}$ and hence, the bounds are not violated.

Stochastic MPC

One method of automatically determining an appropriate amount to tighten the constraints is to formulate them as chance constraints as discussed above. The approach that we take here was introduced in Chapter 4 in Section 4.4.3.

As a first step an optimization problem with the following constraints is solved in order to determine an average feedback matrix $\bar{\mathbf{M}}$ as defined in (4.33). The derivation of this formulation of the constraints can be found in Chapter 4 in Section 4.4.1.

$$(\mathbf{M}_t, \mathbf{h}_t) \text{ satisfies } (4.19) \tag{6.26}$$

$$\mathbf{S}_{(i)}\mathbf{h}_t \leq \mathbf{s}_{(i)} - \Gamma_i \|\mathbf{S}_{(i)}\mathbf{M}\|_2 \qquad \forall i \in \mathbb{N}_1^{qN} \tag{6.27}$$

$$\mathbf{G}_{(j)}(\mathbf{C}x_t + \mathbf{D}\mathbf{h}_t + \mathbf{V}\bar{\mathbf{v}}_t) \leq \mathbf{g}_{(j)} - \Upsilon_j \|\mathbf{G}_{(j)}\mathbf{D}\mathbf{M}_t + \mathbf{G}_{(j)}\mathbf{W}\|_2 \quad \forall j \in \mathbb{N}_1^{rN}\ , \tag{6.28}$$

where

$$\Gamma_i := \Phi^{-1}(1 - \alpha_{\mathbf{u},i}) \tag{6.29}$$

$$\Upsilon_j := \Phi^{-1}(1 - \alpha_{\mathbf{x},j}) \ . \tag{6.30}$$

With $\bar{\mathbf{M}}$, in a second step an optimization problem with the following constraints is solved.

$$\begin{aligned} \mathbf{S}_{(i)}\mathbf{h}_t &\leq \mathbf{s}_{(i)} - \Gamma_i \|\mathbf{S}_{(i)}\gamma\bar{\mathbf{M}}\|_2 && \forall i \in \mathbb{N}_1^{qN} && (6.31)\\ \mathbf{G}_{(j)}(\mathbf{A}x_t + \mathbf{B}\mathbf{h}_t) &\leq \mathbf{g}_{(j)} - \Upsilon_j \|\mathbf{G}_{(j)}(\mathbf{B}\gamma\bar{\mathbf{M}} + \mathbf{E})\|_2 && \forall j \in \mathbb{N}_1^{r(N+1)} && (6.32)\\ \gamma \in [0,1] \ . & && && (6.33) \end{aligned}$$

(c) Cost Function

According to the definitions in Section 6.4, the cost function depends on the choice of the control cost ($\{c_{\mathrm{NRPE}}, c_{\mathrm{el},t}\}$), the scaling vector ξ that takes into account the actuator efficiencies, and the control inputs. Let $\mathbf{c} \in \mathbb{R}^{n_u N}$ denote the product of the chosen control cost and the scaling factor ξ along the horizon N. The cost function can then be written as

$$\min_{\mathbf{u}_t} \mathrm{E}\left[\mathbf{c}^T \mathbf{u}_t\right] \ . \tag{6.34}$$

Deterministic MPC/ Performance Bound

For DMPC and PB the cost function simplifies to

$$\min_{\mathbf{u}_t} \mathbf{c}^T \mathbf{u}_t \ . \tag{6.35}$$

Stochastic MPC

For SMPC Affine Disturbance Feedback is applied, hence the cost function is depending on $\mathbf{w}_t$ and reads

$$\min_{(\mathbf{M}_t, \mathbf{h}_t)} \mathrm{E}\left[\mathbf{c}^T(\mathbf{M}\mathbf{w}_t + \mathbf{h}_t)\right] \ . \tag{6.36}$$

With a linear cost function and with $\mathrm{E}\left[\mathbf{w}_t\right] = 0$ this yields

$$\min_{(\mathbf{M}_t, \mathbf{h}_t)} \mathrm{E}\left[\mathbf{c}^T \mathbf{h}_t\right] \ . \tag{6.37}$$

Note that although $\mathbf{M}_t$ does not enter the cost function directly, it appears in the constraints and therefore influences the choice of the optimal $\mathbf{h}_t$ indirectly.

(d) Soften Constraints

It is not always possible to satisfy all constraints of the building and so a standard relaxation-procedure, the so-called *soft constraints* [Mac02, RM09], are required that

choose automatically which constraints are to be violated first. This is achieved by adding variables to the optimization routine that allow every constraint to be violated. The variables are then heavily penalized, which forces them to zero and the satisfaction of all constraints, if at all possible. If this is not possible, then these additional variables give the optimizer sufficient flexibility to always find a solution that can be applied to the building. One can define the relative importance of each constraint by tuning the relevant weighting matrices and thereby have the system violate the least important constraints first.

6.8.4 Step 4: Solve Optimization Problem

Once the constraints and cost have been formulated, the resulting problem can be passed to a standard optimization routine. We made use of the commercial package CPLEX [sof11a], which is effective for the large-scale and sparse problems that result.

6.8.5 Step 5: Apply Control Action

The optimal solution of the linear program consists of a sequence of planned inputs over the prediction horizon into the future. Only the first of these inputs $u_{t|t}$ is applied to the building, before re-solving the entire problem at the next time step $t + 1$.

6.9 Overview of Simulation Settings

Table 6.7 provides an overview of the simulation settings, which are used in the simulations throughout this thesis. These comprise all choices from the parameter sets of the controller $\mathbb{C}$, of the building type $\mathbb{B}$, of the HVAC system $\mathbb{S}$, of the control settings $\mathbb{A}$, and of the disturbances $\mathbb{D}$.

Table 6.7: Overview of the parameter sets of the controller, building type, HVAC system, control settings, and disturbances.

Parameter Set	Parameter	Value	Identifier
$\mathbb{C}$	Controller	Rule-based control	RBC
		Deterministic MPC	DMPC
		Stochastic MPC	SMPC
		Performance Bound	PB
$\mathbb{B}$	Building standard	Swiss Average	sa
		Passive House	pa
	Construction type	Heavy	h
		Light	l
	Window area fraction	Low	wl
		High	wh
	Facade orientation	North (normal office)	N
		South (normal office)	S
		South+East (corner office)	SE
		South+West (corner office)	SW
$\mathbb{S}$	HVAC system (see Table 6.2)	System 1	S1
		System 2	S2
		System 3	S3
		System 4	S4
		System 5	S5
$\mathbb{A}$	Control costs	NRPE	c_{NRPE}
		Monetary	$c_{\text{el},k}$
	Room temperature range	narrow	nar
		wide	wid
	Setback	Yes	SBon
		No	SBoff
	Ventilation	Fixed schedule	IAQoff
		IAQ-controlled	IAQon
$\mathbb{D}$	Weather location (see Table 6.4)	Zurich	SMA
		Lugano	LUG
		Marseille	MSM
		Wien Hohe Warte	WHW
	Internal gains level (see Table 6.5)	High	ih
		Low	il

7 Use of Weather Predictions and MPC

7.1 Introduction

This chapter deals with the investigation of the energy savings potential of applying MPC and using weather predictions in building climate control.

Several works in the literature point at the usefulness of weather predictions for energy efficient building control (see Literature survey in Section 2.2 of Chapter 2). This chapter describes a large-scale factorial simulation study that was carried out for investigating the energy savings potential for different buildings and HVAC systems under different weather conditions.

In this investigation four control strategies were compared: a state-of-the-art *Rule Based Controller* (RBC) was compared to a standard *Deterministic MPC* (DMPC) formulation. Furthermore, the *Stochastic MPC* (SMPC) introduced in Chapter 4 was investigated and all controllers were compared with the theoretical benchmark, the *Performance Bound* (PB). The investigated control strategies are explained in detail in Section 6.7 of Chapter 6.

Due to the importance of the uncertainty in the weather predictions, this investigation focuses on the stochastic MPC formulation. In particular, the necessary prediction horizon length, the importance of weather predictions for a good control performance, and the tunability of the controller are addressed.

7.1.1 Main Idea and Ouline

The aim in this chapter is to compare the performance of the different controllers and to assess the energy savings potential of using MPC with weather predictions. In Section 7.2 the simulation framework is described and in Section 7.3 the performance assessment concept is introduced. The investigations are detailed in Section 7.4 and the results are given in Section 7.5. Conclusions are drawn in Section 7.6.

7.2 Building Simulation Framework

The building simulation framework for the study on weather prediction is the previously defined simulation setup (see Chapter 6). For this study no modifications were done. The investigated cases are defined in Section 7.4.

7.3 Controller Assessment Concept

In this section the controller assessment concept is presented. In order to assess the performance of the controllers, their behavior during one simulated year was considered. Generally, the simulation of PB and RBC was computationally simple and, therefore, it was possible to run a large number of simulations for different building setups. The simulation of DMPC and SMPC was computationally more expensive. Therefore, the investigation was done in two steps: First, a large-scale simulation was carried out with PB and RBC; and second, based on these results, DMPC and SMPC were compared with PB and RBC for some chosen example cases. The assessment concept is shown in Figure 7.1 and explained below.

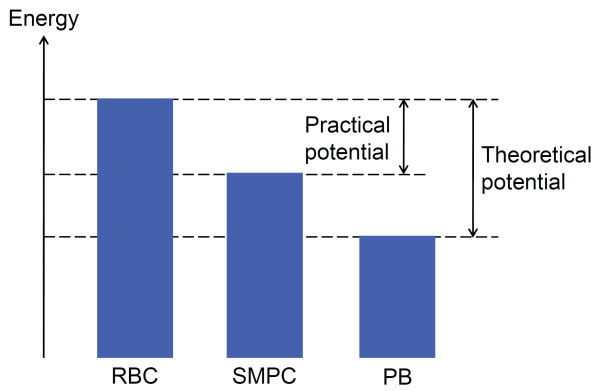

Figure 7.1: Controller assessment concept. First, the theoretical potential was assessed (comparison of RBC and PB) and then the practical potential (comparison of RBC and SMPC).

Theoretical potential: The first step consisted of the comparison of RBC and PB. This was done because there is only hope for a significant improvement if the gap between RBC and PB is large. This investigation was done in a systematic large-scale factorial simulation study for a broad range of cases representing different buildings and different weather conditions, as described below. For further details see [GLW+09,GWL09]. The aim was to answer the following questions:

Q1 Theoretical savings potential: How big are the theoretical savings potentials in IRA?
Q2 Prediction horizon length: What is a suitable prediction horizon length when using MPC with weather predictions for building control (depending on the building and HVAC system)?

Practical potential: In this investigation the performance of RBC and SMPC strategies was compared, but only for selected cases based on the theoretical potential study. The performance of DMPC was also compared, which is expected to perform worse than SMPC since it does not take into account the uncertainty in the problem. Further details can be found in [OGJ+09]. For the practical potential the aim was to answer the following questions:

Q3 Performance of CE: How good is the performance of DMPC in building climate control?
Q4 Performance of SMPC: What is the added value of SMPC in building climate control?
Q5 Importance of Weather Predictions: What impact do weather forecasts and their quality have?
Q6 Tunability: How can MPC help to describe the tradeoff between energy use and comfort?

7.4 Investigations

In this study, the *non-renewable primary energy* (NRPE) usage was assessed as well as the amount and number of violations. A reasonable violation level as it would be tolerated according to the building standards is about 70 Kh/a[1] [EN 07].

In the investigation of the theoretical potential of using weather predictions (W,th) the parameter set $\mathbb{P}^{\mathrm{W,th}} := \{(B, S, A, D) | B \in \mathbb{B}, S \in \mathbb{S}, A \in (c_{\mathrm{NRPE}}, \text{wid}, \text{SBoff}, \text{IAQon}), D \in \mathbb{D}\}$ was considered for all controllers $C \in \mathbb{C}$, with $\mathbb{B}$, $\mathbb{S}$, $\mathbb{D}$, $\mathbb{C}$ defined in Chapter 6. This means that the variation of the whole parameter set as given in Table 6.7 was considered except for the control settings that were restricted to NRPE costs, a wide comfort range, no setback, and IAQ-controlled ventilation. The combination of all possible variants of $\mathbb{P}^{\mathrm{W,th}}$ makes in total 1,280 cases.

In the investigation of the practical potential of using weather predictions (W,pr)

[1] 1 Kh/a (=KelvinHour/annum) corresponds to exceeding the temperature constraint by 1 Kelvin for 1 hour within 1 year

the cases listed in Table 7.1 were considered, which implicitly determine the parameter set $\mathbb{P}^{\mathrm{W,pr}}$. These cases were selected to reflect frequent and interesting building setups, with typical to large theoretical savings potentials [OGJ+09]. Note that also two cases with IAQ-controlled ventilation were investigated. For the MPC controllers (DMPC and SMPC) a Kalman-filter was applied as described in Section 6.8.1. For PB and RBC, no Kalman-filter was necessary, since PB has a perfect prediction available and RBC does not have any prediction available. All simulations were carried out for one year and used weather data of the year 2007. In the following it is detailed how Questions **Q1** to **Q6** were addressed.

7.4.1 Theoretical Energy Savings Potential

Q1 - Theoretical savings potential

For the corresponding analysis PB and RBC were compared for 1,280 cases. A case was given by one choice of the parameters in $\mathbb{P}^{\mathrm{W,th}}$. The aim was to compute the relative theoretical energy savings

$$\Delta E_{\mathrm{RBC}}(B,S,A,D) := \frac{E(\mathrm{RBC},B,S,A,D) - E(\mathrm{PB},B,S,A,D)}{E(\mathrm{PB},B,S,A,D)} \quad \forall (B,S,A,D) \in \mathbb{P}^{\mathrm{W,th}} , \tag{7.1}$$

where $E(\cdot)$ denotes the energy use for a particular case, as well as the amount of violations with RBC

$$V(\mathrm{RBC},B,S,A,D) \quad \forall (B,S,A,D) \in \mathbb{P}^{\mathrm{W,th}} , \tag{7.2}$$

where $V(\cdot)$ denotes the amount of violation for a particular case. Note that the absolute value of violations is considered since $V(\mathrm{PB},B,S,A,D)$ is equal to zero for all cases.

Q2 - Prediction horizon length

For the corresponding analysis PB with a prediction horizon of seven days was compared with PB simulations with shorter prediction horizons for the 1,280 cases.

7.4.2 Practical Energy Savings Potential

Q3 - Performance of DMPC

For the corresponding analysis DMPC was employed using weather forecasts from the COSMO-7 numerical weather prediction model. All cases from Table 7.1 were

Table 7.1: Investigated cases for investigation of practical savings potential, sorted by HVAC system. Bold case numbers indicate the cases investigated for Q4.

	$\mathbb{S}$	$\mathbb{B}$				$\mathbb{D}$		$\mathbb{A}$
Case	**HVAC system**	**Building standard**	**Constr. type**	**Window fraction**	**Facade orient.**	**Location**	**Int. gains**	**Ventilation**
1	2	sa	h	wl	S	LUG	ih	IAQon
2	2	sa	h	wl	S	LUG	ih	IAQoff
3	2	sa	h	wl	S	MSM	ih	IAQon
4	2	sa	l	wl	S	MSM	ih	IAQon
5	2	pa	h	wh	SW	SMA	ih	IAQon
6	2	sa	h	wl	SW	SMA	ih	IAQon
7	2	pa	h	wh	S	SMA	ih	IAQon
8	2	pa	l	wh	S	SMA	ih	IAQon
9	2	sa	h	wl	S	SMA	ih	IAQon
10	2	sa	h	wl	S	SMA	ih	IAQoff
11	2	pa	h	wh	SW	WHW	ih	IAQon
12	2	sa	h	wl	S	WHW	ih	IAQon
13	3	sa	h	wl	S	SMA	ih	IAQon
14	3	pa	h	wh	SW	WHW	il	IAQon
15	4	sa	h	wl	S	LUG	ih	IAQon
16	4	pa	h	wh	S	SMA	ih	IAQon
17	5	pa	h	wh	S	SMA	ih	IAQon
18	5	pa	h	wh	S	WHW	ih	IAQon

analyzed. As benchmarks PB and RBC were used. The aim was to compute the relative energy savings of DMPC

$$\Delta E_{\mathrm{DMPC}}(B,S,A,D) := \frac{E(\mathrm{DMPC},B,S,A,D) - E(\mathrm{PB},B,S,A,D)}{E(\mathrm{PB},B,S,A,D)} \qquad \forall (B,S,A,D) \in \mathbb{P}^{\mathrm{W,pr}} \tag{7.3}$$

as well as the amount of violations with DMPC

$$V(\mathrm{DMPC}, B, S, A, D) \quad \forall (B, S, A, D) \in \mathbb{P}^{\mathrm{W,pr}} \ . \tag{7.4}$$

Note that again the absolute value of violations is considered since $V(\mathrm{PB}, B, S, A, D)$ is equal to zero for all cases.

Q4 - Performance of SMPC

For the corresponding analysis SMPC was employed using weather forecasts from the COSMO-7 numerical weather prediction model. Six example cases from Table 7.1 which are indicated with bold numbers were analyzed. As benchmarks PB and RBC were used. $\Delta E_{\mathrm{SMPC}}(B, S, A, D)$ and $V(\mathrm{SMPC}, B, S, A, D)$ were computed as for DMPC.

Q5 - Importance of Weather Predictions

This question was treated by comparing SMPC performance using COSMO-7 weather predictions, i.e. provided by a weather service, versus using 24h persistence predictions, i.e. continuous recycling of the data from the last 24h. Persistence is a common benchmark in meteorology to assess the quality of predictions. Again, the same six example cases from Table 7.1 were analyzed.

Q6 - Tunability

It was investigated for Building Case 1 in Table 7.1 how the desired comfort level can be achieved with MPC considering the tradeoff between energy use and comfort violations. For this, the parameter α was varied.

7.5 Results

7.5.1 Theoretical Energy Savings Potential

Q1 - Theoretical savings potential

In the investigated 1,280 cases, the reasonable amount of violations of 70 Kh/a was exceeded for many cases when using the RBC controller. We chose to only consider amounts of violation by RBC of < 300 Kh/a. In this category fell 1,228 of the 1,280 cases. Figure 7.2 shows the joint cumulative distribution function of the theoretical energy savings potential (as additional NRPE use in % of PB) and the amount of comfort violations in Kh/a. It can be seen that more than half of the considered cases show an additional NRPE use of more than 40 % (rightmost brown column). Thus, for

many cases there is a significant savings potential, which can potentially be exploited by SMPC. The selection of cases for the practical potential analysis was based both on common building setups and large theoretical savings potentials. The cases set is given in Table 7.1.

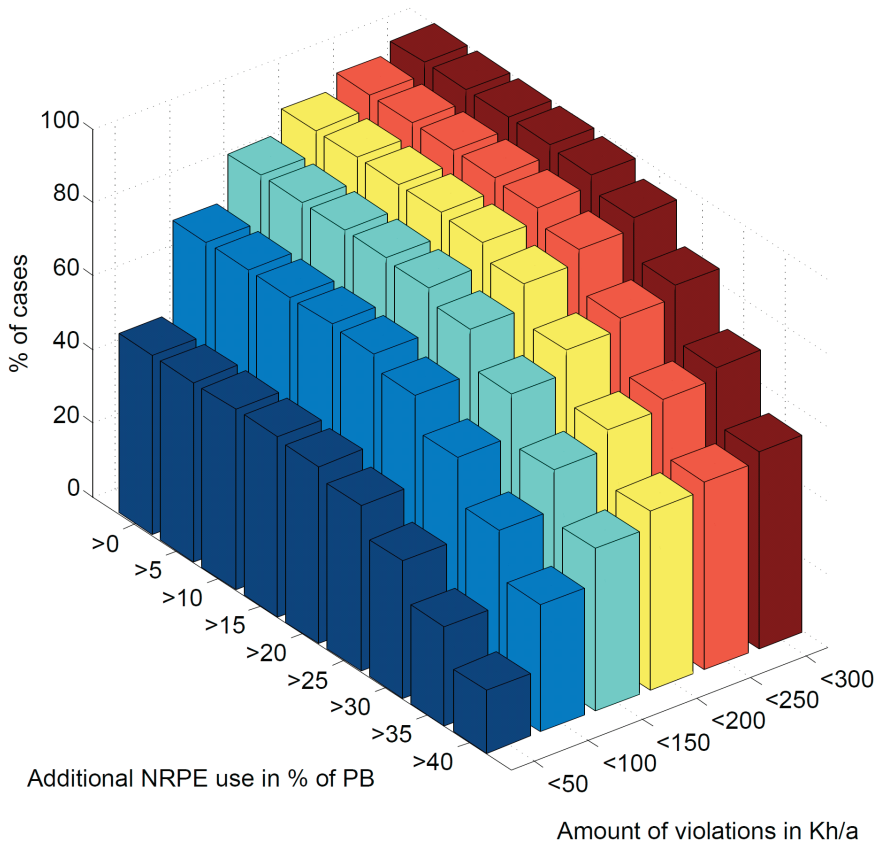

Figure 7.2: Joint cumulative distribution function of a particular additional energy use with RBC in % of PB and a particular amount of violations in Kh/a.

Q2 - Prediction horizon length

In Figure 7.3 the average prediction horizon length (averaged over all cases from the theoretical potential analysis) is plotted which is necessary for reaching errors less than 5% compared to PB. The analysis is separated for different HVAC systems and the two building standards. It can be seen that for most systems (on average) a prediction horizon of 24h is sufficient to deviate not more than 5% from the PB performance, that is why it was decided to use a 24h prediction horizon for all investigated cases (except for PB simulations).

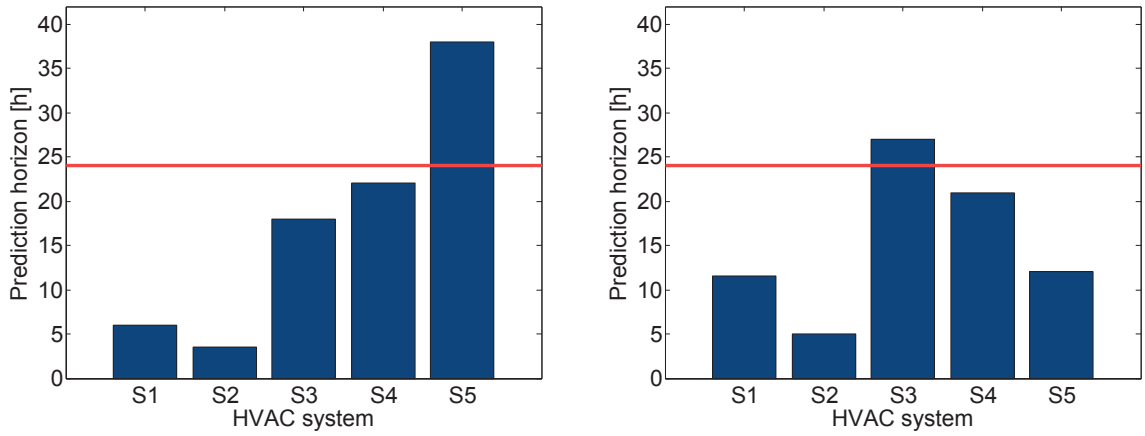

(a) Swiss average (b) Passive house

Figure 7.3: Average prediction horizon length necessary for error in NRPE use to PB of less than 5% for different HVAC systems and separated by swiss average (a) and passive house (b).

7.5.2 Practical Energy Savings Potential

Q3 - Performance of DMPC

In order to answer Q3, the performance of DMPC in terms of NRPE use and violations for the cases in Table 7.1 was compared to PB and RBC and is plotted in Figure 7.4. DMPC and RBC had a larger NRPE use than PB and had both many violations. When comparing RBC and DMPC, both, RBC as well as DMPC, exceeded 70 Kh/a, but DMPC violated this threshold more clearly. The number of violations were also typically larger for DMPC. Note, for both RBC and DMPC the data points for Cases 4 and 8 are not shown because they were beyond the axes ranges of the plots.

Q4 - Performance of SMPC

In order to assess the possible added value of SMPC as compared to the simpler DMPC controller, we considered PB, DMPC, RBC and SMPC for the cases in Table 7.1. Note for SMPC only Cases 1, 2, 3, 7, 17, and 18 were available. The results for SMPC are also shown in Figure 7.4. SMPC resulted in clearly less violations than DMPC and for the available cases also had a comparable or smaller NRPE use. The amount of violation was in all cases less than 70 Kh/a.

In Figure 7.5 SMPC is directly compared for the same six cases with the performance of RBC. It is shown that SMPC has always clearly less NRPE use than RBC and in four of six cases smaller amounts of violations (below the violation limit of 70 Kh/a).

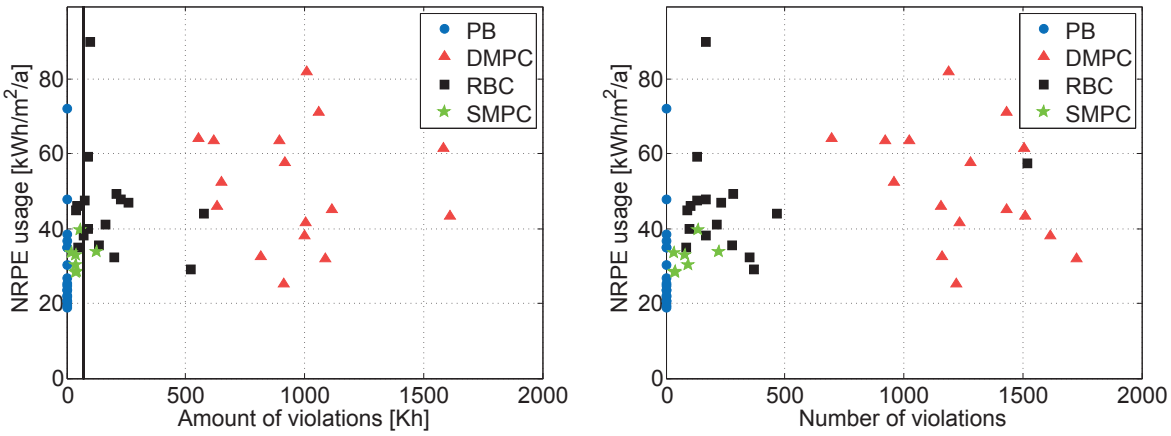

(a) (b)

Figure 7.4: Comparison of PB, DMPC, RBC, and SMPC in terms of NRPE usage versus amount of violations (a) as well as number of violations (b).

This indicates that the additional NRPE use with RBC can be reduced significantly with SMPC.

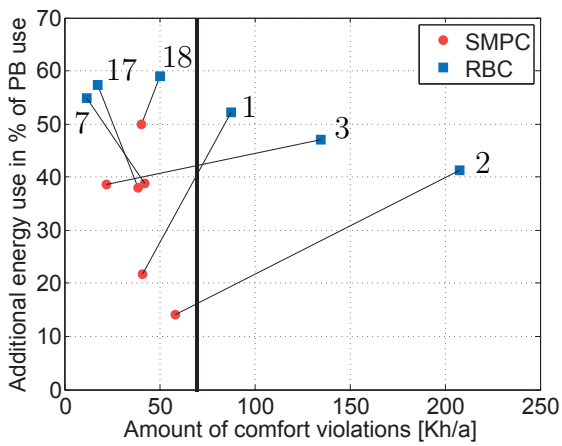

Figure 7.5: Comparison of SMPC and RBC for Cases 1, 2, 3, 7, 17, and 18 in Table 7.1.

Figures 7.6 and 7.7 show the resulting room temperature profiles throughout the whole year for Case 3 in Table 7.1 when using RBC and SMPC, respectively. It can be seen that SMPC has smaller and less frequent violations than RBC. Furthermore, the diurnal temperature variations are much smaller with SMPC, which is a more favorable behavior in terms of comfort. This behavior is similarly observed for the other cases.

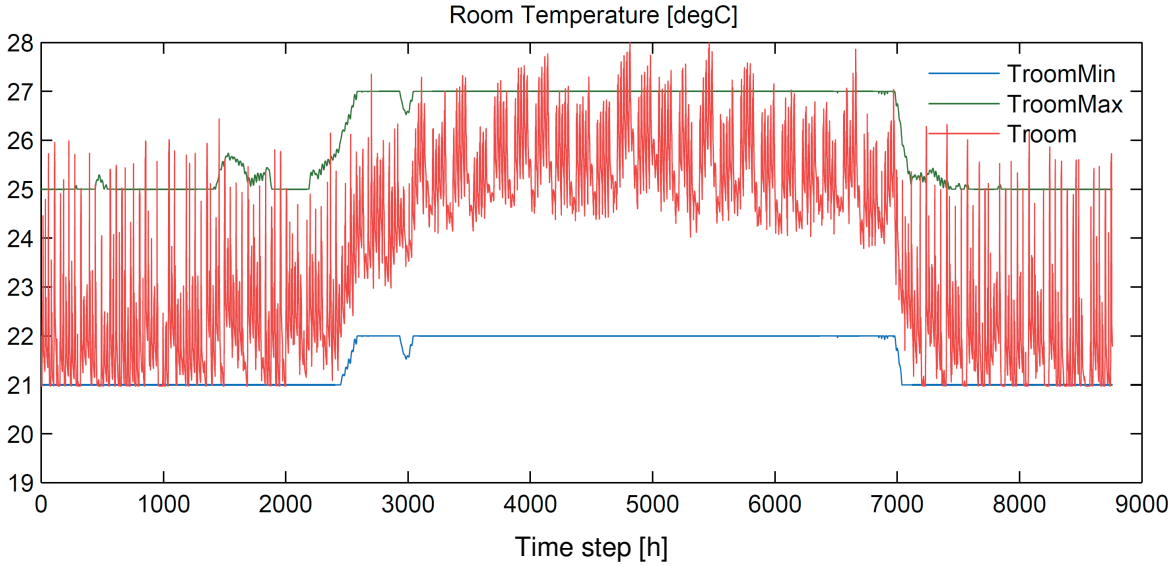

Figure 7.6: Room temperature profile of Case 3 in Table 7.1 using RBC for year 2007.

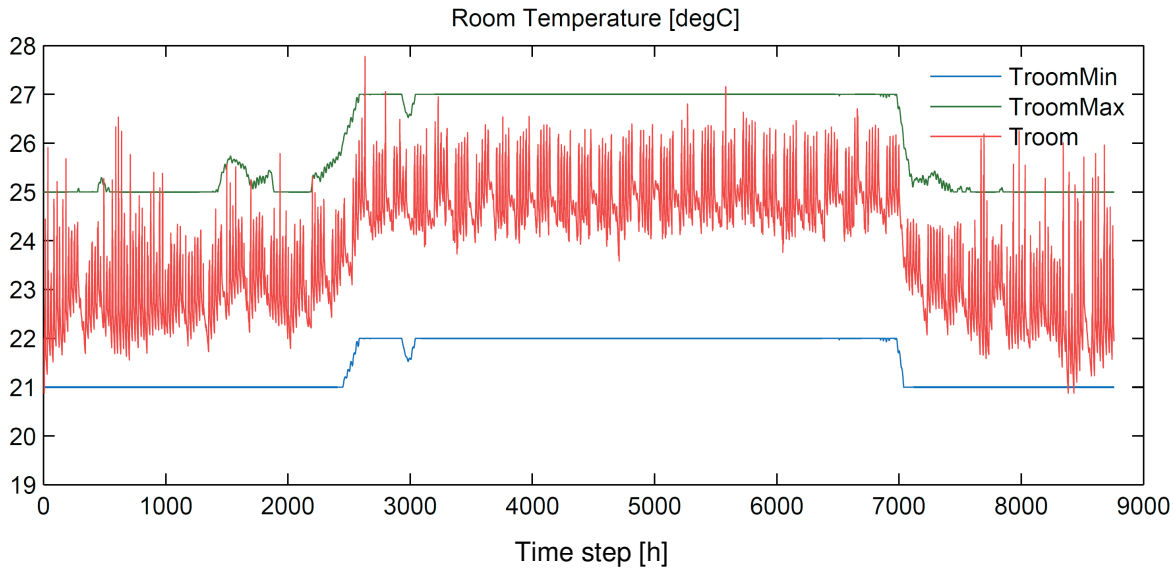

Figure 7.7: Room temperature profile of Case 3 in Table 7.1 using SMPC for year 2007.

Q5 - Importance of Weather Predictions

Figure 7.8 depicts the performance of SMPC with persistence predictions ($\text{SMPC}_{\text{pers}}$) versus COSMO-7 weather predictions (SMPC_{C7}). $\text{SMPC}_{\text{pers}}$ shows in all cases clearly more NRPE use. In two cases each, $\text{SMPC}_{\text{pers}}$ shows slightly less violations, equal amounts of violations, and clearly larger violations than SMPC_{C7}.

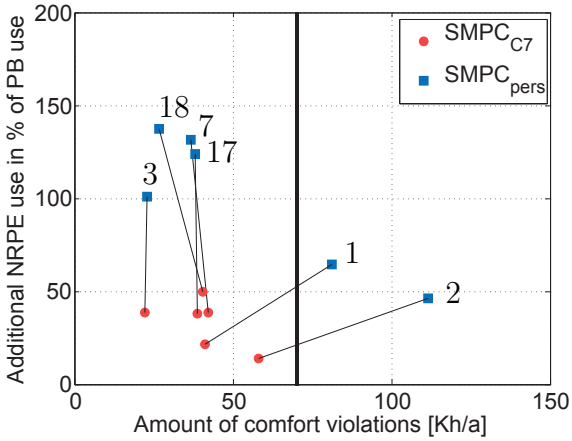

Figure 7.8: Comparison of SMPC with different weather predictions for Cases 1, 2, 3, 7, 17, and 18 in Table 7.1.

Q6 - Tunability

For Case 1 from Table 7.1 the obtained Pareto frontier with respect to the annual NRPE use and annual amount of comfort violations is shown in Figure 7.9. The curve shows a smooth behavior and it can be seen that a decrease in the amount of violations from 70 to 40 Kh/a goes along with an additional NRPE use of 10%.

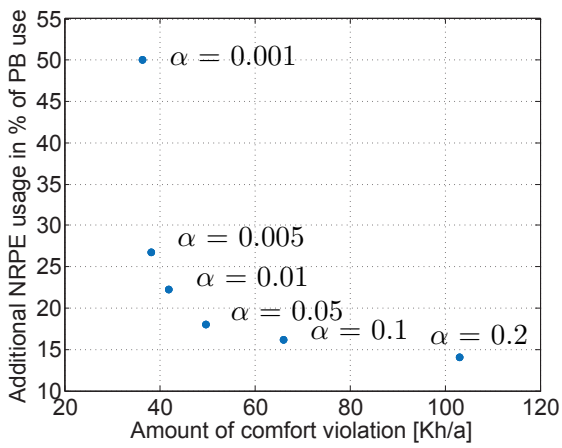

Figure 7.9: Tuning of SMPC for Case 1 in Table 7.1. Pareto frontier of additional NRPE use in % of PB use versus amount of comfort violations.

7.6 Conclusions

In this chapter investigations of the energy savings potential in Integrated Room Automation (IRA) both when comparing the current control practice (RBC) with a theoretical benchmark, the Performance Bound (PB), and when comparing it with Deterministic MPC (DMPC) and Stochastic MPC (SMPC) were presented. Unlike other works that often focus on a particular example, the energy savings potential was estimated in a large-scale simulation study for a large number of different cases varying in the building type, HVAC system, and weather conditions. The results of the large-scale simulation study, that compared the performance of PB and RBC, showed that there is a significant energy savings potential for MPC in many cases.

The newly developed SMPC strategy for building climate control was tested. This controller makes use of weather forecasts in order to compute how much energy and which low/high energy cost actuators are needed to keep the room temperature in the required comfort levels. SMPC was shown to outperform RBC, which is the current control practice, not only in terms of non-renewable primary energy (NRPE) usage and thermal comfort statistics, but also in terms of advantageous room temperature dynamics. SMPC resulted in much smaller diurnal temperature variations, and this behavior can be considered more favorable since the occupants are exposed to much smaller temperature variations during the day. When comparing to DMPC, SMPC was found to be superior both in terms of NRPE usage and comfort violations. This is due to the fact that, unlike DMPC, SMPC is able to directly account for the uncertainty of the weather forecast in its control decisions. It was also shown that the performance of SMPC depends on the quality of the weather prediction; SMPC performed clearly better using COSMO-7 predictions compared to the simple persistence predictions. A further benefit of SMPC is the easy tunability of the tradeoff between NRPE usage and comfort violations with the tuning parameter α, that reflects the level of constraint violations.

In summary, SMPC is a promising approach for building control. However, its performance in real applications can be expected to vary with the quality of the model and the available input data (model parameters, system states, weather predictions etc.) to an extent that remains to be investigated.

8 Use of Occupancy Predictions and MPC

8.1 Introduction

Besides the weather, a second important influence on the thermal behavior of buildings originates from its occupants, both in terms of the heat gains that are introduced to the building and in terms of the constraints describing the occupants' comfort requirements. Today, occupancy information is used only in form of schedules in building climate control, often in addition with instantaneous adjustments of lighting, sometimes in addition with instantaneous adjustment of both lighting and ventilation based on occupancy sensor measurements. The question arises whether the use of occupancy predictions has a significant energy savings potential.

In [BF77] the authors showed that significant savings can be achieved by optimizing a nighttime temperature setback strategy (i.e., during night the thermal comfort constraints are relaxed). This suggests that also information about long-term vacancies (business trips, holidays, illnesses) can contribute to increase energy efficiency in building control, or, more generally speaking, it suggests that taking into account occupancy predictions can contribute to energy savings. This chapter focuses on quantifying the savings potential of long-term occupancy/vacancy predictions by means of simulations.

8.1.1 Use of Occupancy Information for Building Automation

As some of the first dealing with occupancy information for building automation, the authors in [New95] tried to estimate the benefit of occupancy sensor based lighting control. The same question was addressed in [BRM06] where a more detailed occupancy-based control coupled with an ESP-r [rs12] simulation was considered. In [DA09] a learned pattern recognition algorithm was using multi-sensor data to identify how long occupants are typically staying in a room. If this expected period was long enough, the HVAC control would start to bring the room temperature to a certain comfort level while otherwise the room would stay at its setback temperature.

All these works focused on exploiting short-term (in the range of minutes) occupancy information for increasing energy efficiency in buildings. To the best of the author's knowledge, the influence of long-term (in the range of days) occupancy information on the building energy consumption has not yet been investigated systematically.

8.1.2 Use of Occupancy Models in for Building Automation

Since occupancy is of stochastic nature, in this study the average energy use of a controller taking into account occupancy information was evaluated by means of a Monte Carlo study. In order to generate random sequences of occupancy and vacancy days, a suitable model had to be found. Several works exist in the literature on modeling occupancy, some of which are summarized in the following.

The authors of [LB10a] and [LB10b] were interested in modeling occupancy to fuse sensor data with model predictions of a complex stochastic agent-based model for estimating the number of people present in an office. In [BRM06] and [PRMS05] Markov models were used to model the occupant's behavior over a time period. In [Yu10] a genetic programming algorithm was applied to learn the behavior of an occupant in a single-person office based on motion sensor data. In [WFR05] it was hypothesized that the occupancy and vacancy intervals in a single person office are distributed exponentially. Using motion sensor data collected from 35 single room offices to verify the hypothesis, it was found to hold for the vacancy intervals but had to be rejected for the occupancy intervals.

All of the works found on occupancy modeling aim at modeling short-term occupancy. Hence for the presented study a new model describing long-term occupancy had to be devised.

8.1.3 Main Idea and Outline

The aim in this chapter is to quantify the importance of occupancy predictions for energy efficient building control by means of a simulation study. In Section 8.2 the building simulation framework is described, i.e. it is presented which cases defined in Chapter 6 are investigated and which changes in the simulation setup are done for the occupancy study. In Section 8.3 the occupancy model is presented, Section 8.4 describes the investigations, and Section 8.5 is devoted to the results. Section 8.6 provides a discussion, and in Section 8.7 conclusions are drawn.

8.2 Building Simulation Framework

This section describes the building simulation framework for the occupancy study, in particular, it explains the necessary modifications to the previously defined simulation setup (see Chapter 6) and details the cases that were investigated.

8.2.1 Building and HVAC Model

The building and HVAC model employed in the occupancy study was based on the one-zone model in Figure 6.1 of Chapter 6, which is described in (6.8) of Chapter 6 and can be rewritten as

$$\begin{aligned} x_{t+1} &= Ax_t + Bu_t + Ev_t + \sum_{i=1}^{n_u}[(B_{vu,i}v_t + B_{xu,i}x_t)u_{t,i}] \\ y_t &= Cx_t + Du_t + Vv_t + \sum_{i=1}^{n_u}[(D_{vu,i}v_t)u_{t,i}] \ . \end{aligned} \tag{8.1}$$

In this one-zone model it was assumed that the boundary conditions originating from neighboring zones are identical to the modeled zone. In order to account for the heat transfer between zones which are occupied and zones which are vacant in inhomogeneous occupied buildings, a two-zone model was constructed for the occupancy investigation. This two-zone model was obtained by connecting the room nodes of two one-zone models as in (6.8) via their inner walls (see Figure 6.1) as well as connecting the branch originating from the first room node going through the floor to the ceiling of the second zone and the other way around. This gives rise to the following chessboard-like structure:

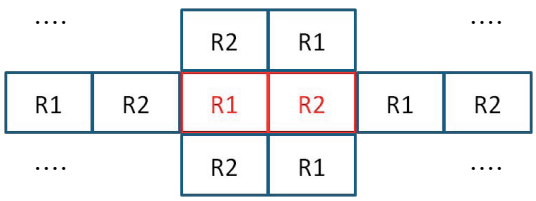

Figure 8.1: Two-zone model.

This two-zone model enables two occupancy layouts: a *homogeneous occupancy*, where the occupancy in both zones is identical and an *alternating occupancy*, where the occupancy in the two zones is different, i.e. one zone is occupied while the other one is vacant. Due to the chessboard-like structure of the model, these two layouts can be expected to represent the extremes.

8.2.2 Building Cases and HVAC Systems

The occupancy investigation was limited to two building types B1 and B2 (as defined in Table 8.1 and two HVAC systems S1 and S5 (as defined in Chapter 6). The considered building types were chosen such as to represent common building types in Switzerland [GE09] as well as to have different thermal characteristics. A description of the two building types and their parameters is given in Table 8.1. The numerical values of the system matrices that reflect these two building types can be found in [LWC+09]. We have that $\mathbb{B}^{\text{occ}} := \{\text{B1, B2}\} \subset \mathbb{B}$.

Table 8.1: Building types for investigation of occupancy information.

	$\mathbb{B}^{\text{occ}}$			
Building type	**Building standard**	**Constr. type**	**Window fraction**	**Facade orient.**
B1	sa	h	l	S
B2	pa	h	h	S

The two HVAC systems considered in this study were S1 and S5 as described in Table 6.2 of Chapter 6. Both HVAC systems included blind positioning and electric lighting, but they differed in terms of availability of ventilation as well as means for heating and cooling. HVAC system S1 was chosen due to the fact that it is a very simple HVAC system, which facilitates the analysis and it is a common setup. HVAC system S5 included TABS, where large savings potentials from occupancy predictions are expected due to its usually very long time constants. We have that $\mathbb{S}^{\text{occ}} := \{\text{S1, S5}\} \subset \mathbb{S}$.

8.2.3 Control settings

The definition of the constraints in this study varied from the definition in Chapter 6 in two respects. First, the thermal comfort range was defined to be constant instead of being a function of the exponentially weighted running mean of the past measured outside air temperature values. The reason for this was that the dependency of energy savings on occupancy patterns is easier to analyze, if a constant comfort band is assumed. Second, setbacks were assumed to be applied depending on the occupancy and the comfort range for the thermal setback was adjusted. The reason for making the thermal comfort range very large during setback was to prevent limitations in savings effects by constraining the temperature during vacancy times. The constraints were defined as follows

$$
\begin{aligned}
y_{t,(1)} = \;& \text{room temperature [°C]} \\
& \text{if occupied} \quad 21 \leq y_{t,1} \leq 26 \qquad \text{else} \quad 5 \leq y_{t,1} \leq 40 \\
y_{t,(2)} = \;& \text{room illuminance [lux]} \\
& \text{if occupied} \quad 500 \leq y_{t,2} \qquad \text{else} \quad 0 \leq y_{t,2} \\
y_{t,(3)} = \;& \text{ceiling surface temperature [°C]} \\
& 18 \leq y_{t,3} \\
y_{t,(4)} = \;& \text{total air change rate } \left[\mathrm{h}^{-1}\right] \\
& \text{if occupied} \quad 1.54 \leq y_{t,4} \leq 4 \qquad \text{else} \quad 0 \leq y_{t,4} \leq 4 \;.
\end{aligned}
$$

Note that in case of low internal gains, the lower bound on the air change rate during occupancy is 0.86.

There was just one choice of control settings considered in the occupancy study, which is $\mathbb{A}^{\mathrm{occ}} := \{(c_{\mathrm{NRPE}}, \mathrm{wid}, \mathrm{SBon}, \mathrm{IAQon}\} \subset \mathbb{A}$.

8.2.4 Disturbances

The building was (as in the definitions of Chapter 6) assumed to be subject to two kinds of disturbances, originating from weather and from internal gains (occupants, equipment). The disturbances v_t are

$$
\begin{aligned}
v_{t,(1)} &= \text{solar radiation } \left[\mathrm{W/m^2}\right] \\
v_{t,(2)} &= \text{outside air temperature [°C]} \\
v_{t,(3)} &= \text{outside air wetbulb temperature [°C]} \\
v_{t,(4)} &= \text{internal gains occupants } \left[\mathrm{W/m^2}\right] \\
v_{t,(5)} &= \text{internal gains equipment } \left[\mathrm{W/m^2}\right].
\end{aligned}
$$

The assumptions on weather and internal gains were changed compared to Chapter 6 as follows.

Weather

For the weather variables, it was assumed that all *predictions* are perfect, i.e. the weather *prediction* is equal to the (future) weather *realization*. The reason for the weather variables being assumed in this idealized fashion was the focus of this investigation on occupancy information and the aim to be able to isolate its effect on energy savings. All other parameter settings were therefore assumed ideal (i.e. perfect weather prediction, no model-plant parameter mismatch, idealized daily weather cycle, etc.).

For the *realization* of weather variables, only two seasons were considered, summer and winter, again to simplify the analysis of occupancy information. For creating weather data, the average hourly values of the corresponding season from a design reference year (i.e. a representative annual data set, which follows the compilation of the standards of the SIA Merkblatt 2028 (2008)) were taken and a daily cycle of the considered variables was created. The so created average daily cycle of the corresponding season was repeated in the simulation to create several days, such that it resulted in a periodic signal. This signal was used for two reasons: First, it had a realistic diurnal profile; and second, it facilitated the analysis of the occupancy influence due to its simplicity.

Internal gains

Internal gains due to *people* and internal gains due to *equipment* were assumed to be perfectly correlated, i.e. while people were present, the equipment was used, during vacancy times the equipment was not used. Only some base load from the equipment was assumed to be constant throughout the simulation. In the following, if referred to occupancy or vacancy, then it is assumed that the equipment is varying accordingly.

The choice of the occupancy *prediction* was the core part of this investigation. In current practice, a *standard weekly profile* is assumed as a fixed schedule for occupancy prediction. This is sometimes improved by additionally including an instantaneous *measurement* of occupancy, i.e. information about the *realization* at the current time step, and adjusting lighting and/or ventilation accordingly. To estimate the potential benefit of more sophisticated occupancy predictions, these methods were compared with a controller that had perfect information about the occupancy *realization*, i.e. the *prediction* was equal to the future *realization* (see also the definition of controllers in Section 8.4). In the following, the standard weekly profile and the realization are defined.

The *standard weekly profile* (see also Section 8.3) was constructed based on the definitions in the building standards [SIA06b], with the exception that the occupancy level was held constant during the day. This is summarized as follows.

1. A building zone is either occupied or vacant (no intermediate status allowed).
2. If the status is occupied, the internal gains levels are:
   People: constant between 7:00 and 18:00, zero otherwise.
   Equipment: constant between 7:00 and 18:00, constant low value otherwise.
3. During nights and weekends the zone is always vacant.

The standard weekly profile is shown in Figure 8.2.

The *realization* was assumed to differ from the schedule in terms of additional va-

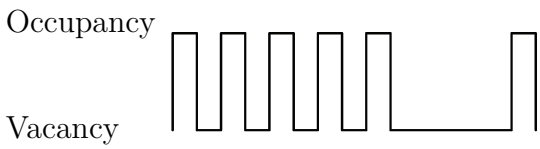

Figure 8.2: A standard weekly occupancy profile is constructed based on the standards [SIA06b] with the exception that the occupancy level is held constant during the day.

cancies, i.e. vacancies occurred during whole working days due to illness, holiday, business trips, etc. This time series with additional vacancy days was randomly created and termed *stochastic varying profile* throughout this work. Since the creation of the stochastic varying occupancy profile and the design of the occupancy model are a central part of this work, they are presented in detail in a separate section, see Section 8.3.

To summarize, for the disturbances two different seasons are considered (summer (sum) and winter (win)) and two different levels of internal gains (high (ih) and low (il)). We have that the set of possible disturbance parameter combinations for the occupancy study is given as $\mathbb{D}^{\text{occ}} := \{(\text{sum}, \text{ih}), (\text{sum}, \text{il}), (\text{win}, \text{ih}), (\text{win}, \text{il})\}$.

8.2.5 Control formulation

As the one-zone model investigated previously, the resulting two-zone model is bilinear, which would lead to a non-convex optimization problem when used in an MPC formulation. Therefore, a form of Sequential Linear Programming was applied [GS61] for linearizing the model at each time step yielding a time-varying linear model of the form

$$\begin{aligned} x_{t+1} &= Ax_t + B_t u_t + Ev_t \\ y_t &= Cx_t + D_t u_t + Vv_t \ . \end{aligned} \tag{8.2}$$

The MPC problem is then given as follows.

Problem 8.1 (MPC for occupancy study).

$$J^*_{\text{occ}}(x_t) = \min_{u_{t|t},\dots,u_{t+N-1|t}} \sum_{k=0}^{N-1} c_{\text{NRPE}} \cdot \xi^T \cdot u_{t+k|t} \tag{8.3}$$

subject to

$$Su_{t+k|t} \leq s \qquad \forall k \in \mathbb{N}_0^{N-1} \tag{8.4}$$

$$Gy_{t+k|t} \leq g_k \qquad \forall k \in \mathbb{N}_0^{N} \tag{8.5}$$

$$x_{t+k+1|t} = Ax_{t+k|t} + B_t u_{t+k|t} + Ev_{t+k|t} \qquad x_{t|t} = x_t \tag{8.6}$$

$$y_{t+k|t} = Cx_{t+k|t} + D_t u_{t+k|t} + Vv_{t+k|t} \ , \tag{8.7}$$

where c_{NRPE} and ξ are defined in Section 6.4 of Chapter 6, (8.4) denotes the input constraints, (8.5) denotes the output constraints, which are time-varying due to the setbacks, and (8.6) and (8.7) denote the building and HVAC dynamics.

For all formulations in the occupancy study a perfect weather prediction was assumed. In that sense, the control formulation was very similar to the PB as defined in Chapter 7. The formulation used an hourly time step. The prediction horizon N was chosen as 72 which corresponds to three days. Choosing a longer prediction horizon was shown not to improve the energy use, i.e. the improvement was below 1% compared to a prediction horizon of one week. The control horizon was 1. Two variants of the formulation were considered, which differed in the handling of occupancy predictions. This is detailed in Section 8.4.

8.3 Occupancy Model

This section is devoted to the construction of occupancy *realizations* and the modeling of occupancy necessary for creating these realizations.

The relative energy savings which may result from taking into account occupancy information in building climate control compared to using only schedules (i.e. assuming the standard weekly profile) can be expected to significantly depend on the occupancy realization. For instance, if the occupancy realization does not deviate much from the standard weekly profile, more sophisticated occupancy predictions are not important, whereas their importance grows with more deviating occupancy realizations. It was therefore decided to carry out a simulation study with different occupancy patterns. Hence, a model of occupancy was needed for generating random occupancy time series for a Monte Carlo study, in which the relative energy savings were estimated.

In order to determine how to model occupancy, as a first step, occupancy data from an office building in Zurich was analyzed. These data comprised occupancy and vacancy days of 50 different persons throughout five years, whereas not all people were present throughout all years. The histograms for occupancy and vacancy of all people throughout the five years are given in Figure 8.3. Both histograms resemble geometric distributions.

Motivated by the work in [WFR05], where exponential distributions for vacancy and occupancy in the range of minutes are assumed, and the desire to use a simple model for occupancy in order to easily analyze effects of occupancy patterns, geometric distributions (i.e. the discrete version of the exponential distribution) for vacancy and occupancy days were assumed.

With this assumption, occupancy time series were created with the procedure given

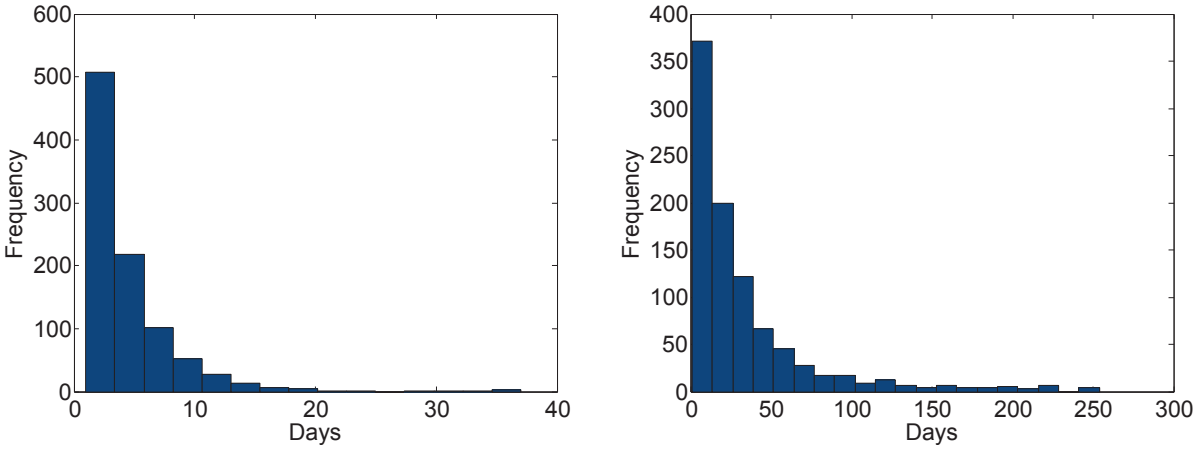

(a) Vacancy (b) Occupancy

Figure 8.3: Vacancy (8.3(a)) and occupancy (8.3(b)) histograms of 50 persons throughout five years. The duration of the vacancy/occupancy intervals is plotted on the x-axis in days whereas on the y-axis the frequency of occurrence of the corresponding interval is shown.

in Algorithm 3. The time series of occupancy are created for a particular pair of

Algorithm 3 Occupancy time series generation

1. Choose expected number of consecutive vacancy days β_{vac} and expected number of consecutive occupancy days β_{occ}.
2. Assume a geometric distribution f_{vac} for x_{vac}, where x_{vac} = number of consecutive vacancy days and $\mathbb{E}(x_{\text{vac}}) = \beta_{\text{vac}}$.
3. Assume a geometric distribution f_{occ} for x_{occ}, where x_{occ} = number of consecutive occupancy days and $\mathbb{E}(x_{\text{occ}}) = \beta_{\text{occ}}$.
4. Sample alternately from distributions f_{vac} and f_{occ} to create an occupancy status time series.
5. Insert a weekend (two vacant days) every five days.

($\beta_{\text{vac}}, \beta_{\text{occ}}$) and are representing the *stochastic varying occupancy profile*, which is used as *realization* of occupancy (see Section 8.2.4). For the Monte Carlo study, a large number of these time series were created and the average energy use and standard deviation with these realizations were computed assuming different occupancy information (see Section 8.4). The number of simulations was chosen such that the estimator for a particular comparison of two controllers with different occupancy information had a standard deviation of less than 1.5% with a confidence interval of 90%. One example of the stochastic varying occupancy profile is shown in Figure 8.4.

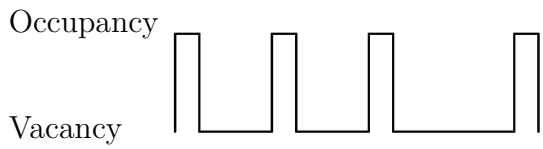

Figure 8.4: Several occupancy profile time series are created for a Monte Carlo study.

Since a separate investigation (see Appendix D) showed the average energy savings to be a monotonously increasing function of $\beta_{\text{vac}}/\beta_{\text{occ}}$, the investigation was limited to the following set $(\beta_{\text{vac}}, \beta_{\text{occ}}) \in \{(1, 10), (1, 5), (5, 10)\}$.

8.4 Investigations

In this section the investigations are described. A large number of simulations was performed, varying three components: the controller (chosen from some set $\mathbb{C}^{\text{occ}}$, which deviated from set $\mathbb{C}$ as explained in the following), the occupancy pattern (chosen from some set $\mathbb{O}$) and the (remaining) simulation parameters (chosen from some set $\mathbb{P}^{\text{occ}}$). The options amongst the three components are detailed in the following.

Controller

All controllers considered in this investigation are based on the MPC algorithm described in Section 8.2, although the current practice in building automation is to use RBC. The reason is the direct comparability and focus on the effect of occupancy prediction, which is easily achievable when using MPC. If one wanted to compare the value of different occupancy predictions with a RBC controller, the performance would highly depend on the rules applied and it would be very hard to isolate the effect of the occupancy prediction. In contrast, with MPC, the occupancy prediction directly enters in the optimization problem and therefore, one can easily compare the same MPC controller with different predictions, and can directly see the difference. The performance of a MPC controller with a particular occupancy information can be thought of as bound on the performance of a RBC controller with the identical available occupancy information.

Four different forms of occupancy information are considered in this investigation, an overview can be found in Table 8.2. $C^{\text{std}}_{-,-}$ reflects the standard controller as currently implemented, where the superscript denotes the prediction and the subscript the adaptation to measurements. This controller assumes as occupancy prediction the standard weekly profile (*std*) and makes no further adjustments based on measurements $(-, -)$.

$C^{\text{std}}_{\text{li},-}$ is identical to the first controller, but adjusts lighting according to instantaneous measurements $(li, -)$, i.e. if the occupancy sensor detects vacancy, the lighting is turned off, meaning that the constraints on illuminance are set to their vacancy value in the MPC problem for the rest of the corresponding day. The remaining constraints and predicted occupancy values are kept as in the first controller to ensure that the comfort requirements can be met again quickly in case the occupants are returning. $C^{\text{std}}_{\text{li,ve}}$ is identical to the first controller, but adjusts lighting and ventilation (li, ve) according to instantaneous measurements, i.e. if the occupancy sensor detects vacancy, lighting and ventilation are turned off, meaning that the constraints on illuminance and air change rate are set to their vacancy value in the MPC problem for the rest of the corresponding day. Finally, $C^{\text{perf}}_{-,-}$ reflects a controller which is possible at best, since it has a perfect prediction (*perf*) of the occupancy realization available, i.e. it knows a priori the occupancy pattern that is realized in the future.

The key question is how big the energy savings potential of taking into account occupancy predictions is compared to using occupancy schedules. This savings potential is directly obtained by the comparison of $C^{\text{perf}}_{-,-}$ and $C^{\text{std}}_{-,-}$ since they only differ in terms of the considered occupancy prediction. One should note that both of these controllers, $C^{\text{perf}}_{-,-}$ and $C^{\text{std}}_{-,-}$, are idealized versions of building controllers (e.g., also RBC controllers) in the sense that they provide a bound on the performance given the model of the building is correct. However, in current building setups, if measurements of the occupancy are available, one can adjust lighting and ventilation based on instantaneous occupancy measurements. So, another equally important question is, whether occupancy *predictions* are necessary to realize significant energy savings or if already adjustments according to occupancy *measurements* provide a significant energy savings potential.

Note that it only makes sense to adjust lighting and ventilation to instantaneous occupancy measurements, but not heating and cooling, since the former two are very fast reacting systems, such that the comfort constraints can be guaranteed again after a short time when occupants have returned unexpectedly, whereas for heating and cooling there is no quick return to the comfort range once the room is at its setback temperature.

Also note that since in reality no perfect occupancy prediction is available, the energy savings potential of using these occupancy predictions will be an upper bound on the energy savings which are possible to achieve in reality.

Occupancy Pattern

The occupancy pattern is defined by its layout denoted with a superscript and by the choice of combination of average vacancy days and average occupancy days $(\beta_{\text{vac}}, \beta_{\text{occ}})$

Table 8.2: Variants of occupancy handling in controller.

Controller	Description
$C^{\text{std}}_{-,-}$	standard controller, assumes standard weekly profile as prediction
$C^{\text{std}}_{\text{li},-}$	same as $C^{\text{std}}_{-,-}$, but adjustment of lighting to instantaneous measurements
$C^{\text{std}}_{\text{li,ve}}$	same as $C^{\text{std}}_{-,-}$, but adjustment of lighting and ventilation to instantaneous measurements
$C^{\text{perf}}_{-,-}$	perfect prediction of occupancy

denoted with a subscript.

As already introduced in Section 8.2.1, two occupancy layouts are considered, an overview can be found in Table 8.3. $O^{\text{hom}}_{(\beta_{\text{vac}},\beta_{\text{occ}})}$ denotes homogeneous occupancy in the building, which means that the occupancy is identical in all zones of the building. $O^{\text{alt}}_{(\beta_{\text{vac}},\beta_{\text{occ}})}$ denotes alternating occupancy, which means that the occupancy in the two considered zones is different, i.e. while one zone always follows the standard schedule, the other one has random vacancies. The two different zones are arranged in a chessboard-like structure, see Figure 8.1.

For the average vacancy days and average occupancy days $(\beta_{\text{vac}}, \beta_{\text{occ}})$, it is sufficient to investigate only a subset of possible combinations {(1,10),(1,5),(5,10)} due to the monotonicity of the resulting energy savings (see Appendix D). These choices reflect that one out of 11 days is vacant, one out of six days is vacant, and five out of 15 days are vacant on the average, respectively. Let $\mathbb{O}$ denote the set of possible occupancy layouts, with $\mathbb{O} := \{O^{\text{hom}}_{(1,10)}, O^{\text{hom}}_{(1,5)}, O^{\text{hom}}_{(5,10)}, O^{\text{alt}}_{(1,10)}, O^{\text{alt}}_{(1,5)}, O^{\text{alt}}_{(5,10)}\}$.

Table 8.3: Occupancy patterns.

Occupancy pattern $(\beta_{\text{vac}}, \beta_{\text{occ}}) \in \{(1,10),(1,5),(5,10)\}$	Description
$O^{\text{hom}}_{(\beta_{\text{vac}},\beta_{\text{occ}})}$	occupancy is identical in all zones
$O^{\text{alt}}_{(\beta_{\text{vac}},\beta_{\text{occ}})}$	chessboard-like structure of two different zones, one zone always follows standard schedule, the other has random vacancies

Parameters

In order to determine the influence of the building type ($\in \mathbb{B}^{\text{occ}}$) and HVAC system

($\in \mathbb{S}^{\text{occ}}$), the season ($\in \mathbb{D}^{\text{occ}}$), as well as the internal gains level ($\in \mathbb{D}^{\text{occ}}$) on the energy savings potential, the parameters as listed in Table 8.4 were varied in this study. Two different building types {B1,B2} were simulated, two different HVAC systems {S1,S2}, summer and winter season {sum,win}, as well as two different levels for the internal gains {ih,il}. The choice of the control settings was constant throughout this investigation, i.e. $\mathbb{A}^{\text{occ}} = \{(c_{\text{NRPE}}, \text{wid}, \text{SBon}, \text{IAQon})\}$.

Let P denote a particular combination of parameters (B, S, A, D). The set of possible parameter combinations is denoted by $\mathbb{P}^{occ} := \{(B, S, A, D) | B \in \mathbb{B}^{\text{occ}}, S \in \mathbb{S}^{\text{occ}}, A \in \mathbb{A}^{\text{occ}}, D \in \mathbb{D}^{\text{occ}}\}$.

Table 8.4: Parameters for investigation of occupancy information.

Parameter	**Value**
Building type	B1, B2, see Table 8.1
HVAC system	S1, S5
Season	summer(sum), winter(win)
Internal gains level	high(ih), low(il)

Simulations

As a first step, the simulations for homogeneous occupancy were carried out and in a second step the simulations for alternating occupancy. Denote with $E(C, O, P)$ the average energy use for a particular choice of a controller C, an occupancy layout O and a combination of parameters P.

The energy use obtained by using the standard controller assuming a standard weekly profile $C^{\text{std}}_{-,-}$ was used as a benchmark. The aim was to identify the relative savings potential to this benchmark by using the other three controller options: $C^{\text{std}}_{\text{li},-}$, $C^{\text{std}}_{\text{li,ve}}$, and $C^{\text{perf}}_{-,-}$. These were computed as

$$\Delta E^{\text{std}}_{\text{li},-}(O, P) := \frac{E(C^{\text{std}}_{-,-}, O, P) - E(C^{\text{std}}_{\text{li},-}, O, P)}{E(C^{\text{std}}_{-,-}, O, P)} \tag{8.8}$$

$$\Delta E^{\text{std}}_{\text{li,ve}}(O, P) := \frac{E(C^{\text{std}}_{-,-}, O, P) - E(C^{\text{std}}_{\text{li,ve}}, O, P)}{E(C^{\text{std}}_{-,-}, O, P)} \tag{8.9}$$

$$\Delta E^{\text{perf}}_{-,-}(O, P) := \frac{E(C^{\text{std}}_{-,-}, O, P) - E(C^{\text{perf}}_{-,-}, O, P)}{E(C^{\text{std}}_{-,-}, O, P)} \tag{8.10}$$

$\forall\ O \in \mathbb{O}$ and $\forall\ P \in \mathbb{P}^{\text{occ}}$. It can clearly be expected that $0 \leq \Delta E^{\text{std}}_{\text{li},-}(O, P) \leq \Delta E^{\text{std}}_{\text{li,ve}}(O, P) \leq \Delta E^{\text{perf}}_{-,-}(O, P)$.

Whereas the controllers deviated in the occupancy prediction and instantaneous adjustment of lighting and ventilation, they all encountered the same occupancy realization in the simulations, which was obtained from creating occupancy time series according to Algorithm 3. The number of runs of the Monte Carlo study, i.e. the number of simulated realization scenarios, was determined such that the estimator of the relative energy savings potential had a standard deviation of less than 1.5% with a confidence interval of 90%.

8.5 Results

8.5.1 Homogeneous occupancy

Figure 8.5 depicts the simulation results for the case of homogeneous occupancy. It shows the relative energy savings $\Delta E^{\text{std}}_{\text{li},-}$, $\Delta E^{\text{std}}_{\text{li,ve}}$, and $\Delta E^{\text{perf}}_{-,-}$ as defined in (8.8)-(8.10) for all $P \in \mathbb{P}^{\text{occ}}$ and all $O^{\text{hom}}_{(\beta_{\text{vac}},\beta_{\text{occ}})} \in \mathbb{O}$, i.e. for all building types and HVAC systems, both seasons {sum,win}, both internal gains levels {il,ih}, and the three combinations of $(\beta_{\text{vac}}, \beta_{\text{occ}})$. Note that HVAC system S1 does not have ventilation, therefore, only two bars are shown.

It can clearly be seen that for all cases the energy savings potential is increasing for an increasing vacancy to occupancy ratio $\beta_{\text{vac}}/\beta_{\text{occ}}$. The savings potential is significant, ranging up to 34%. However, for almost all cases, a large fraction of this potential can already be captured by adjusting lighting and ventilation to instantaneous measurements, which can be seen from the fact that $\Delta E^{\text{perf}}_{-,-}$ is not significantly higher than $\Delta E^{\text{std}}_{\text{li,ve}}$. Only for very long vacancy to occupancy ratios as $(\beta_{\text{vac}}, \beta_{\text{occ}}) = (5, 10)$ there is still a significant savings potential of $C^{\text{perf}}_{-,-}$ compared to $C^{\text{std}}_{\text{li,ve}}$ (for building type B1 mainly in winter, for building type B2 mainly in summer).

Furthermore, for building type B1 in winter there is almost no energy savings potential with $C^{\text{perf}}_{-,-}$ compared to $C^{\text{std}}_{\text{li,ve}}$. A closer analysis revealed that due to the good insulation and large window area of this building, the controller is able to meet the comfort constraints almost only by changing the blind position, which does not contribute to the energy use.

8.5.2 Alternating occupancy

This investigation was carried out to analyze the sensitivity of the savings potential if vacancies only appear in every second room of the building. Figure 8.6 depicts the simulation results for alternating occupancy. It shows the relative energy savings

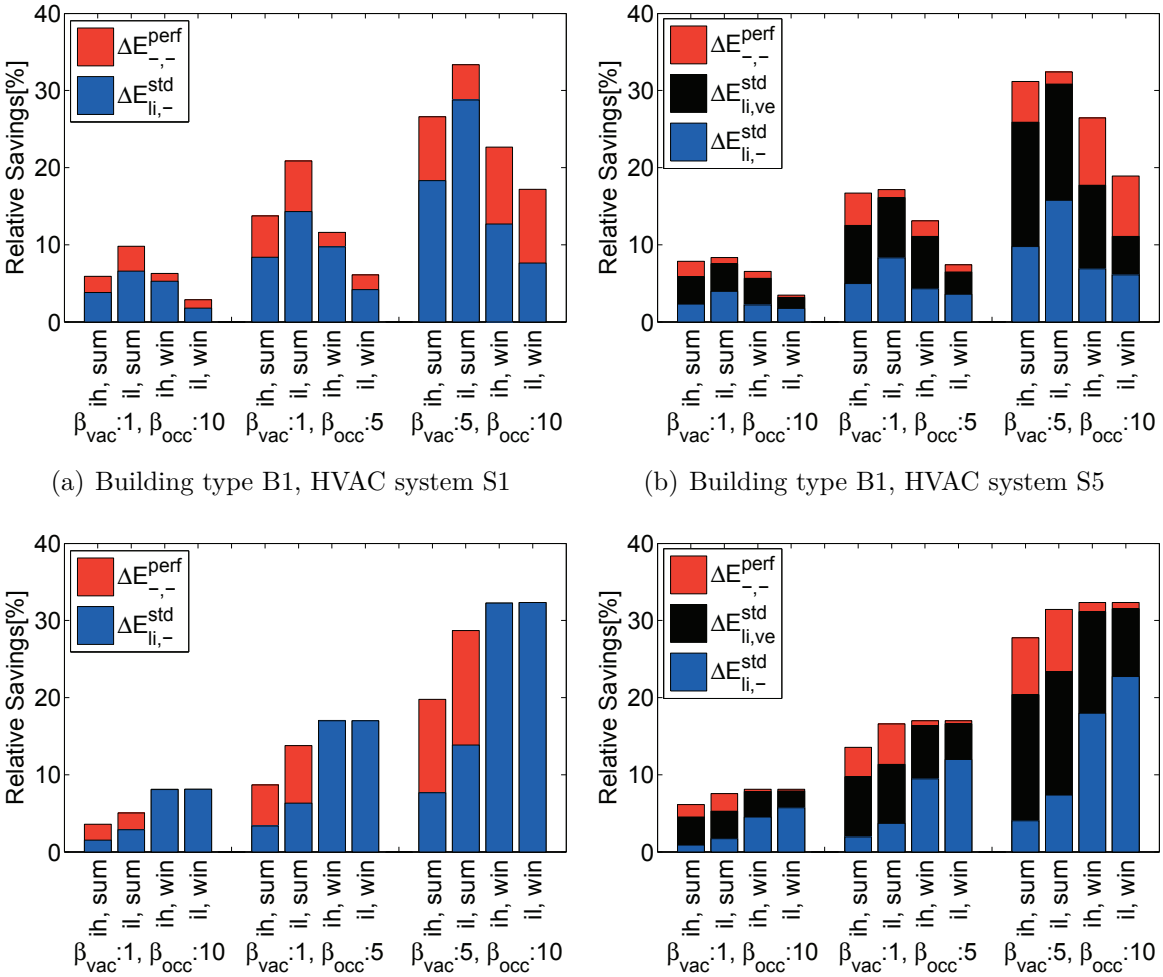

(a) Building type B1, HVAC system S1

(b) Building type B1, HVAC system S5

(c) Building type B2, HVAC system S1

(d) Building type B2, HVAC system S5

Figure 8.5: Homogeneous occupancy. The relative energy savings $\Delta E^{\text{std}}_{\text{li},-}$, $\Delta E^{\text{std}}_{\text{li,ve}}$, and $\Delta E^{\text{perf}}_{-,-}$ as defined in (8.8)-(8.10) are plotted for all $P \in \mathbb{P}^{\text{occ}}$ and all $O^{\text{hom}}_{(\beta_{\text{vac}},\beta_{\text{occ}})} \in \mathbb{O}$, i.e. for all building types and HVAC systems, both seasons {sum,win}, both internal gains levels {il,ih}, and the three combinations of $(\beta_{\text{vac}}, \beta_{\text{occ}})$.

$\Delta E^{\text{std}}_{\text{li},-}$, $\Delta E^{\text{std}}_{\text{li,ve}}$, and $\Delta E^{\text{perf}}_{-,-}$ as defined in (8.8),(8.9), and (8.10) for all $P \in \mathbb{P}^{\text{occ}}$ and all $O^{\text{alt}}_{(\beta_{\text{vac}},\beta_{\text{occ}})} \in \mathbb{O}$, i.e. for all building types and HVAC systems, both seasons {sum,win}, both internal gains levels {il,ih}, and the three combinations of $(\beta_{\text{vac}}, \beta_{\text{occ}})$.

Similarly to the case of homogeneous occupancy, the energy savings are increasing with an increasing vacancy to occupancy ratio $\beta_{\text{vac}}/\beta_{\text{occ}}$. Furthermore, for the investigated cases, the energy savings are about 50% of the corresponding cases with homogeneous occupancy. This is to be expected if one neglects the heat transfer be-

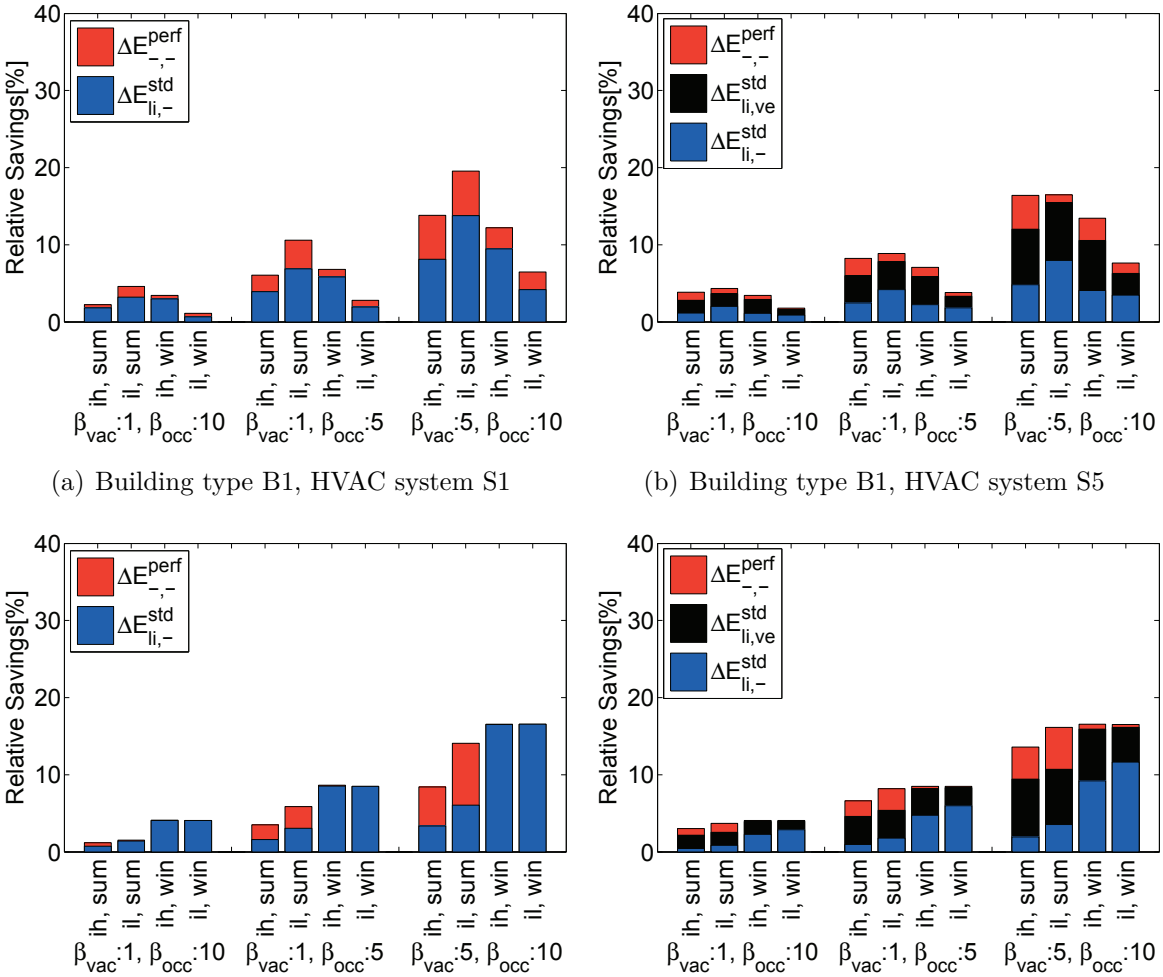

(a) Building type B1, HVAC system S1

(b) Building type B1, HVAC system S5

(c) Building type B2, HVAC system S1

(d) Building type B2, HVAC system S5

Figure 8.6: Alternating occupancy. The relative energy savings $\Delta E^{\text{std}}_{\text{li},-}$, $\Delta E^{\text{std}}_{\text{li,ve}}$, and $\Delta E^{\text{perf}}_{-,-}$ as defined in (8.8)-(8.10) are plotted for all $P \in \mathbb{P}^{\text{occ}}$ and all $O^{\text{alt}}_{(\beta_{\text{vac}},\beta_{\text{occ}})} \in \mathbb{O}$, i.e. for all building types and HVAC systems, both seasons {sum,win}, both internal gains levels {il,ih}, and the three combinations of $(\beta_{\text{vac}}, \beta_{\text{occ}})$.

tween zones, since the savings are only realized in half of the building zones. Therefore it can be concluded, that the influence of heat transfer between different zones had no significant effect on the energy savings potential in the current setup. In reality the heat transfer can be expected to be more important, due to open doors etc.

8.6 Discussion

This section is devoted to discuss the choice of the investigation setup as well as the obtained results.

8.6.1 Choice of Investigation Setup

All controllers considered in this investigation are based on MPC since it enables a direct comparability and focus on the effect of different occupancy information. If one wanted to compare the value of different occupancy predictions with RBC, the performance would highly depend on the rules applied and it would be very hard to isolate the effect of the occupancy prediction. In contrast, with MPC, the occupancy prediction directly enters in the optimization problem and therefore, one can easily compare the same MPC controller with different predictions. The performance of an MPC controller with a particular occupancy information can be thought of as an upper bound on the performance of an RBC controller with the identical available occupancy information. Therefore, if two MPC controllers with different occupancy information are compared, this yields the value of the occupancy information one would also obtain when comparing RBC controllers with the same occupancy information, but which are perfectly tuned. Hence, the use of MPC provides a unifying and simplifying framework for this investigation.

When investigating the energy savings potential of occupancy predictions, a perfect prediction of the occupancy realization was considered. In reality one could think of using for instance Outlook calendars in order to be aware of business trips, holidays, etc. in advance. However, illnesses can appear suddenly or people can also make mistakes when scheduling business trips. Therefore, in reality a perfect prediction of the realization will never be achieved and it should be pointed out that the computed energy savings potential reflects an upper bound on the potential.

In all simulations it was assumed that the model of the building and HVAC system is perfectly known and that the weather is perfectly predicted. This is clearly not the case in reality; however, since this assumption was made for all investigations, the effect on the relative savings can be expected to be small (i.e. in reality both controllers will perform worse, but the difference should not be much affected).

The choice of buildings and HVAC systems was driven by two factors: First, the choices represent common setups in Switzerland; and second, they are chosen such that they represent rather extreme outcomes of energy savings potentials, e.g., HVAC system S5 has TABS and is a slow reacting system, whereas HVAC system S1 is faster and has no ventilation. Also the buildings represent extreme scenarios, since building

type B1 is swiss average with small windows, whereas building type B2 is a passive house, which is well insulated and has large windows. The choice was made such that it can be expected that the resulting energy saving potentials of most other relevant building cases are lying in the spanned range of these cases.

Summarizing, the described investigation setup provides a general methodology for investigating questions related to energy savings potentials of occupancy information in building control.

8.6.2 Simulation Results

The most relevant case of the average vacancy and average occupancy days seems to be $(\beta_{\text{vac}}, \beta_{\text{occ}}) = (1, 5)$ since it represents a case which is still reasonable for many offices, but has quite a large energy savings potential of taking into account occupancy information. However, for this case, the relative energy savings of $C^{\text{perf}}_{-,-}$ compared to $C^{\text{std}}_{\text{li},-}$ and $C^{\text{std}}_{\text{li,ve}}$ are only significant in summer and even for these cases, the absolute energy savings are only about $1\,\text{kWh/m}^2\text{a}$ (see Appendix E).

One can clearly see that even though there is a significant energy savings potential, a large part of it can already be obtained by taking into account instantaneous occupancy measurements, i.e. with using $C^{\text{std}}_{\text{li},-}$ and $C^{\text{std}}_{\text{li,ve}}$. Hence, there is strong indication that adjustments based on instantaneous measurements have a significant energy savings potential, in particular the adjustment of ventilation (see also absolute savings in Appendix E). Using on top of that more sophisticated occupancy prediction is questionable in terms of energy savings potential since the estimated savings potential is already very small but represents an upper bound on the energy savings, which can be achieved in reality with occupancy predictions that are not perfect.

The comparison of homogeneous and alternating occupancy revealed that the influence of heat transfer between different zones had no significant effect on the energy savings potential in the current setup. In reality the heat transfer can be expected to be more important, due to open doors etc. The effect of this depends on the season: In winter heat transfer to vacant rooms is expected to increase energy use. In summer the effect of heat transfer on the energy use is unclear, since there can be a heat transfer to the cooled (occupied) room, which would increase energy use or a heat transfer to the vacant room, because this is colder due to missing internal gains.

8.7 Conclusions

This investigation estimated the energy savings potential of using occupancy information for common office buildings in Switzerland equipped with Integrated Room Automation depending on the occupancy pattern (i.e. frequency of vacancy days) as well as on the building type, HVAC system, and season. It was found that energy savings are increasing with respect to increasing vacancy and decreasing occupancy days.

The simulations with homogeneous occupancy showed a savings potential of up to 34% for the case of average vacancy and occupancy intervals of 5 and 10 days, respectively. In the simulations with alternating occupancy, the savings are in the range of 50% of the savings with homogeneous occupancy.

Taking into account occupancy information in building control has a significant energy savings potential. However, a large part of this potential can already be captured by taking into account instantaneous occupancy information.

To summarize, adjusting lighting and especially ventilation to instantaneous measurement can clearly be recommended for saving energy in building control. This recommendation is in line with many other works emphasizing the importance on so-called demand-driven ventilation. Using on top of that more sophisticated occupancy predictions does not provide a significant energy savings potential, keeping in mind that the estimated potential in this study is an upper bound, but only quite small.

9 Use of Dynamic Electricity Prices and MPC

9.1 Introduction

This chapter presents an investigation of how peak electricity demand can be reduced by adopting a dynamic electricity tariff and MPC in building control.

The International Energy Agency (IEA) recommended in particular for Switzerland additional efforts to increase *Demand Response* (DR) [(IE07]. Demand response means the management of the customer's electricity consumption in response to supply conditions, market prices, etc. In other European countries such as Germany or France, it is already made obligatory for utilities to offer variable end-consumer tariffs [Law09, Tar10].

The idea in this work is to use the thermal storage capacity of the building, as it was done in Chapters 7 and 8 for adapting to changing boundary conditions originating from weather and occupancy, and extend this to also adapt to external price signals in order to induce a grid-friendly behavior. In this work the focus is on the reduction of peak electricity demand, which is important from a grid perspective, since the peaks determine the necessary capacity of the network.

For building control, intuitively, the goal to minimize total electricity consumption seems to be well-chosen. In practice, however, such an optimization strategy can lead to remarkable peaks in electricity demand that can, and in light of grid stability, should preferably be avoided. Furthermore, electricity is consumed at times when, in the context of liberalized electricity markets, it is most expensive. The evolution of electricity prices is, however, external information that is not known to a conventional building controller.

Since the building envelope itself constitutes a thermal storage, there inherently exists the possibility to shift electricity demand from high price to low price times or from high grid load to low grid load times, respectively. The controller should therefore be enabled to take advantage of demand shifting. This is possible, if information on both electricity spot prices and grid load levels can be incorporated directly in the controller.

Note that time-series for spot prices and grid load levels should, fundamentally, be well correlated over time. Electricity demand for a given hour is strongly linked to grid load levels. And a high electricity demand will act as a driver towards high spot market prices, whereas low electricity demand has the opposite effect. However, this correlation, based on the fundamental linking of electricity demand and supply, does not hold if, e.g., speculation is driving the spot market price (see also Remark 9.3). Thus, using only the spot market price as tariff can induce negative effects, i.e. increasing already existing peak load levels in the electricity grid. Therefore, the use of MPC and a dynamic electricity tariff that is based both on spot market prices as well as on actual electricity grid load levels is proposed. This proposed tariff truly reflects the marginal costs of electricity provision for the end-user.

The electricity tariff can be readily included into the MPC cost function, however, since this electricity tariff is only available for a limited time window into the future, *Least-Squares Support Vector Machines* (LS-SVM) for electricity tariff price forecasting are used to provide the MPC controller with the necessary estimated time-varying costs for the whole prediction horizon. In the given context, the hourly pricing provides an economic incentive for a building controller to react sensitively with respect to high spot market electricity prices and high grid load levels, respectively. It can be shown that peak electricity demand of buildings can be significantly reduced, which makes this study an example for the successful implementation of Demand Response (DR) in the field of building control.

9.2 Building Simulation Framework

This section describes the building simulation framework for the study on dynamic electricity prices, in particular, it defines and explains the necessary modifications to the previously defined simulation setup in Chapter 6 and defines the cases, which were investigated.

9.2.1 Building and HVAC Model

As building and HVAC model in this study, the one-zone-model in Figure 6.1 of Chapter 6 was used, which is described by (6.8) and can be rewritten as

$$\begin{aligned} x_{t+1} &= Ax_t + Bu_t + Hv_t + \sum_{i=1}^{n_u}[(B_{vu,i}v_t + B_{xu,i}x_t)u_{t,i}] \\ y_t &= Cx_t + Du_t + Vv_t + \sum_{i=1}^{n_u}[(D_{vu,i}v_t)u_{t,i}] \ . \end{aligned} \tag{9.1}$$

9.2.2 Building Cases and HVAC Systems

In this study the definitions for the building parameters and HVAC system from Chapter 6 have not been modified. However, only a subset of the simulation cases was investigated and an overview of the investigated parameters can be found in Table 9.1. The building type parameters for the price investigation $\mathbb{B}^{\text{ep}} \subset \mathbb{B}$ is given by all combinations of $\mathbb{B}$ with facade orientation South. Concerning the HVAC system the investigation is restricted to HVAC system S1, $\mathbb{S}^{\text{ep}} := \{\text{S1}\} \subset \mathbb{S}$.

Table 9.1: Building types for investigation of dynamic electricity prices including building standard, construction type, window area fraction, and facade orientation.

Parameter	**Value**	**Identifier**
Building standard	Swiss average	sa
	Passive house	pa
Construction type	Heavy	h
	Light	l
Window area fraction	Low	wl
	High	wh
Facade orientation	South	S

9.2.3 Control Settings

The control settings for the price investigation are restricted to one case. $\mathbb{A}^{\text{ep}} := \{(c_{\text{NRPE}}, \text{wid}, \text{SBon}, \text{IAQon})\} \subset \mathbb{A}$.

9.2.4 Disturbances

For both weather and internal gains perfect predictions were assumed. For the weather predictions, weather data of the city of Zurich of the year 2007 were taken, to match with the electricity tariff data of Zurich which were available for the same year. For internal gains the assumptions defined in Chapter 6 were employed. The disturbance parameter set for the price investigation is given as $\mathbb{D}^{\text{ep}} := \{(\text{SMA, ih}), (\text{SMA, il})\} \subset \mathbb{D}$.

9.2.5 Control Formulation

Employing the same procedure for obtaining a time-varying linear model as described in Section 6.8.2 of Chapter 6 and applied in Section 8.2.5 of Chapter 8, the MPC problem is given as follows.

Problem 9.1 (MPC for with dynamic electricity tariff).

$$J^*_{\text{occ}}(x_t) = \min_{u_{t|t},\dots,u_{t+N-1|t}} \sum_{k=0}^{N-1} c^{\text{tariff}}_{t+k} \cdot \xi^T \cdot u_{t+k|t} \tag{9.2}$$

subject to

$$Su_{t+k|t} \leq s \qquad \forall k \in \mathbb{N}_0^{N-1} \tag{9.3}$$

$$Gy_{t+k|t} \leq g_k \qquad \forall k \in \mathbb{N}_0^{N-1} \tag{9.4}$$

$$x_{t+k+1|t} = Ax_{t+k|t} + B_t u_{t+k|t} + Ev_{t+k|t} \qquad x_{t|t} = x_t \tag{9.5}$$

$$y_{t+k|t} = Cx_{t+k|t} + D_t u_{t+k|t} + Vv_{t+k|t}\ , \tag{9.6}$$

where ξ is defined in Section 6.4 of Chapter 6, (9.3) denotes the input constraints, (9.4) denotes the output constraints, which are time-varying due to the setbacks, and (9.5) and (9.6) denote the building and HVAC dynamics. The time-varying electricity price enters directly in the objective function. How it is constructed is explained in Section 9.3. The formulation uses an hourly time step, a prediction horizon of 24 (one day), and a control horizon of one (one hour).

9.2.6 Electricity Tariffs

In the investigation three different tariff schemes are used for the building control simulations: a *constant* electricity tariff c_t^{con}, a typical *peak/ off-peak* tariff c_t^{pop}, and a recently proposed *dynamic* tariff c_t^{dyn} [UA10].

Table 9.2: Overview of electricity tariffs. The index t denotes the time dependency, i.e. c_t is the tariff at time t.

Tariff	Description
c_t^{con}	constant tariff
c_t^{pop}	peak/ off-peak tariff
c_t^{dyn}	dynamic tariff

All tariffs are based on the price regime for electricity provision, transmission as well as fees and taxes that are currently charged by the local utility "Elektrizitätswerk der Stadt Zürich" (ewz) in the city of Zurich, Switzerland. For the *constant* tariff, a time-independent fixed rate for electricity consumption based on the average electricity costs is assumed (CHF 0.147/kWh). As *peak/ off-peak* tariff, the existing ewz tariff scheme is used, in which electricity prices during night time and on Sundays as well as public holidays (Mon.-Sat. 22h-6h, Sun. 0h-24h – CHF 0.095/kWh) are about half of the prices as during week-days (Mon.-Sat. 6h-22h – CHF 0.185/kWh) [eDoecet10]. Both of these tariffs are used as benchmarks for the performance of the *dynamic tariff*. The dynamic tariff and its construction is detailed in the next section.

9.3 Dynamic Electricity Tariff

In this section a dynamic tariff that can be used for Problem 9.1 is presented. Since spot market prices, which are used for the tariff construction, are only available for a limited time window into the future, LS-SVM for electricity tariff price forecasting are used to provide the MPC controller with the necessary estimated time-varying prices for the whole prediction horizon. This section therefore presents the basic construction of the dynamic tariff, the support vector regression for estimating the missing data including numerical results for short-term tariff forecasting, and the construction of the whole electricity price vector for the MPC problem.

9.3.1 Basic Construction

The basic dynamic tariff is a recently developed time-varying, hourly-based tariff that reflects the true marginal cost of electricity consumption, i.e. the sum of the time-varying cost components for electricity provision and transport as well as fixed cost components in the form of fees and taxes (all given on a per kWh basis) [UA10]. This tariff scheme is used here as a dynamic benchmark tariff for assessing and evaluating the demand response potential of price-responsive loads on the end-consumer side. It is based on time-series of Swiss spot market prices (Swissix) as traded on the European Energy Exchange (EEX) [Exc10] and a generic electricity load curve, reconstructed from grid load measurements (full-year time series, 15 min sampling) of the city of Zurich [eDoecet10]. The reference year is 2007. The construction of the dynamic tariff is as follows:

1. Time-series of spot market prices and load curves are used to calculate the average spot price and average grid load level for the given time period.

2. The relative weights of the individual cost components of electricity consumption, e.g. α, β, and γ, are calculated using tariff data from ewz [eDoecet10]. The average electricity price for the constructed full-year time-series is $c_{\text{avg}} =$ CHF 0.1465/kWh.
3. The construction of the spot/ load-based tariff is then accomplished using (9.7). More details on the tariff construction can be found in [UA10].

The hourly dynamic electricity tariff c_k^{dyn} is defined as

$$c_t^{\text{dyn}} := \left(\alpha \cdot \frac{\mathsf{Spot\ price(k)}}{\mathsf{Spot\ price}_{\text{avg}}} + \beta \cdot \frac{\mathsf{Load\,level(k)}}{\mathsf{Load\,level}_{\text{avg}}} + \gamma\right) \cdot c_{\text{avg}} \tag{9.7}$$

$$\text{with} \left\| \begin{array}{lcl} \alpha & := & \%\,\mathsf{Electricity}_{\text{avg}} \\ \beta & := & \%\,\mathsf{Grid\ utilization}_{\text{avg}} \\ \gamma & := & \%\,\mathsf{City\ concession}_{\text{avg}} \end{array} \right\| ,$$

where t is the hourly time step and c_{avg} is the average tariff price. For the considered case, α, β, and γ are 41.0 %, 53.7 %, and 5.4 %, respectively.

Remark 9.2. By construction, (9.7) involves a normalization, i.e. an electrical load which is constant throughout the whole time period will incur the same costs with the time-varying tariff scheme as if the constant average electricity price would be applied. Note that this level can be chosen by the utility company to scale the resulting time-varying electricity price and determine the price level.

The tariff construction is implemented in a day-ahead fashion: Next day's EEX spot market prices are announced shortly after noon on weekdays. An exact day-ahead variable tariff price vector can then be constructed in line with the announcements of day-ahead EEX spot prices. This leads to a varying prediction horizon for the variable tariff's day-ahead prices of a 12 h minimum, just before the announcement of the next day's EEX spot prices, to a 36 h maximum, just after the announcement. Since the MPC optimization approach uses a 24 h prediction horizon, the missing tariff prices of the first 12 hours of the next day have to be estimated, which is done via SVM, see Section 9.3.2.

The proposed spot/load-based tariff scheme exhibits a good correlation, measured via the coefficient of determination (R^2), with both spot price and grid load time-series for the whole year 2007 ($R^2 = 0.91$ and $R^2 = 0.54$, respectively). In contrast, the direct correlation between spot price and grid load is remarkably low ($R^2 = 0.25$). An illustration of the correlation is shown in Figure 9.1. The spot/load-based tariff is compared to the currently existing ewz day/night tariff scheme, in which electricity prices during night time (Mon.-Sat. 22h–6h, Sun. 0h–24h) are only about half that of prices during day time (Mon.-Sat. 6h–22h) [eDoecet10], see Table 9.3.

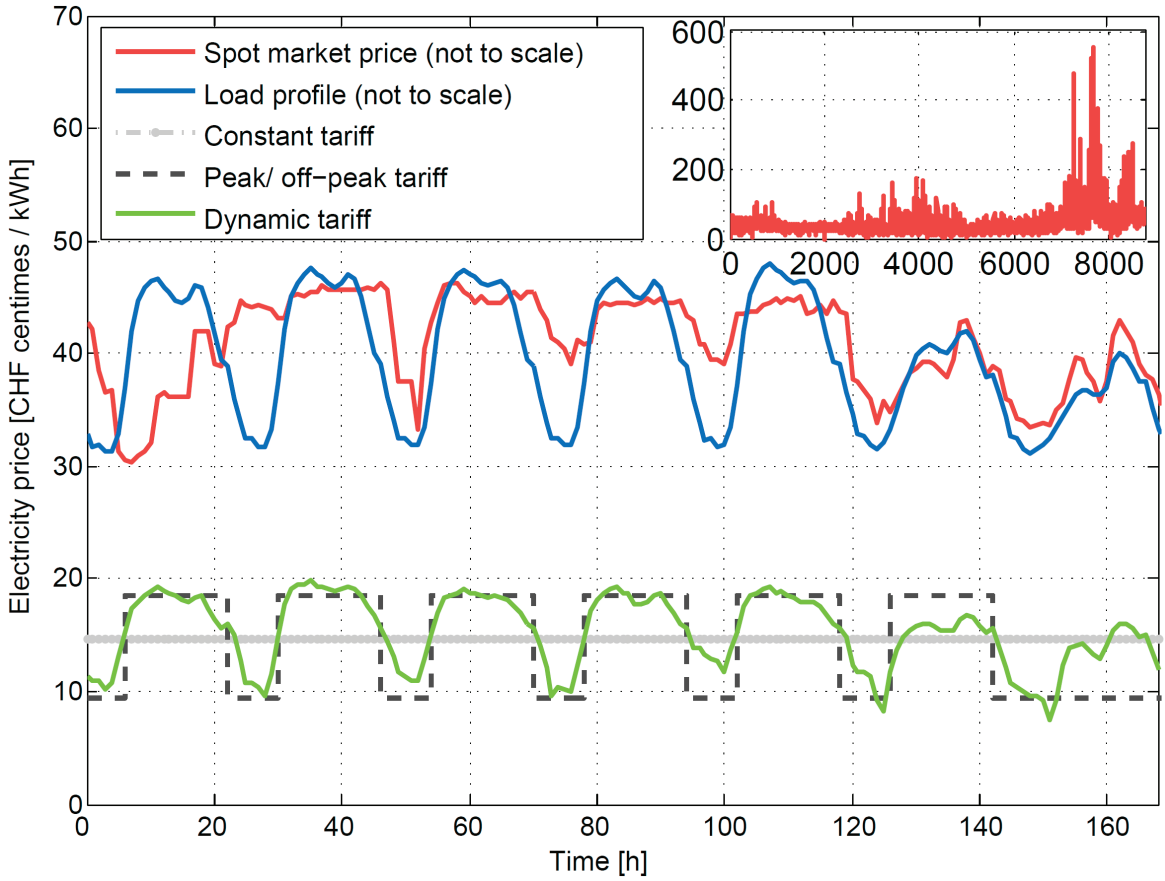

Figure 9.1: Evolution of spot prices, grid load, and dynamic tariff.

Remark 9.3. When considering only the first three quarters of 2007, the correlation with the load time-series are actually significantly higher: tariff–load $R^2 = 0.86$ and spot–load $R^2 = 0.54$. This remarkable difference is due to significant spot price peaks towards the end of 2007, shown in the inlay of Figure 9.1, which distorts the otherwise very good correlation.

The results from the correlation analysis are a strong indication that the spot/load-based tariff can act as a communication signal for price-responsive end-consumers, truly relaying information on spot market price and grid load levels. It provides the necessary price information and economic incentive for end-consumers to react accordingly.

The spot/load-based tariff scheme allows to find a consensus between the end-consumer's individual goal of minimizing the cost for electricity and the superordinate goal of reducing peak electricity demand and peak grid load levels.

Table 9.3: Correlation of variable tariffs with spot price and grid load time-series for the first three quarters of the year 2007.

Tariff scheme	Spot time-series R^2 =	Load time-series R^2 =
ewz Day/Night	0.13 (0.30)	0.63 (0.63)
Spot-based	1.00 (1.00)	0.25 (0.54)
Spot/Load-based	0.91 (0.88)	0.54 (0.86)

9.3.2 Support Vector Regression

The knowledge of electricity price patterns based on what happened on the electricity spot market and with electricity grid load levels during previous days can improve the performance of DR initiatives. In essence this means to help the customers in deciding when and how to change their energy demand in light of dynamic electricity prices. Since the electricity tariff is only available for a limited time window into the future the hourly prices at the end of the prediction horizon need to be estimated in order to provide the MPC controller with the necessary estimated time-varying electricity prices for the whole prediction horizon. The tariff time series is generally non-stationary with an hourly sampling time; it exhibits high-frequency fluctuations and peak shifting, also influenced by calendar effects, i.e. weekends and holidays. Therefore it is a relatively hard task to capture the dynamics of the tariff time series and fit a model out of the given data set. Several methodologies have been adopted for electricity price forecasting. Broadly exploited approaches are time series models, such as Autoregressive Integrated Moving Average (ARIMA) [CRNC03], Artificial Neural Network (ANN) [SSD99], and Support Vector Machines (SVM) [OFG97]. Here the Least-Squares Support Vector Machines (LS-SVM) method is used to forecast day-ahead electricity prices based on past spot market prices and grid load levels. Recently the SVM technique was successfully applied to find price patterns in the energy market [LMC+08, GBNC07, SDS03a]. The training algorithm of a SVM involves a quadratic optimization program, which provides a unique solution and does not require the random initialization of weights, as in ANN training. Given N_s samples of system input patterns E_i and the associated output values S_i, where i represents the sample, LS-SVR approximates the relationship between the outputs and inputs using the following equation.

Definition 9.4.

$$S_i = \sum_{i=1}^{N_s} w_i \phi(E_i) + b_i \ , \tag{9.8}$$

where $\phi(E_i)$ is a nonlinear mapping of the input data to a higher-dimensional feature space, b_i is the scalar threshold, and w_i is the weight coefficient. The parameters w_i and b_i are estimated solving a linear regression problem in this feature space, which requires the assignment of the *kernel function* $K(E_i, E_j) = \phi(E_i)^T \phi(E_j)$ and the tuning of a predefined set of parameters. Then the SVR can avoid under- and over- fitting by tuning the parameter set. Formulas for parameter selection are used which can be found in [CM04]. More information regarding SVMs can also be obtained in [ker11].

The LS-SVR method described above is applied to compute tariff forecasts. The hourly spot market prices and grid load levels for Zurich 2007 are considered for the training of the LS-SVR. The training data set is defined as follows: at each hour, the input patterns are based on the spot market prices, the grid load level, and the electricity prices 4 months back into the past and the corresponding outputs are the electricity price one hour ahead. To improve the training accuracy and prevent over-fitting and under-fitting, statistical analysis of 'studentized' residuals was applied and the outliers were removed [Fox97]. Then the nonlinear regressor is trained and used to predict the hourly electricity prices for the next day. Figure 9.2 shows forecasted and actual hourly electricity prices of the first three weeks of July 2007. The value of the coefficient of determination R^2 for the three weeks presented is 0.94, showing the goodness of fit.

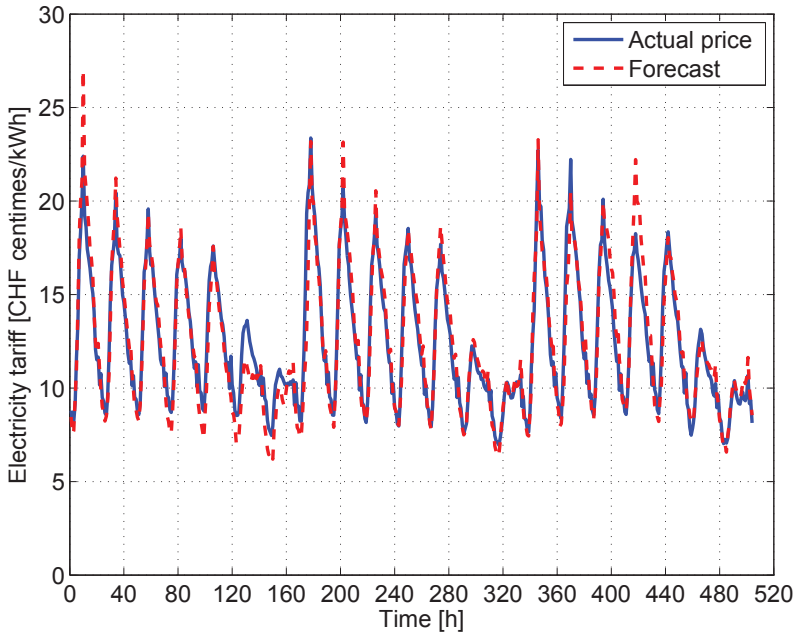

Figure 9.2: Hourly electricity tariff forecasts for Zurich, 1-22 July 2007.

All the numerical results presented in this subsection are obtained by Matlab's SVM toolbox, an LS-SVM training and simulation environment written in C-code [PSG+].

9.3.3 Construction of Price Vector for MPC Controller

At each time step t, the MPC controller must be provided with the electricity prices for the whole prediction horizon, i.e. 24h. As the prediction horizon for the variable tariff's day-ahead prices is varying, predicted electricity prices are not always available over a $24h$ time window, the missing price data need to be estimated. Denote by $\mathsf{c}_\mathsf{i}^{\mathsf{tariff}}, i \in \{1, ..., 24\}$ the 24 electricity tariffs valid between 0:00 and 0:00 on day t and by $\hat{\mathsf{c}}_\mathsf{j}^{\mathsf{tariff}}, j \in \{1, ..., 12\}$ the electricity forecasts valid between 0:00 and 12:00 on day $t+1$. For every day, from hour $k = 1$ to hour $k = 12$, the electricity price vector with regression, $c^{\mathrm{reg}} \in \mathbb{R}^{24}$, is built as follows:

$$c^{\mathrm{reg}} = [\mathsf{c}_{k+1}^{tariff} \dots \mathsf{c}_{24}^{tariff} \hat{\mathsf{c}}_1^{tariff} \dots \hat{\mathsf{c}}_k^{tariff}]. \tag{9.9}$$

The electricity price vector for MPC at the remaining hours of a day is computed out of the time-varying electricity tariff prices, which are available over 24h.

9.4 Investigations

In order to determine the effect of different electricity tariffs, the four tariff options, constant tariff c^{con}, peak/ off-peak tariff c^{pop}, dynamic tariff c^{dyn} (perfectly predicted dynamic tariff) and the *regression tariff* c^{reg} (dynamic tariff based on predictions and regression), were compared for varying building types and internal gains levels. An overview of the available simulation parameters is given in Table 9.4.

Table 9.4: Parameters for investigation of electricity prices.

Parameter	**Value**
Tariff	c^{con}, c^{pop}, c^{dyn}, c^{reg}
Building standard	sa, pa
Construction type	h, l
Window area fraction	wh, wl
Internal gains level	ih, il

9.5 Results

9.5.1 Qualitative Differences

A qualitative graphical depiction of the electricity consumption for the considered office room is given in Figure 9.3. The time frame is the third week of December 2007. The evolution of room temperature for three different cases is presented: A MPC controller using the constant electricity tariff and a MPC controller using the dynamic tariff assuming either perfect prediction or using the regression estimation. In all cases, the room temperature constraints are respected. However, significantly different temperature patterns appear during night time: The dynamic tariff leads to a pre-heating of the office room during the early morning hours when electricity prices are lowest. There exist slight differences between the cases of perfect predicted and estimated dynamic tariffs. When the MPC controller uses tariff estimations, the pre-heating during nighttime occurs 1-2 hours earlier and is on some mornings sub-optimal.

The shift of electricity demand is accomplished mostly by a partial shift of radiator usage from day time to night time. This shift can only be partial as the temperature constraints need to be respected. The MPC controller clearly takes advantage of the office room's thermal inertia in its optimization. The demand of other appliances, such as lighting can mostly not be shifted in time. Some variations and an overall slight reduction in the office lighting's peak usage are noticeable nevertheless. This is accomplished by the control of the window blinds that adds an additional albeit small degree of freedom for the lighting.

9.5.2 Quantitative Differences

A quantitative analysis of the electricity consumption over the whole year 2007 for altogether 16 different room configurations as listed in Table 9.1 shows interesting results, see Figure 9.4. First of all, a noticeable reduction in overall peak electricity demand as compared to the constant tariff: The daily maximum peak electricity demand, i.e the highest load event per day, is on average reduced by 7.9% (peak/ off-peak tariff), by 5.2% (dynamic tariff – perfect prediction) and by 6.1% (dynamic tariff – regression). These aggregated consumption figures, however, are obscured by two facts: First, only a fraction of total electricity consumption can be shifted in time. Demand such as lighting is only barely shiftable, whereas thermal loads (chillers, cooling tower, radiators) are well shiftable in time. Second, the peak demand of the rooms should be compared with the given load curve for Zurich, since only peak consumption occurring when grid load levels are already high is critical.

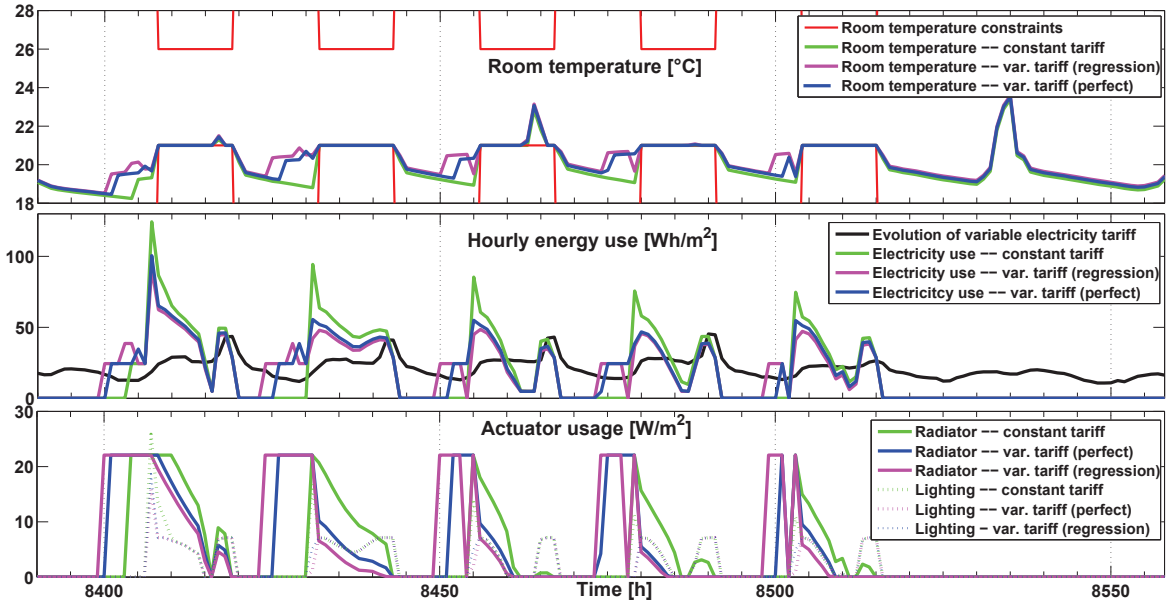

Figure 9.3: Reducing peak electricity demand by shifting radiator usage in winter time.

When comparing directly the peak demand of the different rooms' thermal appliances with the given load curve, the peak shifting is remarkable: The thermal appliances daily maximum peak demand is on average reduced by 31.5% (peak/ off-peak tariff), by 38.9% (dynamic tariff – perfect prediction) and by 39.0% (dynamic tariff – regression). Total electricity consumption stays the same for all swiss average buildings and is marginally reduced for all passive houses, by -1%, when using an MPC setup with any of the given dynamic electricity tariffs.

A rather unexpected result occurred when looking at electricity costs: Total costs for the whole year were significantly lower when using a constant tariff that charges the average cost of the dynamic tariff (CHF $0.1465/kWh$). When using an optimizing over the dynamic tariffs, costs are 11.6% (peak/ off-peak tariff) and 26.3% (dynamic tariff – perfect/regression) higher. At first this result comes as a surprise. However, only a part of the office room's electric consumption can be shifted in time. Lighting can almost not be shifted and occurs when the office is by definition occupied, i.e. during the expensive day time. By construction (see Remark 9.2) the prices during the day are much higher than with the constant tariff. Consequently, if a significant amount of the load cannot be shifted to less expensive times, then the electricity costs increase.

When looking at the costs incurred by the given thermal appliances, significant cost reductions can be seen: On average 15% (peak/ off-peak tariff) and $7-9\%$ (dynamic tariff – perfect/regression) lower. Depending on building type, differing trends can be

seen: Swiss average buildings see increasing costs: by 0.3% (day/night tariff) and by 12.2 – 14.1% (dynamic tariff – perfect/regression). This is due to the specifically high cooling/heating demand of such buildings and comparatively low thermal inertia. In contrast, the costs for passive houses decline steeply: by 29.5% (peak/ off-peak tariff) and by 28.4 – 31.2% (dynamic tariff – perfect/regression).

This economic disadvantage for swiss average houses could however be addressed by a scaling of the proposed tariff structure, such that, e.g., an average household would under a dynamic tariff scheme pay the same as before, but would have the opportunity to pay considerably less if it behaved price-responsive. This way, an economic incentive would be created to behave grid-friendly.

Additionally, it is expected that the positive effect on the peak demand reduction that was observed can be further exploited by considering buildings with more storage devices (e.g., a hot water boiler which can be heated during night) as well as systems with TABS, which has long time constants. This is expected to enable further load shifting and consequently also result in lower electricity consumption costs.

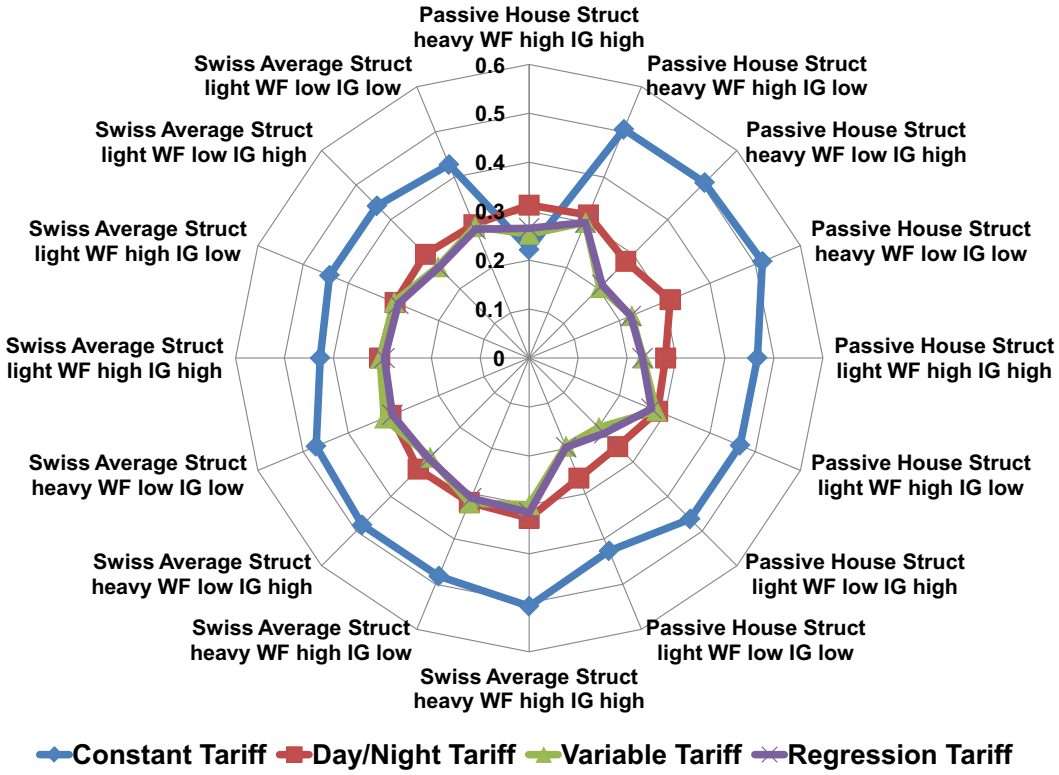

Figure 9.4: Relative peak demand reduction for different room setups.

9.6 Conclusions

This study shows that peak electricity demand in building climate control relative to a given reference load curve can effectively be reduced by incorporating an appropriately designed variable electricity tariff directly into the cost function of an MPC setup. This load shifting effort for thermal loads comes at the cost of higher electricity consumption. Overall electricity costs are clearly increased for the given 16 test cases, as thermal loads here do not represent the majority of electricity consumption. Electricity costs only for the thermal loads fall steeply for passive houses and increase slightly for swiss average houses.

The proposed scheme is well suited to reach the goal of load shifting and decreasing of peak electricity demand with respect to a given load profile. The scaling of the tariff needs, however, to be tuned, such that an average household is not paying more than before; and an economic incentive is given for adhering to such DR schemes.

Appendix

A Expression of Matrices in Augmented Model

$$\mathbf{A} := \begin{bmatrix} \mathbf{I} \\ A \\ A^2 \\ \vdots \\ A^N \end{bmatrix} \qquad \mathbf{B} := \begin{bmatrix} B & \mathbf{0} & \dots & \dots & \dots \\ AB & B & \mathbf{0} & \dots & \dots \\ A^2B & AB & B & \mathbf{0} & \dots \\ \vdots & \vdots & \vdots & \ddots & \dots \\ A^NB & A^{N-1}B & \dots & \dots & \ddots \end{bmatrix}$$

$$\mathbf{H} := \begin{bmatrix} H & \mathbf{0} & \dots & \dots & \dots \\ AH & H & \mathbf{0} & \dots & \dots \\ A^2H & AH & H & \mathbf{0} & \dots \\ \vdots & \vdots & \vdots & \ddots & \dots \\ A^NH & A^{N-1}H & \dots & \dots & \ddots \end{bmatrix} \qquad \mathbf{E} := \begin{bmatrix} E & \mathbf{0} & \dots & \dots & \dots \\ AE & E & \mathbf{0} & \dots & \dots \\ A^2E & AE & E & \mathbf{0} & \dots \\ \vdots & \vdots & \vdots & \ddots & \dots \\ A^NE & A^{N-1}E & \dots & \dots & \ddots \end{bmatrix}$$

$$\mathbf{C} := \begin{bmatrix} C \\ CA \\ CA^2 \\ \vdots \\ CA^{N-1} \end{bmatrix} \qquad \mathbf{D} := \begin{bmatrix} D & \mathbf{0} & \dots & \dots & \dots \\ CB & D & \mathbf{0} & \dots & \dots \\ CAB & CB & D & \mathbf{0} & \dots \\ \vdots & \vdots & \vdots & \ddots & \dots \\ CA^{N-1}B & CA^{N-2}B & \dots & \dots & \ddots \end{bmatrix}$$

$$\mathbf{V} := \begin{bmatrix} V & \mathbf{0} & \dots & \dots & \dots \\ CH & V & \mathbf{0} & \dots & \dots \\ CAH & CH & V & \mathbf{0} & \dots \\ \vdots & \vdots & \vdots & \ddots & \dots \\ CA^{N-1}H & CA^{N-2}H & \dots & \dots & \ddots \end{bmatrix} \qquad \mathbf{W} := \begin{bmatrix} W & \mathbf{0} & \dots & \dots & \dots \\ CE & W & \mathbf{0} & \dots & \dots \\ CAE & CE & W & \mathbf{0} & \dots \\ \vdots & \vdots & \vdots & \ddots & \dots \\ CA^{N-1}E & CA^{N-2}E & \dots & \dots & \ddots \end{bmatrix}$$

B Proof of Theorem 4.16

In order to use results from [BS06], we restate (4.29) equivalently as

$$\left(\begin{bmatrix} \mathbf{G}_j\mathbf{B} & \mathbf{0}_{\{1\times n_u n_p N^2\}} \end{bmatrix} + \begin{bmatrix} \mathbf{0}_{\{1\times n_u N\}} & (\Xi_j \mathbf{w})^T \end{bmatrix} \right) \mathbf{z} \tag{10}$$

$$+ (\mathbf{G}_j \mathbf{A} x_0 - \mathbf{g}_j + \mathbf{G}_j \mathbf{E} \mathbf{w}) \leq 0 \ ,$$

where $\mathbf{z} := \begin{bmatrix} \mathbf{h}^T & \mathbf{m}^T \end{bmatrix}^T$ contains the vectors $\mathbf{h}$ and $\mathbf{m}$, where $\mathbf{m}$ is a vectorized version of $\mathbf{M}$ with a particular structure defined as

$$\begin{aligned} \mathbf{m} := [\mathbf{0} \ \ \mathrm{vec}(M_{1,0})^T \ \ \mathrm{vec}(M_{2,0})^T \ ... \ \mathrm{vec}(M_{N-1,0})^T \\ \mathbf{0} \ \ \mathbf{0} \ \ \mathrm{vec}(M_{2,1})^T \ ... \ \mathrm{vec}(M_{N-1,1})^T \ ... \ \mathbf{0}]^T \end{aligned} \tag{11}$$

and Ξ_j is defined as follows: In order to show equivalence of (4.29) and (10), the only non-obvious part is to show that $\mathbf{G}_j \mathbf{B} \mathbf{M} \mathbf{w} = (\Xi_j \mathbf{w})^T \mathbf{m}$. First, note that $\mathbf{G}_j \mathbf{B} \mathbf{M} \mathbf{w}$ is scalar $\Rightarrow \mathbf{G}_j \mathbf{B} \mathbf{M} \mathbf{w} = (\mathbf{G}_j \mathbf{B} \mathbf{M} \mathbf{w})^T$. Similarly, $(\Xi_j \mathbf{w})^T \mathbf{m} = \mathbf{m}^T \Xi_j \mathbf{w}$. Thus, we need to show that $\mathbf{G}_j \mathbf{B} \mathbf{M} = \mathbf{m}^T \Xi_j$.

Let $f^T := \mathbf{G}_j \mathbf{B}$, with $f^T = \begin{bmatrix} f_1 & \dots & f_N \end{bmatrix}$. $\Rightarrow \mathbf{G}_j \mathbf{B} \mathbf{M} = f^T \mathbf{M}$. For each $j \in \mathbb{N}_0^{N-1}$ we can write

$$f_j M_{k,l} = \mathrm{vec}(M_{k,l})^T \left(\mathbf{I}_{mp} \otimes f_j \right) \ .$$

Define $\hat{F}^j := \begin{bmatrix} \mathbf{I}_{mp} \otimes f_0 \\ \mathbf{I}_{mp} \otimes f_1 \\ \vdots \end{bmatrix}$, which multiplies each column of $\mathbf{M}$. Consequently, if $\Xi_j := \left(\mathbf{I} \otimes \hat{F}^j \right)$, $f^T \mathbf{M}$ can be written as $\mathbf{m}^T \Xi_j$. Having the inequality in this form, the assertion now follows from Theorem 2b of [BS06].

C Computation of Problem 4.18

The aim is to formulate a standard QP. We show it here for the state constraints, the input constraints can be handled in the same fashion. The state constraints in $\Pi_{BDS}(x_0)$ can be rewritten as

$$\begin{aligned} &\max \mathbf{G}_j \mathbf{A} x_0 + \mathbf{G}_j \mathbf{B} \mathbf{h} - \mathbf{g}_j + \mathbf{m}^T \Xi_j + \mathbf{G}_j \mathbf{E}_j) \mathbf{w} \leq 0 \\ &s.t. \ \ -\Omega_{\mathbf{x},j} \mathbf{1} \leq \mathbf{w} \leq \Omega_{\mathbf{x},j} \mathbf{1} \ , \end{aligned} \tag{12}$$

where the maximization is meant to be taken row-wise. We follow the approach made standard in robust programming and take the dual of this optimization problem

$$\begin{aligned} &\min \Omega(\mathbf{1}^T \lambda_l^j + \mathbf{1}^T \lambda_u^j) + \mathbf{G}_j \mathbf{A} x_0 + \mathbf{G}_j \mathbf{E} \mathbf{h} - \mathbf{g}_j \leq 0 \\ &s.t. \ \ \lambda_l^j - \lambda_u^j = \mathbf{m}^T \boldsymbol{\Xi}_\mathbf{j} + \mathbf{G}_j \mathbf{E}_j \\ &\qquad \lambda_l^j, \ \lambda_u^j \geq 0 \ , \quad \forall j \in \mathbb{N}_1^{r(N+1)} \ , \end{aligned} \tag{13}$$

where λ_l^j and λ_u^j are Lagrange multipliers corresponding to row j.

By duality, we have that any feasible λ in (13) will upper bound the maximization in (12). We are therefore free to drop the minimization in the constraint of (13) and by strong duality on linear programming, this relaxation will be tight. We can hence state Problem 4.18 equivalently as

$$
\begin{aligned}
&(\mathbf{M}^*(x_0), \mathbf{h}^*(x_0)) := \arg \min_{(\mathbf{M},\mathbf{h})} J_N^{ADF}(x_0, \mathbf{M}, \mathbf{h}) \\
&s.t.\ \Omega(\mathbf{1}^T \kappa_l^i + \mathbf{1}^T \kappa_u^i) + \mathbf{S}_i \mathbf{h} - \mathbf{s}_i \geq 0 \\
&\quad \kappa_l^i - \kappa_u^i = \mathbf{m}^T \mathbf{\Theta_i} \\
&\quad \kappa_l^i,\ \kappa_u^i \geq 0\ , \qquad \forall i \in \mathbb{N}_1^{qN} \\
&\quad \Omega(\mathbf{1}^T \lambda_l^j + \mathbf{1}^T \lambda_u^j) + \mathbf{G}_j \mathbf{A} x_0 + \mathbf{G}_j \mathbf{B} \mathbf{h} - \mathbf{g}_j \geq 0 \\
&\quad \lambda_l^j - \lambda_u^j = \mathbf{m}^T \mathbf{\Xi_j} + \mathbf{G}_j \mathbf{E}_j \\
&\quad \lambda_l^j,\ \lambda_u^j \geq 0\ , \qquad \forall j \in \mathbb{N}_1^{r(N+1)}\ ,
\end{aligned}
\tag{14}
$$

where Θ_i is defined from showing that $\mathbf{S}_i \mathbf{M} \mathbf{w} = (\Theta_i \mathbf{w})^T \mathbf{m}$ equivalently as shown for Ξ_j in Appendix B.

D Monotonicity of NRPE Use Depending on $(\beta_{\text{vac}}, \beta_{\text{occ}})$

In order to analyze the behavior of energy use depending on the average occupancy β_{vac} and average vacancy β_{occ}, the relative energy savings $\Delta E_{\text{li},-}^{\text{std}}$ are plotted versus all combinations of $\beta_{\text{vac}} \in \{2, 4, 8, 16\}$ and $\beta_{\text{occ}} \in \{4, 8, 16, 32\}$ for the parameters $P =$ (Building type B1, HVAC system S1, il, win). The behavior of the savings with respect to changes in vacancy and occupancy appears to be monotonous. As can be expected, for increasing vacancy values and for decreasing occupancy values the relative energy consumption increases. For the investigated range of parameters and the investigated case the dependency appears to be approximately linear. This observation justifies the choice of only three different $(\beta_{\text{vac}}, \beta_{\text{occ}})$ combinations, i.e. (1,10), (1,5), (5,10), used in all investigations.

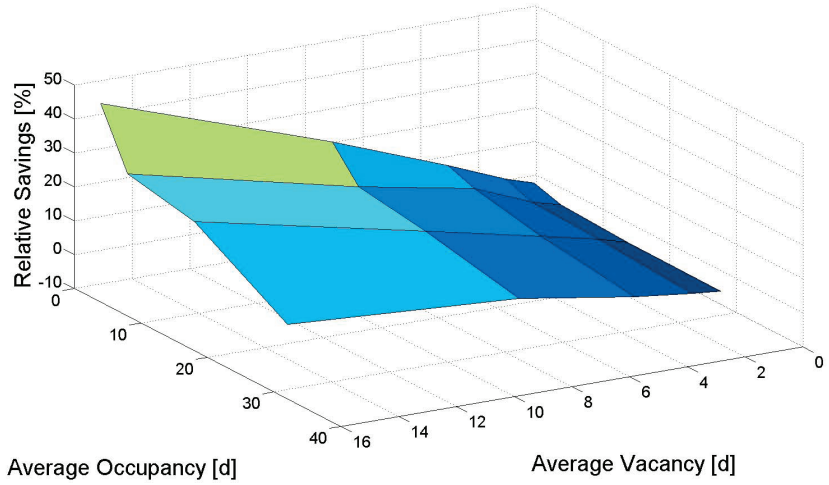

Figure D.1: Homogenous occupancy. The relative energy savings $\Delta E^{\mathrm{std}}_{\mathrm{li},-}$ are plotted versus different values of $(\beta_{\mathrm{vac}}, \beta_{\mathrm{occ}})$ for the parameters $P =$ (Building type B1, HVAC system S1, il, win).

E Homogeneous Occupancy, Absolute Savings

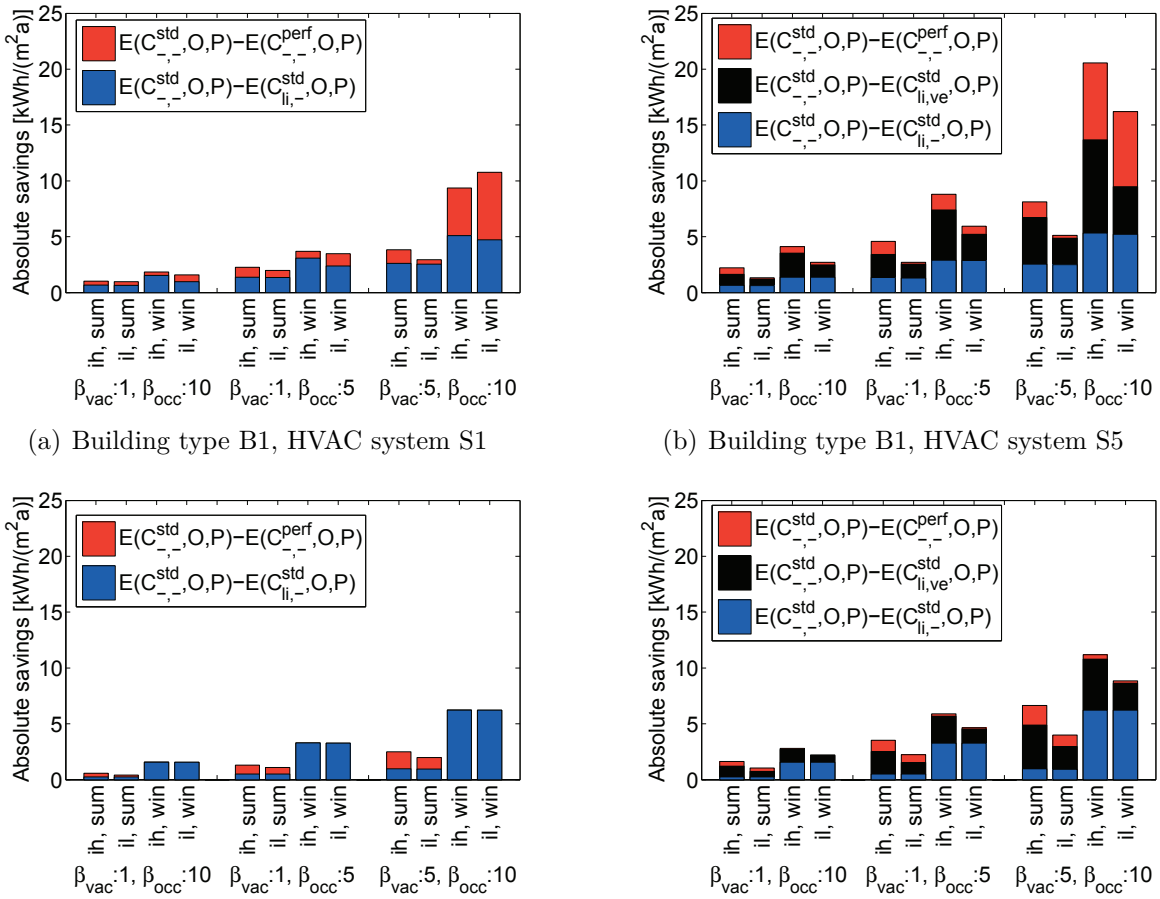

(a) Building type B1, HVAC system S1

(b) Building type B1, HVAC system S5

(c) Building type B2, HVAC system S1

(d) Building type B2, HVAC system S5

Figure E.2: Homogenous occupancy. The absolute energy savings $E(C^{\text{std}}_{-,-}, O, P) - E(C^{\text{perf}}_{-,-}, O, P)$, $E(C^{\text{std}}_{-,-}, O, P) - E(C^{\text{std}}_{\text{li,ve}}, O, P)$, and $E(C^{\text{std}}_{-,-}, O, P) - E(C^{\text{std}}_{\text{li},-}, O, P)$ are plotted in [kWh/(m^2a)] for all $P \in \mathbb{P}^{\text{occ}}$ and all $O^{\text{hom}}_{(\beta_{\text{vac}},\beta_{\text{occ}})} \in \mathbb{O}$, i.e. for all building cases and HVAC systems, both seasons {sum,win}, both internal gains levels {il,ih}, and the three combinations of $(\beta_{\text{vac}}, \beta_{\text{occ}})$.

Bibliography

[AM79] F.D.O. Anderson and J.B. Moore. *Optimal Filtering*. Prentice-Hall, Englewood Cliffs, N.J., 1979.

[AOT07] R.V. Andersen, B. Olesen, and J. Toftum. Simulation of the effects of occupant behaviour on indoor climate and energy consumption. In *Proc. of the Clima - RHEVA World Congress*, 2007.

[BB09] D. Bernardini and A. Bemporad. Scenario-based model predictive control of stochastic constrained linear systems. In *Proc. of the 48th IEEE Conference on Decision and Control*, pages 6333–6338, 2009.

[Bem98] A. Bemporad. Reducing conservativeness in predictive control of constrained systems with disturbances. In *Proc. of the 37th IEEE Conference on Decision and Control*, pages 1384–1391, 1998.

[BF77] D.P. Bloomfield and D.J. Fisk. The optimisation of intermittent heating. *Building and Environment*, 12(1):43–55, 1977.

[BK04] S. Bischof and H.R. Kranz. *Gebäudeautomation*. In: Energieeinsparung in Gebäuden, L. Joos (Hrsg.), Vulkan, 2004.

[BL97] J.R. Birge and F. Louveaux. *Introduction to Stochastic Programming*. Springer Series in Operations Research, 1997.

[Bla99] F. Blanchini. Set invariance in control. *Automatica*, 35(11):1747–1767, 1999.

[BRM06] D. Bourgeois, C. Reinhart, and I. MacDonald. Adding advanced behavioural models in whole building energy simulation: A study on the total energy impact of manual and automated lighting control. *Energy and Buildings*, 38:814–823, 2006.

[BS06] D. Bertsimas and M. Sim. Tractable approximations to robust conic optimization problems. *Mathematical Programming*, Ser. B 107(1):5–36, 2006.

[BTGGN04] A. Ben-Tal, A. Goryashko, E. Guslitzer, and A. Nemirovski. Adjustable robust solutions of uncertain linear programs. *Mathematical Programming*, 99(2):351–376, 2004.

[Cal10] G. Calafiore. Random convex programs. *Siam Journal on Optimization*, 20(6):3427–3464, 2010.

[CC05] G. Calafiore and M. Campi. Uncertain convex programs: Randomized solutions and confidence levels. *Mathemtical Programming*, 102(1):25–46, 2005.

[CC06] G. Calafiore and M. Campi. The scenario approach to robust control design. *IEEE Transactions on Automatic Control*, 51(5):742–753, 2006.

[CCS58] A. Charnes, W.W. Cooper, and G.H. Symonds. Cost horizons and certainty equivalents: an approach to stochastic programming of heating oil. *Management Science*, 4(3):235–263, 1958.

[CGKM07] R. Cagienard, P. Grieder, E.C. Kerrigan, and M. Morari. Move blocking strategies in receding horizon control. *Journal of Process Control*, 17(6):563–570, 2007.

[CKRC10] M. Cannon, B. Kouvaritakis, S. Rakovic, and Q. Chen. Stochastic tubes in model predictive control with probabilistic constraints. In *Proc. of the American Control Conference*, 2010.

[CM04] V. Cherkassky and Y. Ma. Practical selection of svm parameters and noise estimation for svm regression. *Neural Networks*, 17(1), 2004.

[CRNC03] J. Contreras, R.Espinola, F.J. Nogales, and A.J. Conejo. Arima models to predict next-day electricity prices. *IEEE Transaction on Power Systems*, 18(3), 2003.

[CRZ01] L. Chisci, J.A. Rossiter, and G. Zappa. Systems with persistent state disturbances: predictive control with restricted constraints. *Automatica*, 37:1019–1028, 2001.

[CZU03] S.H. Cho and M. Zaheer-Uddin. Predictive control of intermittently operated radiant floor heating systems. *Energy and Conversion Management*, 44:1333–1342, 2003.

[DA09] B. Dong and B. Andrews. Sensor-based occupancy behavioral pattern recognition for energy and comfort management in intelligent buildings. In *Proc. of 11th International IBPSA Conference*, 2009.

[eDoecet10] ewz Details of end-consumer electricity tariffs. *www.stadt-zuerich.ch/content/ewz/de/index/energie/stromprodukte_zuerich/privatkunden*, last accessed 10 March 2010.

[EN 04] EN 16484-2:2004. *Building Automation and control systems (BACS)*. 2004.

[EN 07] EN 15251:2007. *Indoor environmental input parameters for design and as-*

sessment of energy performance of buildings addressing indoor air quality, thermal environment, lighting and acoustics. 2007.

[EN 09] EN 13790:2009. *Energy performance of buildings - Calculation of energy use for space heating and cooling.* 2009.

[Exc10] EPEX European Power Exchange. *http://static.epexspot.com/document/7157/EPEXSpot_info_20091221_EEG_en.pdf*, last accessed 10 March 2010.

[Fan70] P.O. Fanger. *Thermal Comfort.* Danish Technical Press (republished by McGraw-Hill, New York, 1973), 1970.

[Fox97] J. Fox. *Applied Regression Analysis, Linear Models, and Related Methods.* Sage Publications, 1997.

[GBNC07] C. Gao, E. Bompard, R. Napoli, and H. Cheng. Price forecast in the competitive electricity market by support vector machine. *Physica A*, 382:98–113, 2007.

[GE09] D. Gyalistras and M. Gwerder (Eds.). Use of weather and occupancy forecasts for optimal building climate control (opticontrol): Two years progress report. Technical report, ETH Zurich and Siemens Building Technologies Division, Siemens Switzerland Ltd., Zug, Switzerland, 2009.

[GGO+10] D. Gyalistras, M. Gwerder, F. Oldewurtel, C.N. Jones, M. Morari, B. Lehmann, K. Wirth, and V. Stauch. Analysis of energy savings potentials for integrated room automation. In *Proc. of the Clima - REHVA World Congress*, 2010.

[GI10] R. Gondhalekar and J. Imura. Least-restrictive move-blocking model predictive control. *Automatica*, 46(7):1234–1240, 2010.

[GIK09] R. Gondhalekar, J. Imura, and K. Kashima. Rigorous determination of maximum controlled invariant feasible sets. In *In Proc. of EUCA European control Conference*, pages 2821–2826, 2009.

[GKM06] P.J. Goulart, E.C. Kerrigan, and J.M. Maciejowski. Optimization over state feedback policies for robust control with constraints. *Automatica*, 42(4):523–533, 2006.

[GLW+09] D. Gyalistras, B. Lehmann, K. Wirth, M. Gwerder, F. Oldewurtel, and V. Stauch. Performance bounds and potential assessment. Technical report, 2009. In [GE09].

[GPM89] C.E. Garcia, D.M. Prett, and M. Morari. Model predictive control: Theory and practice–a survey. *Automatica*, 25:335–348, 1889.

[GS61] R.E. Griffith and R.A. Steward. A nonlinear programming technique for

the optimization of continuous processing systems. *Journal of Management Sciece*, 7:379–392, 1961.

[GT85] W.J. Grünenfelder and J. Tödtli. The use of weather predictions and dynamic programming in the control of solar demestic hot water systems. In *Proc. of the Mediterranean Electrotechnical Conference (Melecon)*, 1985.

[GT05] M. Gwerder and J. Tödli. Predictive control for integrated room automation. In *Proc. of the Clima - RHEVA World Congress*, 2005.

[GTG09] M. Gwerder, J. Toedtli, and D. Gyalistras. Ruled-based control strategies. Technical report, 2009. In [GE09].

[GWL09] D. Gyalistras, K. Wirth, and B. Lehmann. Analysis of savings potentials and peak electricity demand. Technical report, 2009. In [GE09].

[HCL09] P. Hokayem, D. Chatterjee, and J. Lygeros. On stochastic receding horizon control with bounded control inputs. In *Proc. of the 48th IEEE Conference on Decision and Control*, pages 6359–6364, 2009.

[HFK04a] G.P. Henze, C. Felsmann, and G. Knabe. Evaluation of optimal control for active and passive building thermal storage. *International Journal of Thermal Sciences*, 43(2):173–183, 2004.

[HFK04b] G.P. Henze, C. Felsmann, and G. Knabe. Impact of forecasting accuracy on predictive optimal control of active and passive building thermal storage inventory. *International Journal of HVAC & Research*, 10(2):153–178, 2004.

[HKLF05] G.P. Henze, D.E. Kalz, S. Liu, and C. Felsmann. Experimental analysis of model-based predictive optimal control for active and passive building thermal storage inventory. *International Journal of HVAC & Research*, 11(2):189–214, 2005.

[(IE07] International Energy Agency (IEA). *Energy Policies of IEA Countries - Switzerland 2007 Review.* OECD/IEA, 2007.

[Ker00] E.C. Kerrigan. *Robust constraint satisfaction: Invariant sets and predictive control.* PhD thesis, 2000.

[ker11] http://www.kernel-machines.org. last visited June 2011.

[KM03] E.C. Kerrigan and J.M. Maciejowski. On robust optimization and the optimal control of constrained linear systems with bounded state disturbances. In *Proc. of the European Control Conference*, 2003.

[KM05] P. Kall and J. Mayer. *Stochastic Linear Programming.* Kluwer Academic Publishers, 2005.

[LÖ3] J. Löfberg. Approximation of closed-loop MPC. In *Proc. of 42nd IEEE Conference on Decision and Control*, pages 1438–1442, 2003.

[Lau08] J. Laustsen. *Energy Efficiency Requirements in Building Codes, Energy Efficiency Policies for New Buildings*. International Energy Agency, 2008.

[Law09] EnWG Energiewirtschaftsgesetz (German Energy Economy Law). 2009.

[LB10a] C. Liao and P. Barooah. An integrated approach to occupancy modeling and estimation in commercial buildings. In *Proc. of the American Control Conference*, pages 3130–3135, 2010.

[LB10b] C. Liao and P. Barooah. An integrated approach to occupancy modeling and estimation in commercial buildings. Technical report, Cambridge University Press, 2010.

[LMC+08] Q. Li, Q. Meng, J. Cai, H. Yoshino, and A. Mochida. Applying support vector machine to predict hourly cooling load in the building. *Applied Energy*, 86(10):2249–2256, 2008.

[LPL08] C. Pout L. Perez-Lombarda, J. Ortiz. A review on buildings energy consumption information. *Energy and Buildings*, 40(3):394–398, 2008.

[LWC+09] B. Lehmann, K. Wirth, S. Carl, V. Dorer, T. Frank, and M. Gwerder. Modeling of buildings and building systems. Technical report, 2009. In [GE09].

[LWD+09] B. Lehmann, K. Wirth, V. Dorer, T. Frank, and M. Gwerder. Control problem and experimental setup. Technical report, 2009. In [GE09].

[Mac02] J.M. Maciejowski. *Predictive Control with Constraints*. Prentice Hall, Essex, England, 2002.

[MBH+09] Y. Ma, F. Borrelli, B. Hencey, A. Packard, and S. Bortoff. Model Predictive Control of thermal energy storage in building cooling systems. *Proc. of the 48h IEEE Conference on Decision and Control*, pages 392–397, 2009.

[ML99] M. Morari and J.H. Lee. Model predictive control: past, present and future. *Computers & Chemical Engineering*, 23(4):667–682, 1999.

[MRRS00a] D.Q. Mayne, J.B. Rawlings, C.V. Rao, and P.O.M. Scokaert. Constrained model predictive control: Stability and optimality. *Automatica*, 36(6):789–814, 2000.

[MRRS00b] D.Q. Mayne, J.B. Rawlings, C.V. Rao, and P.O.M. Scokaert. Constrained model predictive control: Stability and optimality. *Automatica*, 36(6):789–814, 2000.

[MW65] B. Miller and H. Wagner. Chance-constrained programming with joint constraints. *Operations Research*, 13(6):930–945, 1965.

[New95] G.R. Newsham. Lightswitch: A stochastic model for predicting office lighting energy consumption. *Proc. of Right Light Three, 3rd European Conference on Energy Efficient Lighting*, pages 59–66, 1995.

[OFG97] E.E. Osuna, R. Freund, and F. Girosi. Support vector machines: training and applications. Technical report, 1997.

[OGG+10] F. Oldewurtel, D. Gyalistras, M. Gwerder, C.N. Jones, A. Parisio, V. Stauch, B. Lehmann, and M. Morari. Increasing energy efficiency in building climate control using weather forecasts and model predictive control. In *Proc. of the Clima - REHVA World Congress*, 2010.

[OGJ+09] F. Oldewurtel, D. Gyalistras, C.N. Jones, A. Parisio, and M. Morari. Analysis of model predictive control strategies. Technical report, 2009. In [GE09].

[OGJM09] F. Oldewurtel, R. Gondhalekar, C.N. Jones, and M. Morari. Blocking parameterizations for improving the computational tractability of affine disturbance feedback mpc problems. In *Proc. of the 48th IEEE Conference on Decision and Control*, pages 7381–7386, 2009.

[OJM08] F. Oldewurtel, C.N. Jones, and M. Morari. A tractable approximation of chance constrained stochastic mpc based on affine disturbance feedback. In *Proc. of the 47th Conference on Decision and Control*, pages 4731–4736, 2008.

[OPJ+10] F. Oldewurtel, A. Parisio, C.N. Jones, M. Morari, D. Gyalistras, M. Gwerder, V. Stauch, B. Lehmann, and K. Wirth. Energy Efficient Building Climate Control using Stochastic Model Predictive Control and Weather Predictions. In *Proc. of the American Control Conference*, pages 5100–5105, 2010.

[OPJ+12] F. Oldewurtel, A. Parisio, C.N. Jones, D. Gyalistras, M. Gwerder, V. Stauch, B. Lehmann, and M. Morari. Use of model predictive control and weather predictions for energy efficient building climate control. *Energy & Buildings*, 45:15–27, 2012.

[Opt11] OptiControl Project. *www.opticontrol.ethz.ch*, last accessed 28 July 2011.

[OUP+10] F. Oldewurtel, A. Ulbig, A. Parisio, G. Andersson, and M. Morari. Reducing Peak Electricity Demand in Building Climate Control using Real-Time Pricing and Model Predictive Control. In *Proc. of the 49th IEEE Conference on Decision and Control, CDC*, pages 1927–1932, 2010.

[Par09] A. Parisio. *Handling uncertainty with application to indoor climate control and resource allocation planning, PhD thesis.* University of Sannio, Benevento, Italy, 2009.

[PDED04] B. Pasik-Duncan, R. Elliott, and M. Davis. Guest editorial, special issue on stochastic control. *IEEE Trans. on Automatic Control*, 49(3):321–323, 2004.

[Pre70] A. Prekopa. On probabilistic constrained programming. In *in Proc. of the Princeton Symposium on Mathematical Programming*, pages 113–138. Princeton University Press, Princeton, NJ, 1970.

[Pre95] A. Prekopa. *Stochastic Programming.* Kluwer Academic Publishers, Dordrecht, The Netherlands, 1995.

[PRMS05] J. Page, D. Robinson, N. Morel, and J.-L. Scartezzini. A generalised stochastic model for the simulation of occupant presence. *Energy and Buildings*, 40(2):83–98, 2005.

[PSG+] K. Pelckmans, J.A.K. Suykens, T. Van Gestel, J. De Brabanter, L. Lukas, B. Hamers, B. De Moor, and J. Vandewalle. LS-SVMlab: a MATLAB/C toolbox for least squares support vector machines. Technical report.

[RM09] J.B. Rawlings and D.Q. Mayne. *Model Predictive Control: Theory and Design.* Nob Hill Publishing, 2009.

[Roc70] R.T. Rockafellar. *Convex Analysis.* Princeton University Press, 1970.

[rs12] ESP r software. *http://www.esru.strath.ac.uk/Programs/ESP-r.htm*, last accessed 31 January 2012.

[SDS03a] D.C. Sansom, T. Downs, and T.K. Saha. Support vector machine based electricity price forecasting for electricity markets utilising projected assessment of system adequacy data. In *Proc. of the Sixth International Power Engineering Conference (IPEC)*, pages 783–788, 2003.

[SDS+03b] J. Steppeler, G. Doms, U. Schättler, H. Bitzer, A. Gassmann, U. Damrath, and G. Gregoric. Meso-gamma scale forecasts using the non-hydrostatic model lm. *Meteorology and Atmospheric Physics*, 82:75–96, 2003.

[SIA] *SIA Design Tool "Klimatisierung", based on SIA standards 380/4 and 382/1.*

[SIA06a] *Lüftungs- und Klimaanlagen - Allgemeine Grundlagen und Anforderungen.* SIA Standard 382/1, 2006.

[SIA06b] *Standard-Nutzungsbedingungen für die Energie- und Gebäudetechnik.* SIA Standard 2024, 2006.

[SOCP11] J. Siroky, F. Oldewurtel, J. Cigler, and S. Privara. Experimental analysis of model predictive control for an energy efficient building heating system. *Applied Energy*, 88(9):3079–3087, 2011.

[sof11a] CPLEX software. *http://www-01.ibm.com/software/integration/optimization/cplex-optimizer/*, last accessed 28 July 2011.

[sof11b] EnergyPlus software. *http://apps1.eere.energy.gov/buildings/energyplus/*, last accessed 28 July 2011.

[sof11c] TRNSYS software. *http://sel.me.wisc.edu/trnsys/*, last accessed 28 July 2011.

[SSD99] B.R. Szkuta, L.A. Sanabria, and T.S. Dillon. Electricity price short-term forecasting using artificial neural networks. *IEEE Transaction on Power Systems*, 14(3):851–857, 1999.

[SSS09] V. Stauch, F. Schubiger, and P. Steiner. Local weather forecasts and observations. Technical report, 2009. In [GE09].

[Tar10] EDF Tariffs. www.edf-bleuciel.fr. last accessed 10 March 2010.

[UA10] A. Ulbig and G. Andersson. Towards variable end-consumer electricity tariffs reflecting marginal costs: A benchmark tariff. *Proc. of the 7th Conference on the European Energy Market (EEM)*, pages 1–6, 2010.

[vHB02] D.H. van Hessem and O.H. Bosgra. A conic reformulation of model predictive control including bounded and stochastic disturbances under state and input constraints. In *Proc. of the 41st IEEE Conference on Decision and Control*, pages 4643–4648, 2002.

[WB09] Y. Wang and S. Boyd. Performance bounds for linear stochastic control. *Systems & Control Letters*, 58(3):178–182, 2009.

[WFR05] D. Wang, C. Federspiel, and F. Rubinstein. Modeling occupancy in single person offices. *Energy and Buildings*, 37(2):121–126, 2005.

[Yu10] T. Yu. Modeling occupancy behavior for energy efficiency and occupants comfort management in intelligent buildings. In *Proc. of the 9th International Conference on Machine Learning and Applications (ICMLA)*, pages 726–731, 2010.

Curriculum Vitae

Frauke Oldewurtel
born on the 9th of November 1980, in Oldenburg, Germany.

2006-2011	Doctorate at the Automatic Control Laboratory, ETH Zurich, Switzerland (Dr. sc. ETH Zurich)
2005	Internship at Siemens Corporate Technology, Munich, Germany
2004-2006	Diploma studies in Electrical Engineering and Business Administration, TU Braunschweig, Germany (Dipl.-Wirtsch.-Ing.)
2003-2004	Master studies in Electrical Engineering, Georgia Institute of Technology, USA (Master of Science)
2000-2003	Undergraduate studies in Electrical Engineering and Business Administration TU Braunschweig, Germany (B.Sc.)
1993-2000	Neues Gymnasium Oldenburg, Germany (Abitur, High school)